2017

The myocyte enhancer factor-2 (MEF2) family mediates complex gene regulation in skeletal and cardiac myocytes

BOSTON UNIVERSITY

GRADUATE SCHOOL OF ARTS AND SCIENCES

Dissertation

The Myocyte Enhancer Factor-2 (MEF2) family mediates complex gene regulation in skeletal and cardiac myocytes

by

CODY ALAN DESJARDINS

B.A., Bowdoin College, 2009

Submitted in partial fulfillment of the

requirements of the degree of

Doctor of Philosophy

2017

Approved by

First Reader _____

Francisco J. Naya, Ph.D.
Associate Professor of Biology

Second Reader _____

Trevor W. Siggers, Ph.D.
Assistant Professor of Biology

ACKNOWLEDGMENTS

It has been said that it takes a village to raise a child, and if my graduate career is any indication, it takes a few more to raise a graduate student! I would like to begin by sharing my appreciation for my advisor, Dr. Frank Naya, whose unswerving dedication to mentoring his graduate students is truly the foundation upon which any member of the Naya lab is able to achieve success. I would also like to thank my thesis committee members: Dr. Chip Celenza, Dr. Susan Kandarian, Dr. Angela Ho, and Dr. Trevor Siggers, whose insightful questioning provided me direction when the way was the murkiest. Next I would like to thank the Naya lab, past and present. I could not have asked for a better community in which to pursue my degree, and I am happy to have shared this experience with them. I would like to take an opportunity to thank Dr. Nelsa Estrella and Dr. Mandi Clark whose camaraderie made the Naya lab truly a home. Finally, I would also like to thank all of the innumerable faculty, graduate students, and other members of the Boston University community who have made my graduate career so enjoyable.

Next, I would like to thank my friends outside of the BU community without whose support I could not have managed the focus and dedication I needed to complete my doctorate. I thank them for being sympathetic when I had to go to work instead of spending time with them, and I also thank them for making the time we did spend together that much more meaningful. And while there are far too many to list, I want you all to know how much I love and appreciate you for being there no matter the circumstances.

And most importantly, I would like to thank my family. Especially my father, Alan, and Sue for supporting my decision to become a scientist, even when they were not totally sure where I would end up, and for having confidence in my ability to succeed at whatever I set my mind to. I would like to thank the Amshoffs for taking me in and for providing all the support and excitement they could as I worked towards finishing my degree. Finally, I would like to thank Meredith, whose unwavering acceptance of the weird and wild hours of graduate school is simply beyond miraculous, and without whose love and support I don't know if could have had the strength to finish my degree. We're both finally out of graduate school, and I am excited to see what life has in store for us next.

My name may be the only one attached to this dissertation, but this endeavor was not completed alone and I want you all to know how much I value the support you have given me. Thank you all.

THE MYOCYTE ENHANCER FACTOR-2 (MEF2) FAMILY MEDIATES COMPLEX GENE REGULATION IN SKELETAL AND CARDIAC MYOCYTES

CODY ALAN DESJARDINS

Boston University Graduate School of Arts and Sciences, 2017

Major Professor: Francisco J. Naya, Associate Professor of Biology

ABSTRACT

Regulation of striated muscle differentiation and development are complex processes coordinated by an array of transcription factors. MEF2 is a crucial transcription factor required for muscle differentiation, but the roles of the individual MEF2 family members, MEF2A-D, have not been extensively evaluated. Acute ablation of *Mef2* expression in skeletal myoblasts revealed a required role for MEF2A activity in myoblast differentiation that was not shared with the other MEF2 factors. We hypothesized that a transcriptomic level analysis of *Mef2*-deficient skeletal myoblasts would reveal distinct regulatory roles for each MEF2 isoform. Comparative microarray analysis supported our hypothesis and we observed distinct gene programs preferentially-sensitive to individual MEF2 isoforms. While there was no variance in the consensus binding site associated with regulation by individual MEF2 isoforms, we did observe uniquely enriched binding sites for candidate co-regulatory proteins that mediate these complex regulatory patterns. Based on our observations in skeletal myoblasts, we performed a series of acute *Mef2* knockdowns in neonatal cardiomyocytes and uncovered a requirement for MEF2A and -

D, but not MEF2C in cardiomyocyte survival. Comparative microarray analysis confirmed that, similar to skeletal myoblasts, the MEF2 family regulated distinct but overlapping gene programs in cardiomyocytes. Additionally, this analysis uncovered a previously uncharacterized antagonistic regulation of a subset of cell cycle and sarcomere genes. Interestingly, *Mef2a* and *-d* knockdowns caused an upregulation of cell cycle markers and downregulation of sarcomere genes, with the opposite regulatory pattern in *Mef2c* knockdown. Further investigation of the proximal promoter region of these genes revealed enriched binding sites for transcription factors associated with key signaling pathways in the developing embryo, Hedgehog and Notch. Overexpression of constitutively active components of these signaling pathways revealed that Notch function requires the presence of MEF2A and -D, while Hedgehog does not appear to interact with these two isoforms. We have shown through our studies that MEF2, a core muscle transcription factor, takes part in complex regulatory interactions that are critical for the appropriate development of striated muscle tissues.

TABLE OF CONTENTS

LIST OF TABLES

LIST OF FIGURES

LIST OF ABBREVIATIONS

°C	degrees Celsius
µ-	micro-
2n	diploid
4n	tetraploid
-A	ampere
aa	amino acid
Ac-DEVD-	N-Acetyl-Asp-Glu-Val-Asp-7-amido-4-
AMC	Methylcoumarin
AKAP	A-kinase anchored protein
bHLH	basic Helix-loop-Helix
bp	base pair
BSA	bovine serum albumin
c-	centi-
$CaCl_2$	calcium chloride
CaMK	calcium modulated protein kinase
cDNA	complementary DNA
ChIP	chromatin immunoprecipitation
ChIP-exo	ChIP-exonuclease
ChIP-on-chip	ChIP on microarray
ChIP-seq	ChIP-sequencing
CPE	cytopathic effect

CT	threshold cycle
C-terminal	carboxy terminal
DAPI	4',6-diamidino-2-phenylindole
dH_2O	de-ionized water
DMEM	Dulbecco's Modified Eagle Medium
DNA	deoxyribonucleic acid
DTT	Dithiothreitol
EDTA	ethylenediaminetetraacetic acid
EGR1	Early Growth Response 1
-EnR	Engrailed repressor
ERK	extra-cellular signal regulated kinase
FAK	focal adhesion kinase
FIMO	Find Individual Motif Occurrences
Floxed	flanked by loxP sites
g	gram
GO	gene ontology
HBSS	Hank's Buffered Saline Solution
HCl	hydrochloric acid
HDAC	histone deacetylase
HEPES	4-(2-hydroxyethyl)-1-piperazineethanesulfonic acid
HH	Hedgehog signaling
hr	hour

HRP	horse-radish peroxidase
IACUC	Institutional Animal Care and Use Committee
IPA	Ingenuity pathway analysis
JAK-2	Janus kinase 2
KEGG	Kyoto encyclopedia of genes and genomes
KO	knockout
L	liter
lacZ/βGal	β-Galactosidase (gene/protein)
LB	Luria Broth
LoF	loss-of-function
luc	firefly luciferase
M	molar
m	meter
m-	milli-
MADS-box	MCM1, Agamous Deficiens, SRF box
MAPK	mitogen-activated protein kinase
MEF2	Myocyte Enhancer Factor-2
MHC	Myosin Heavy Chain
min	minute
MOI	multiplicity of infection
mRNA	messenger RNA
MYF5	Myogenic Factor 5

MyoD	Myogenic Differentiation 1
n-	nano
Na_2Co_3	sodium carbonate
Na_2HPO_4	disodium phosphate
NaCl	sodium chloride
NaH_2PO_4	monosodium phosphate
NaOH	sodium hydroxide
NCBI	National Center of Biotechnology Information
NF-κB	nuclear factor kappa-light-chain-enhancer of activated B cells
NICD	Notch intracellular domain
NRVM	neonatal rat ventricular myocyte
N-terminal	amino terminal
OE	overexpression
p-	pico-
PBS	phosphate buffered saline
PCR	polymerase chain reaction
PEI	polyethylamine
pfu	plaque-forming unit
PKA	protein kinase A
PMSF	phenylmethane sulfonyl fluoride
qRT-PCR	quantitative real-time PCR

RNA	ribonucleic acid
RNAi	RNA interference
RNAse	ribonuclease
rpm	rotations per minute
SDS	sodium dodecyl sulfate
sec	second
SHH	Sonic Hedgehog
shRNA	short hairpin RNA
siRNA	short interfering RNA
SRF	Serum Response Factor
TBS	Tris-buffered saline
TF	transcription factor
TFBS	transcription factor binding site
Tris	Tris(hydroxymethyl)aminomethane
UV	ultraviolet light
V	volts
xg	times the acceleration of gravity
Δ	delta (change)

CHAPTER ONE: Introduction

1.1 Introduction

This dissertation focuses on understanding the interplay of regulatory roles of MEF2 isoforms in mammalian striated muscle. Mammalian MEF2 is composed of four transcription factors, MEF2A-D, that share high amino acid conservation, but have distinct roles in development and homeostasis. Prior literature has focused on the study of a single member of the family and extrapolated shared roles to the other family members. This research addresses the MEF2 family members as independent transcription factors.

The dissertation is divided into three parts. In chapter three, evidence is presented supporting unique roles for individual MEF2 factors in an *in vitro* model of skeletal differentiation and reveals distinct and overlapping networks regulated by each member of the MEF2 family. Data presented in chapter four reveals that the MEF2 family also regulates diverse cellular pathways in cardiac muscle, and introduces a novel antagonistic regulatory pattern governing a subset of genes regulated in one direction by MEF2A and -D, and in the opposite direction by MEF2C. We then introduce candidate regulatory pathways that may explain this uncharacterized pattern of regulation. Chapter five is focused on the direct repressive interaction of a single co-regulatory transcription factor, EGR1, and its role in MEF2A-mediated gene regulation. Investigating the complex intra-family MEF2 regulatory networks that exist in striated muscle is critical for understanding muscle development and disease.

1.2 Mammalian striated muscle development

1.2.1 Cardiac muscle development

The mammalian heart develops from specified mesodermal cells originating from the primitive streak. These cells form fields that migrate anteriorly and laterally from the primitive streak to form the anterolateral plate mesoderm which then migrates towards the midline at approximately mouse e7.5. Fusion at the midline of the embryo leads to the first formal cardiac structure, the linear heart tube, which is then elongated by the addition of the secondary heart field. After fusion of the secondary heart field the linear heart tube becomes functional and begins pumping blood from the venous region towards the arterial region at approximately e8.5 (Paige *et al.* 2015). The heart tube then undergoes looping morphogenesis and begins to expand outward as the chambers of the heart begin to mature by e9.5, with distinct ventricles forming by e10.5 (Paige *et al.* 2015).

1.2.2 Skeletal muscle development

The cell lineage that develops into the skeletal muscles of the body wall and limbs resides in the maturing somites. The somites are a series of mesodermal discs that arise from the presomitic mesoderm in a rostral-caudal progression (Molkentin *et al.* 1996). The formation of the somites from the presomitic mesoderm begins at e8.0 in mice (Edmonson *et al.* 1994). The induction of myogenesis in the body wall muscles occurs through activation of two myogenic bHLH factors, Myf5 and MyoD downstream of external signaling cues from the surrounding tissues (Braun *et al.* 1996, Molkentin *et al.* 1996). External signaling cues from the notochord, neural tube, and lateral mesoderm

induce compartmentalization of the somite into several discrete substructures responsible for the development of various body tissues (Molkentin *et al.* 1996).

1.3 Myocyte Enhancer Factor-2 Transcription Factors

1.3.1 Discovery and structure of MEF2 factors

The MEF2 family was discovered as DNA binding activity on an A/T-rich sequence upstream of the transcriptional start site of the *mck* promoter (renamed *Ckm*; creatine kinase, M-type) (Gossett *et al.* 1989). Expression of the protein binding this site preceded the expression of *mck* and other muscle-specific transcripts (Gossett *et al.* 1989, Pollock *et al.* 1991, Yu *et al.* 1992), establishing a role in early regulation of skeletal muscle gene expression. Initial investigations suggested an overlap in binding specificity with Serum Response Factor (SRF) (Pollock *et al.* 1991) due to the presence of a MADS box, a conserved DNA binding domain that is shared by proteins in the MADS box family: yeast mating-type selection factor MCM1, plant leaf identity homeodomain factor Agamous Deficiens, and human serum response factor SRF (Pollock *et al.* 1991, Yu *et al.* 1992). Further analysis revealed MEF2 activity was specific to a unique consensus sequence, $CTA(A/T)_4TAG$, which differed from the SRF consensus sequence (Pollock *et al.* 1991).

Mammalian MEF2 is composed of four members expressed from distinct genes (Figure 1.1). The highly conserved N-terminal region of each MEF2 factor shares approximately 95% amino acid sequence similarity in the MADS box and MEF2 domains (Black *et al.* 1998, Santelli *et al.* 2000). The MADS box and MEF2 domain are required for DNA binding and dimerization, and play a key role in the binding of co-

regulatory factors (Black *et al.* 1998, Santelli *et al.* 2000, Potthoff *et al.* 2007). The C-terminal region of each MEF2 factor contains the transcriptional activation domain and exhibits considerable amino acid divergence (Potthoff *et al.* 2007), sharing between 6 and 16% amino acid sequence identity. This divergence occurs throughout the region with the exception of an alternatively spliced exon designated β, shared among all four MEF2 isoforms. Inclusion of the β is enriched in tissues with known MEF2 function, and appears important in MEF2-mediated transcriptional activation (Figure 1.2) (Zhu *et al.* 2005).

1.3.2 MEF2 developmental expression patterns

MEF2 family members display a complex developmental expression pattern in striated muscle (Figure 1.3). In mammalian embryos, the heart begins as a curved stripe of cardiac precursor cells, i.e. the cardiac crescent, that have been specified to develop into the heart. Spatiotemporal *in situ* hybridization analysis on developing mouse embryos revealed that *Mef2b* and *Mef2c* are the first *Mef2* isoforms expressed in the cardiac mesoderm at embryonic day 7.5 (E7.5) prior to expression of sarcomeric genes such as cardiac α-actin (Edmonson *et al.* 1994, Molkentin *et al.* 1996). *Mef2c* is also expressed in the sinus venosus which contributes to the cardiac atria. *Mef2a* and *Mef2d* are subsequently expressed in the linear heart tube between E8.0 and E8.5, and after E8.5 all four *Mef2* genes are expressed throughout the developing heart (Figure 1.3). *Mef2b* and *Mef2c* expression begins to decline at E11.5, whereas *Mef2a* and *Mef2d* continue to be expressed. Additionally, *Mef2a* and *Mef2c* are expressed in the cardiac outflow tract as early as E9.5 and their expression seems far more prominent than that of *Mef2d*

(Edmonson *et al.* 1994). Postnatally, *Mef2a* and *Mef2d* are the most abundant isoforms in the heart. However, *Mef2c* expression has also been detected in postnatal cardiomyocytes, and is believed to play a role in homeostasis (Pereira *et al.* 2009)

The induction of myogenesis of the body wall muscles occurs through activation of two myogenic bHLH factors, MYF5 and MyoD (Braun *et al.* 1996, Molkentin *et al.* 1996). Induction of *Mef2* expression occurs concurrently with the appearance of the myogenic bHLH factors. *Mef2b* and *Mef2c* are the first *Mef2* transcripts detected in developing skeletal muscle at E9.0 (Figure 1.3), with the expression of *Mef2a* and *Mef2d* following soon thereafter at E9.5 (Molkentin *et al.* 1996). Expression of all *Mef2* transcripts persists through skeletal muscle development and into mature tissue (Edmonson *et al.* 1994).

1.3.3 MEF2 transcriptional activity in development

The spatiotemporal readout of MEF2 transcriptional activity in developing and adult mice was determined by generating transgenic mice harboring the *lacZ* gene driven by 3 copies of the *desmin* MEF2 site and surrounding flanking sequences (Naya *et al.* 1999). Reporter expression was restricted primarily to the muscle and neuronal lineages, tissues expressing high levels of MEF2 (Figure 1.4). In the heart, activity of the transgene was detected in a cluster of cardiogenic precursors in the cardiac crescent as early as E7.5 consistent with the expression of *Mef2c*. At E8.5, βgal expression appeared to be restricted to myocytes and was observed in the aortic sac, conotruncus, and the developing ventricles and atria. Transgene expression continued to be detected uniformly throughout the developing heart in both the atrial and ventricular chambers through

E14.5. However, despite abundant expression of *Mef2a* and *Mef2d* at this time point and postnatally, βgal expression begins to decline in late fetal cardiac development, and is greatly diminished postnatally. The reduction in postnatal MEF2-dependent reporter expression stems, in part, from the repression of MEF2 activity by histone deacetylases (HDACs) (McKinsey *et al.* 2001, McKinsey *et al.* 2002). Despite the potent repression of MEF2 activity on the transgene, high expression levels of MEF2A and MEF2D and robust *in vitro* DNA binding activity in postnatal cardiac extracts suggest that MEF2 protein isoforms still retain essential transcriptional function in muscle gene regulation in postnatal cardiomyocyte homeostasis. Indeed, as described below, MEF2A and MEF2D are required for proper gene regulation and survival in neonatal cardiomyocytes.

Concurrently, analysis of the *lacZ* reporter transgenic mice reveals robust MEF2 activity in the somites, a developmental structure that will eventually give rise to the body wall muscles of the organism (Figure 1.4). The discovery of MEF2 binding activity upstream of the expression of muscle-specific genes implicates the MEF2 family as central co-regulators of the skeletal and cardiac differentiation programs (Gossett *et al.* 1989, Pollock *et al.* 1991, Yu *et al.* 1992, Potthoff *et al.* 2007). MEF2 binding sites were discovered on promoters containing E-box binding sites, the consensus binding sequence of the myogenic bHLH factors (Wright *et al.* 1991, Black *et al.* 1998, Puri *et al.* 2000). The presence of both binding sites on muscle-specific promoters suggests coordinate regulation of muscle specific genes by the MEF2 family and the myogenic bHLH factors (Black *et al.* 1998, Puri *et al.* 2000). Additionally, protein-protein interactions between

the MEF2 factors and myogenic bHLH heterodimers are sufficient to induce synergistic transcriptional activation in the presence of only a single binding site (Black *et al.* 1998).

1.3.4 Regulation of MEF2 transcriptional activity

The transcriptional activity of the MEF2 transcription factors integrates signals from a variety of signaling cascades, including muscle-specific calcium signaling and more general receptor signal transduction pathways. Multiple calcium signaling pathways converge to regulate the post-translational activity of the MEF2 family (Black *et al.* 1998, Potthoff *et al.* 2007).

Class II HDACs repress MEF2 family members through interaction with a short amino acid sequence conserved among MEF2 factors (Han *et al.* 2005). Activation of the calcium modulated protein kinase (CaMK) signaling pathway precludes association of these HDACs with MEF2, allowing for subsequent MEF2 transcriptional activation (Lu *et al.* 2000, McKinsey *et al.* 2001).

Mitogen-activated protein kinases (MAPKs) are known activators of MEF2 transcriptional activity. Activation of p38 leads to phosphorylation of a conserved sequence in the C-terminal transcriptional activation domain of MEF2 leading to increased activity (McKinsey *et al.* 2002). In parallel, ERK5 is a known MEF2 co-activator and its activation leads to the formation of a complex with MEF2, leading to transcriptional activation (Lu *et al.* 2000).

In the years following the reported links between MEF2 and chromatin modifiers (Sartorelli *et al.* 1997, Miska *et al.* 1999, Sparrow *et al.* 1999), the MEF2-HDAC interaction has been the most extensively investigated pathway in pathophysiological

processes in the heart. It is now firmly established that dissociation of class II HDACs from MEF2 downstream of hypertrophic signaling is a key event in the stimulation of postnatal MEF2 transcriptional activity (Lu *et al.* 2000, Zhang *et al.* 2002, McKinsey *et al.* 2005), a process that ultimately contributes to the genomic reprogramming observed in cardiac pathology. Briefly, these pathological signals activate a number of protein kinases to promote sequestration of class II HDACs in the cytoplasm. Most, if not all, of these protein kinases such as calcium-calmodulin kinases and protein kinase D phosphorylate class II HDACs on specific amino acid residues which serve as docking sites for adaptor protein 14-3-3, resulting in their nuclear export and subsequent MEF2 activation (Backs *et al.* 2006, Parra *et al.* 2010). Additionally, the PKA signaling pathway including the A-kinase anchoring protein, AKAP, have been shown to modulate HDAC and MEF2 activity (Carnegie *et al.* 2008, Lehmann *et al.* 2014). Apart from the pathological findings, the MEF2-HDAC pathway has been implicated in cardiovascular development. Inhibition or activation of HDACs in P19 cells was shown to enhance and impair cardiomyocyte differentiation (Karamboulas *et al.* 2006).

1.3.5 Invertebrate loss of function models

1.3.5.1 *Drosophila*

This classic and powerful animal model has been extensively used to decipher the gene regulatory networks of cardiac development and function (Bryantsev *et al.* 2009, Vogler *et al.* 2015). *Drosophila* has an open circulatory system and hemolymph is pumped throughout the organism by the dorsal vessel, a linear heart-like tube. Despite its apparent simplicity, the dorsal vessel has a well-defined aorta and primary contractile

region, and the developing dorsal vessel consists of two cardiac cell types: cardioblasts and non-muscle pericardial cells. *Drosophila Mef2* (*D-Mef2*) is expressed in cardioblasts, the lineage that will give rise to the myocardial cells that perform the contractile activity of the dorsal vessel (Lilly *et al.* 1994).

Seminal studies in this invertebrate model system unambiguously demonstrated the importance of MEF2 for the differentiation of all muscle types: cardiac, somatic, and visceral. Null mutations of *Drosophila-Mef2* (*D-Mef2*) were generated by genetic deletion or chemical mutagenesis with similar phenotypic results (Bour *et al.* 1995, Lilly *et al.* 1995). Although the dorsal vessel formed in both mutant lines, *D-Mef2* mutant cardiomyocytes failed to express differentiation genes (Table 1.1) (Bour *et al.* 1995, Lilly *et al.* 1995). Recent studies have now implicated D-Mef2 in the regulation of cardiac cell fate, and it was shown to collaborate with the cardiac transcription factors Tinman (Nkx2.5) and Pannier (GATA4) to expand the cardiogenic pool of cells from mesoderm (Lovato *et al.* 2015). Additionally, *D-Mef2*-null flies have a severe body muscle phenotype in which muscle precursors are appropriately specified but fail to differentiate (Ticho *et al.* 1996, Durham *et al.* 2006).

1.3.5.2 *C. elegans*

Nematodes do not have a heart-like organ, but striated muscle cells in the pharynx exhibit cardiomyocyte-like contractile properties. Like flies, nematodes encode a single *Mef2* gene that is ubiquitously expressed (Dichoso *et al.* 2000). Interestingly, two different mutant alleles of *Mef2* were generated, but these mutations did not overtly impair embryonic development or muscle differentiation (Table 1.1) (Dichoso *et al.*

2000). Epistatic analysis was performed to determine the extent to which Mef2 could modulate known muscle phenotypes. Genetic crosses of *C. elegans-Mef2* (*CeMef2*) mutants to *MyoD*, *Twist*, or *pha-1* mutant worms, defective in mesoderm or muscle development failed to exacerbate those muscle defects (Dichoso *et al.* 2000). Despite the lack of obvious morphological defects a more detailed genomic and cellular analysis may be needed to address its specific requirement in muscle in this organism.

1.3.6 Zebrafish loss of function models

Zebrafish have a two chambered heart with a single atrium and ventricle (Moorman *et al.* 2003). The zebrafish genome encodes orthologs of the four mammalian *Mef2* genes, and their expression is largely restricted to muscle and the brain lineages (Ticho *et al.* 1996, Hinits *et al.* 2007, Lazic *et al.* 2011). Zebrafish also encode additional *mef2a* and *mef2c* paralogs, likely due to additional genome duplication events in this evolutionary branch. The paralogs *mef2ca* and *mef2cb* are most closely related to *Mef2c* whereas *mef2aa* and *mef2ab* are likely orthologs of *Mef2a* (Hinits *et al.* 2012). *In situ* expression analysis revealed that *mef2c* (*mef2ca*) transcripts are the earliest detectable *mef2* transcripts expressed in the cardiac primordia (16 h post fertilization [hpf]) whereas *mef2a* (*mef2aa*) transcripts are detected a few hours later (18 hpf) at the time of myocardial differentiation. *Mef2a* and *mef2c* expression is sustained through late development (48 hpf). Surprisingly, despite its abundant expression in skeletal muscle (Hinits *et al.* 2007), *mef2d* transcripts have not been detected at early cardiac developmental time points. Expression analysis of the apparent *Mef2b* homolog remains to be determined.

Several groups have analyzed the *in vivo* role of zebrafish *mef2* genes using morpholino oligonucleotides and/or mutant lines derived from large scale mutagenesis screens (Table 1.1). Mef2a morphants were generated by using two different morpholino oligonucleotides. These morphants display normal cardiac morphology but Mef2a-deficiency caused a significant reduction in cardiac contractility and disorganized sarcomere structure (Wang *et al.* 2005).

The zebrafish *mef2c* genes have also been extensively analyzed in cardiac development. Morpholino inhibition of the *mef2cb* paralog resulted in defects in the second (anterior) heart field as these morphants lacked a subset of cardiomyocytes in the arterial pole of the developing heart (Lazic *et al.* 2011). In a subsequent study, the role of both *mef2c* paralogs, *mef2ca* and *mef2cb*, were analyzed using gain-of-function and loss-of-function approaches. A genetic mutation in *mef2ca* (b1086) resulted in delayed cardiomyocyte differentiation marker expression, but ultimately the hearts developed normally (Hinits *et al.* 2012). By contrast, *mef2cb* morphants displayed shortened hearts characterized by reduced atrial and ventricular volume. However, a *mef2cb* mutant allele (fh288), which causes a premature stop in the MADS box DNA binding domain, displayed no overt cardiac phenotype. Combinatorial *mef2ca* and *mef2cb* deficiency, using various combinations of individual *mef2c* genomic mutant lines and morpholino approaches, resulted in pericardial edema, and impaired cardiomyocyte differentiation and heart tube formation in a substantial percentage of mutant embryos (Hinits *et al.* 2012). A broader ablation of all *mef2* isoforms using a single morpholino (*mef2d/c*) yielded a more severe cardiac phenotype (Hinits *et al.* 2012). These morphants lacked all

myosin heavy chain expression, and most cardiomyocytes failed to differentiate. As the vast majority of *mef2* mutant analyses in this animal model were performed with morpholino oligonucleotides, the distinct cardiac phenotypes associated with each isoform knockdown will need to be further clarified using mutagenized zebrafish lines harboring *bona fide* loss-of-function or null alleles of the *mef2* genes.

Conversely, to determine whether overexpression of Mef2c is sufficient to promote cardiomyocyte determination the Mef2cb isoform was injected at the 1–2 cell stage of zebrafish development. Curiously, Mef2cb caused ectopic skeletal, but not cardiac, muscle formation in the head region. When Mef2cb overexpression was restricted to lineages with endogenous Mef2cb expression, ectopic expression of cardiogenic markers was observed but no skeletal muscle cells were observed, suggesting that the skeletal myogenic effect of Mef2cb overexpression is restricted to cells that do not normally express Mef2cb (Hinits *et al.* 2012). These overexpression experiments suggest that we still fail to have a complete molecular understanding of the cardiac regulatory role of Mef2 in zebrafish.

1.3.7 Mammalian loss of function models

To determine the *in vivo* role of the mammalian MEF2 transcription factor family, knockout (KO) mice have been published for three of the four murine MEF2 genes by deleting the second coding exon (encoding the MADS box DNA binding and MEF2 domains). This deletion effectively abrogates DNA-binding ability and renders the mutant proteins nonfunctional. Additionally, a variety of other genetic MEF2

manipulations have been published, a compiled list of interesting manipulations and their gross morphological phenotypes is described in Table 1.2.

1.3.7.1 MEF2A

The global MEF2A loss of function model revealed an important role for this isoform in the postnatal heart. The majority of MEF2A-null mice exhibit sudden perinatal lethality and display an enlarged heart (Naya *et al.* 2002). Detailed analyses of cardiomyocytes from these mutants revealed severe myofibrillar defects likely resulting from the dysregulation of a MEF2A-dependent costamere gene program (Durham *et al.* 2006, Huang *et al.* 2006, Ewen *et al.* 2011). Neonatal cardiomyocytes depleted of MEF2A using RNA interference (RNAi) also display widespread apoptosis likely resulting from deficiencies in focal adhesion contacts (Ewen *et al.* 2011). To understand the transcriptional mechanisms involved in MEF2A-dependent regulation of costamere genes our group used bioinformatics to identify candidate cofactor binding sites in MEF2A-regulated costamere gene regulatory regions. One of these sites belonged to the EGR1 transcription factor, a factor known to play a regulatory role in cardiovascular pathology (Khachigian 2006). Functional characterization of this computational prediction revealed that EGR1 and MEF2A interact and represses MEF2-dependent reporters (Feng *et al.* 2015). Additionally, overexpression and depletion of *Egr1* in neonatal cardiomyocytes resulted in downregulated and upregulated costamere gene expression, respectively. Finally, while a small percentage of MEF2A KO mice are viable and survive to adulthood, their hearts display mitochondrial deficiency and conduction defects. The genetic basis of survival in a subset of MEF2A KO mice and

molecular mechanisms of the mitochondrial and conduction abnormalities remain to be determined (Naya *et al.* 2002).

Interestingly, while loss of MEF2A activity has a drastic phenotype in cardiac tissue, *Mef2A* KO mice do not appear to have a skeletal muscle phenotype. It is only upon skeletal muscle injury that an impaired regeneration phenotype emerges. Impaired skeletal muscle regeneration in MEF2A KO mice is due to dysregulation of Wnt signaling mediated by MEF2A activation of a microRNA program (Snyder *et al.* 2013)

1.3.7.2 MEF2B

While *Mef2b* transcripts are detected early in cardiac development, and ubiquitously expressed, the *Mef2b*-null mouse reveals very little about the role of *Mef2b*. The *Mef2b*-null mouse is viable and lacking any muscle phenotype. Further characterization is not reported (Black *et al.* 1998). Characterization of the *Mef2b*-null mouse model remains to be published.

1.3.7.3 MEF2C

Of the mammalian MEF2 genes, the MEF2C KO is the only one that results in embryonic lethality. MEF2C KO mice display defective cardiac looping morphogenesis and vascular malformations (Lin *et al.* 1997, Lin *et al.* 1998, Bi *et al.* 1999). However, cardiomyocyte-specific deletion of MEF2C at approximately E10.5 using αMHC-Cre transgenic mice results in viable embryos and normal cardiac development (Vong *et al.* 2005). These findings suggest that MEF2C is dispensable after early embryonic development or that its transcriptional function is compensated for by the remaining MEF2 factors. Given the similarities in their embryonic cardiac developmental defects, mice with a combinatorial deficiency of MEF2C and the cardiac transcription factor,

Nkx2.5, were generated. These double homozygous null embryos developed a heart with a single cardiac chamber expressing atrial and second heart field markers but lacking ventricular markers (Vincentz *et al.* 2008). These results indicate that MEF2C and Nkx2.5 function in the same genetic pathway for the specification and differentiation of ventricular myocytes. Recently, floxed MEF2C have been used to delete this mammalian isoform in the anterior second heart field. These mice display a wide range of outflow tract defects such as overriding aorta and double outlet right ventricle reinforcing the important role of this mammalian MEF2 isoform in embryonic cardiac morphogenesis (Barnes *et al.* 2016).

Targeted KO of *Mef2c* expression in skeletal muscle exhibits normal embryonic development, but leads to rapid perinatal loss of muscle tissue, associated with improper sarcomere organization (Potthoff *et al.* 2007), suggesting that MEF2C plays an integral role in the maintenance of skeletal muscle fibers after birth.

1.3.7.4 MEF2D

Global deletion of MEF2D was generated by crossing floxed MEF2D mice to *Meox*-Cre, which is active in the three germ layers. Loss-of-function of MEF2D resulted in viable mice with normal cardiac structure and function. However, when adult MEF2D KO mice were subjected to cardiac stressors these hearts display attenuated hypertrophy and fibrosis (Kim *et al.* 2008). Additionally, despite the apparent lack of a cardiac phenotype in MEF2D-deficient hearts in homeostasis, we have shown that acute depletion of MEF2D in neonatal cardiomyocytes *in vitro* results in cell cycle re-entry and programmed cell death (Estrella *et al.* 2015). Perhaps these differences relate to the

temporal requirement of MEF2D in postnatal cardiomyocytes or differences between *in vitro* and *in vivo* approaches in analyzing MEF2D deficiency.

The regulatory roles of alternatively spliced MEF2D isoforms have recently been investigated in muscle differentiation (Sebastian *et al.* 2013). Two alternatively spliced MEF2D isoforms, α1 and α2, are expressed in skeletal muscle but the MEF2D α2 isoform appears to be required for differentiation. This α2 isoform includes a coding exon that is resistant to inhibitory phosphorylation mediated by PKA (Du *et al.* 2008) thereby activating muscle transcription. Along these lines, a number of mammalian MEF2 splice isoforms have been previously described (Zhu *et al.* 2005). In particular, an exon (the β+ isoform) near the 3' end of *Mef2a*, *-c*, and *-d* resulted in more potent transactivation compared to MEF2 isoforms lacking this domain. Although the above experiments were performed in skeletal muscle, given the overlapping gene programs in striated muscle, it is tempting to speculate that alternatively spliced isoforms of MEF2 proteins display distinct regulatory properties in cardiomyocytes. Much remains to be determined regarding alternative splice isoforms within each of the MEF2 genes and their specific role in cardiac gene regulation.

Mef2d-null mice do not exhibit a morphological skeletal muscle phenotype (Kim *et al.* 2008). While binding activity is identical among the MEF2 family members, loss-of-function analysis reveals largely non-overlapping phenotypes associated with the loss of each individual MEF2 factor.

1.3.7.5 Additional studies relating aberrant MEF2 expression and activity

In addition to ablation of individual MEF2 isoform activity, a series of dominant negative approaches were used to determine the collective role of MEF2 in cardiomyocytes (Table 1.2). Interestingly, these manipulations yielded different outcomes. Inhibition of MEF2 activity in cardiomyocytes derived from P19 embryonic carcinoma cells resulted in impaired differentiation (Karamboulas *et al.* 2006). This study generated a dominant negative construct of MEF2 by fusing the DNA binding domain of MEF2C (aa1–105) with the potent repressor domain from the Engrailed transcription factor (EnR) and driven by the Nkx2.5 enhancer, which is active at the onset of cardiac development at E7.5. Transient overexpression of this dominant negative construct *in vivo* supports the cardiomyocyte differentiation defect, and yielded two distinct phenotypes classified by the severity of the impact on cardiac development (Karamboulas *et al.* 2006). The most severe transgenic embryos failed to form a heart, but myosin heavy chain (MHC) positive cardiomyocytes were detected, while less severe displayed thin walled myocardium. These results are consistent with an earlier study demonstrating the differentiation promoting effects of MEF2C when overexpressed in P19 embryonal carcinoma cells (Skerjanc *et al.* 1998).

In contrast to the severe cardiac defects in transient mouse embryos, stable transgenic mice expressing dominant-negative forms of MEF2C did not display cardiac developmental defects, but did present a postnatal phenotype. One study described attenuated postnatal growth of the myocardium overexpressing the DNA binding domain of MEF2C (amino acids 1–95) driven by the αMHC promoter (Kolodziejczyk *et al.* 1999). In another independent study, stable transgenic mice harboring a different

dominant negative MEF2 (MEF2C aa 1–117; DNA binding defective R24L mutant) had no measurable phenotypic effects on heart size or function (van Oort *et al.* 2006). However, there were key differences in the approaches that could account for the distinct phenotypes. The truncated MEF2C and MEF2C-EnR constructs are capable of DNA binding whereas the R24L mutant cannot bind to DNA. Moreover, MEF2C R24L transgene was induced using a "floxed ON" approach by crossing to αMHC-Cre transgenic mice. Despite its effectiveness in inducing loxP recombination, transgene levels in the heart may not have been expressed at sufficiently high levels to induce a phenotype.

Conversely, individual mammalian MEF2 proteins have also been overexpressed in neonatal cardiomyocytes and the heart. *In vitro* overexpression of MEF2A, -C, and –D yielded similar morphological phenotypes in neonatal cardiomyocytes, including sarcomere disorganization and focal elongation (Xu *et al.* 2006). Individual overexpression of these MEF2 proteins in the mouse heart using the cardiomyocyte-specific αMHC promoter, which is active in development but massively upregulated postnatally, also resulted in comparable phenotypes. MEF2A and MEF2C overexpression induced dilated cardiomyopathy (Durham *et al.* 2006, van Oort *et al.* 2006, Xu *et al.* 2006), whereas MEF2D overexpression resulted in atrial enlargement and extensive fibrosis (Kim *et al.* 2008). While these results suggest functionally redundant roles of MEF2 family members in postnatal cardiomyocytes it should be noted that the proteins were expressed at supra-physiological levels potentially overcoming isoform-specific

gene regulatory effects. A summary of MEF2 mutant phenotypes in mammalian models systems are listed in Table 1.2.

1.4 Functional genomic analysis of MEF2 in striated muscle

While there is no doubt that MEF2 is an essential transcription factor in the regulation of the muscle cytoarchitectural gene program in virtually all animal model systems (Black *et al.* 1998, Potthoff *et al.* 2007, Estrella *et al.* 2014), a much broader gene regulatory function for MEF2 has recently been uncovered through comprehensive genome-wide studies. Initial studies were carried out primarily in *Drosophila* somatic muscle and the murine C2C12 skeletal myoblast cell line. Findings in these model systems expanded the traditional view of MEF2 from that of an exclusive transcriptional regulator of structural genes to one harboring broader regulatory function through its regulation of varied gene programs in muscle. More recently, next generation genomic technologies have been applied to investigate the role of MEF2 in global gene regulation, i.e., genome-wide binding and target gene expression, in cardiomyocytes. Given the limitation of isoform-specific reagents for mammalian MEF2 proteins, the majority of the genomic studies performed in vertebrate model systems have focused primarily on a single MEF2 isoform or generalized its genome-wide role based on a representative member of the family.

The first *in vivo*, global analysis of MEF2 genome binding was performed in *Drosophila* (Sandmann *et al.* 2006). This study performed chromatin immunoprecipitation followed by genomic DNA microarray (ChIP-on chip) at multiple time points in muscle development. These experiments revealed hundreds of genomic

regions bound by MEF2 at all stages of muscle development and not restricted to terminal differentiation. A number of these bound regions were found to function as enhancers *in vivo* and to drive MEF2-dependent reporter expression in somatic muscle. MEF2 bound to genomic regions predicted to regulate a variety of pathways including myoblast fusion, extracellular matrix-muscle attachment, and somatic and cardiac muscle identity genes such as those belonging to the Notch-Delta signaling pathway, in addition to the previously characterized structural genes. Several MEF2 bound enhancers in the aforementioned study were previously identified in *Drosophila* by combining computational prediction of muscle enhancer elements with ChIP using a MEF2 antibody (Junion *et al.* 2005), lending support to the efficacy of these global analyses.

In vertebrates, genome-wide analyses on muscle regulatory factors including MEF2 were first performed in C2C12 skeletal myoblasts (Paris *et al.* 2004, Blais *et al.* 2005). Consistent with the findings in *Drosophila*, these ChIP-on-chip studies revealed that MEF2 binding was not limited to structural genes but included genes belonging to signal transduction cascades, transcription factors, muscle differentiation, and the neuromuscular junction. It is worth noting that while both groups used the same MEF2 antibody one was reported to be MEF2A-specific and the other MEF2C. Nevertheless, both studies arrive at the conclusion that the MEF2 transcription factor family regulates an array of cellular processes in muscle. Additionally, the distinct functions of MEF2D isoforms were examined in C2C12 myoblasts by subjecting MEF2D isoform specific antibodies to ChIP followed by high-throughput sequencing (ChIP-seq) (Sebastian *et al.* 2013). Despite the different activities of each MEF2D alternatively spliced isoform in

myogenic differentiation, this study revealed similar binding site preferences and extensive overlap of target genes bound by MEF2D isoforms suggesting additional regulatory mechanisms beyond DNA binding. Finally, our group performed a global analysis of the target genes regulated by the four mammalian MEF2 factors in C2C12 myoblasts (Estrella *et al.* 2015). In stark contrast to the longstanding notion of functional redundancy in the family, we discovered that only a small percentage of genes were co-regulated by all four isoforms. Moreover, transcription factor binding site enrichment analysis of the promoters of these genes revealed that individual MEF2-regulated gene sets harbor a distinct cohort of co-regulators.

To investigate genome-wide binding of the mammalian core cardiac transcription factors in cardiomyocytes, an integrative systems level analysis was performed in HL-1 cells, a cardiac atrial cell line. Using a variety of genome scale technologies such as ChIP-on-chip and RNAi, common and unique target genes regulated by GATA4, MEF2A, Nkx2.5, and SRF were determined (Schlesinger *et al.* 2011). This global analysis revealed that different cohorts of target genes in the cardiomyocyte genome were regulated by distinct combination of cardiac transcription factors. For example, MEF2A and Nkx2.5 were found to co-regulate genes belonging to muscle cell differentiation and heart looping pathways. A similar study used HL-1 cells to identify genomic binding of core cardiac transcription factors by inducible overexpression of biotinylation peptide-tagged versions of these regulatory factors, allowing biotinylation by BirA, followed by streptavidin pulldown and ChIP-seq (He *et al.* 2011). These findings revealed co-occupancy of cardiac enhancers with various combinations of GATA4, MEF2A, TBX5,

SRF, and Nkx2.5. Additionally, a number of cardiac enhancers associated with heart development and function were found to be co-regulated by GATA4 and MEF2A. Given the important and common role of GATA and MEF2 transcription factor families in cardiac development and disease, further genomic dissection of this coregulatory pathway is warranted. Finally, genome-wide analysis of Tbx20 bound regions in the heart of transgenic mice overexpressing epitope-tagged Tbx20 revealed a significant enrichment of MEF2 binding sites in these enhancers (Shen *et al.* 2011). Gene ontology analysis of these regions revealed genes associated with ion transport, calcium signaling, and contraction, cellular processes previously attributed to the MEF2 family.

Recently, ChIP-exo, a modification of ChIP-seq that improves sequencing resolution by digesting unbound DNA regions using exonuclease, was used to identify and compare the genome-wide, direct target genes of MEF2A in neonatal cardiomyocytes and C2C12 myoblasts (Wales *et al.* 2014). While there was modest overlap in target genes, the MEF2A bound regions in cardiomyocytes had an overrepresentation of AP-1, CREB, BACH, and ERE transcription factor binding sites. Furthermore, gene ontology analysis revealed that the most significantly enriched genes bound by MEF2A in neonatal cardiomyocytes are involved in actin organization. These results are consistent with the role of MEF2A the regulation of the costamere/focal adhesion complexes which are intimately associated with the actin cytoskeleton (Ewen *et al.* 2011, Estrella *et al.* 2014).

Finally, a mathematical modeling approach was used to identify putative cardiac enhancers in the human genome. A combination of Gibbs sampling and linear regression was utilized to identify significantly enriched transcription factor binding sites from a

large data set of previously validated enhancers active in cardiac development and differentiation (Narlikar *et al.* 2010). Among the known and *de novo* transcription factor binding motifs, MEF2 and SRF binding sites obtained the maximum positive weight scores. In a complementary set of computational experiments, co-occurring binding motifs, including MEF2, and other sequence features were used to predict thousands of putative cardiac enhancers in noncoding regions of the human genome. This study supports extensive experimental data that MEF2 is a major player in cardiac gene regulatory networks.

1.5 Hedgehog and Notch signaling in the heart

1.5.1 Hedgehog signaling

Hedgehog (HH) signaling is a critical pathway in a wide array of mammalian tissues including skeletal and cardiac muscle (Lee *et al.* 2016). Initiation of HH signaling is mediated by the processing and secretion of one of three mammalian hedgehog ligands: Sonic hedgehog (SHH), Indian hedgehog (IHH), or Desert hedgehog (DHH). Secreted HH ligands interact with the Patched-1 (PTCH1) transmembrane receptor to induce HH signal transduction in the target cell (Figure 1.5).

In the absence of HH ligand, PTCH1 prevents HH signaling through an uncharacterized mechanism that prevents Smoothened (SMO), a critical HH signaling activator, from being integrated into the cell membrane (Figure 1.5, right). In the absence of SMO activity, HH downstream effectors Glioma-associated oncogene 2 and 3 (GLI2 and -3, respectively) are bound by a repressive protein complex. Persistence in this complex leads to proteosomal degradation of the GLI factors. GLI2 is a positive

transcriptional regulator, and targeting for proteosomal degradation leads to complete destruction of the protein. On the other hand, GLI3 is a transcriptional repressor, and upon targeting for proteosomal degradation, yields a truncated GLI3 protein which is capable of entering the nucleus and repressing expression of HH-dependent genes (Lee *et al.* 2016, Pak *et al.* 2016)

Upon HH ligand binding to PTCH1, SMO repression is relieved and GLI2 and -3 escape cytoplasmic sequestration and enter the nucleus (Figure 1.5, left). GLI2 acts as a transcriptional activator and induces the expression of a number of downstream effectors including GLI1, a GLI-family homolog that acts as an additional transcriptional activator. Full-length GLI3 retains its repressive characteristics and acts as a brake and negative feedback loop to maintain signal integrity (Lee *et al.* 2016, Pak *et al.* 2016).

1.5.2 Role of HH signaling in cardiac development

HH signaling appears to play a key role in cardiac specification and development. Several of loss-of-function mice have been created to assess the roles of the various members of the HH signaling cascade in cardiac development. *Shh*-null and *Gli2*-null/*Gli3*-heterozygous mice both show cardiac looping defects (Motoyama *et al.* 1998, Tsukui *et al.* 1999). Additionally, *Smo* knockout models were embryonic lethal with severe cardiac abnormalities (Zhang *et al.* 2001) and a constricted expression pattern of the early cardiac marker, *Nkx2.5*. Conversely, *Ptch1*-null mice exhibited an expanded field of *Nkx2.5* positive cardiac precursors during embryonic development (Zhang *et al.* 2001).

Additionally, work performed in zebrafish and mouse has shown that activation of HH-signaling in cardiac precursor cells is required for cardiac specification and reduction in SHH expression led to fewer cardiomyocytes. Ectopic SHH expression was sufficient to increase cardiomyocyte number in the developing zebrafish heart. This study also shows that SHH ligand binding by cardiac progenitors and HH signaling is required in a cell autonomous manner, suggesting that activation of HH signaling is required in the cells that will give rise to the cardiomyocyte population in the developing heart (Thomas *et al.* 2008).

In vitro investigation of HH signaling has supported its role in cardiac specification and development. Most notably, overexpression of SHH in P19 embyronal carcinoma cells is sufficient to induce commitment to a cardiac lineage with concordant expression of myosin heavy chain 7 (MYH7) and cardiac α-actin (ACTC1), and morphological changes that closely recapitulate that of a cardiomyocyte. Additionally, SHH overexpression was sufficient to induce expression of core cardiac transcriptional regulators: *Mef2c*, *Nkx2.5*, and *Gata4* (Gianakopoulos *et al.* 2005).

Previous *in vitro* analysis implicated HH signaling as a potential regulator of core cardiac transcription factors, including MEF2 (Gianakopoulos *et al.* 2005). Further analysis revealed that GLI2 and MEF2C appear to be capable of regulating the other's expression in P19 embryonal carcinoma cells, and mouse embryonic stem cells. Additionally, protein interaction assays have revealed a direct complex of GLI2 and MEF2C in P19 cells that was capable of synergistic activation of a luciferase reporter *in vitro* (Voronova *et al.* 2012).

1.5.3 Notch signaling

Notch signaling is mediated by four mammalian Notch receptors that are composed of a heterodimeric combination of an extracellular ligand binding domain with a transmembrane and intracellular transcriptional activation domain. Interaction of the extracellular receptor with transmembrane ligands of the Delta-like and Jagged family induces cleavage of the intracellular domain from the transmembrane region by prenisilin-γ-secretase. The released Notch intracellular domain (NICD) translocates into the nucleus where it interacts with the RBP-Jκ transcriptional activation complex to induce transcription of Notch target genes, including *Hey* and *Hes* families (Figure 1.6) (Ntziachristos *et al.* 2014).

1.5.4 Notch signaling in cardiac development

The role of Notch signaling in cardiac development has been well studied. Notch signaling components are expressed in all three tissue layers of the developing heart (D'Amato *et al.* 2016), and are key mediators of tissue cross-talk within the developing heart. Additionally, appropriate Notch signaling activation is required for appropriate specification of cardiac sub-structures including valve and trabeculation formation (D'Amato *et al.* 2016). *In vitro* studies support the importance of Notch signaling in cardiac development. RBP-Jκ-mediated NICD transcriptional activation is sufficient to induce cell-cycle reentry in quiescent neonatal ventricular cardiomyocytes via modulation of Cyclin D1 expression and nuclear localization (Campa *et al.* 2008). Additionally, ectopic activation of Notch signaling reveals G_2/M checkpoint activation that prevents older cardiomyocytes from proceeding into mitosis downstream of Notch

activation, shedding potential light on the mechanism mediating the loss of regenerative capacity of the adult heart. G_2/M checkpoint override with caffeine led to mitotic catastrophe and apoptosis in Notch-induced cardiomyocyte cell cycle re-entry, suggesting DNA replication defects associated with G_0 exit (Campa *et al.* 2008).

Unfortunately, the regulatory interactions between Notch signaling and the MEF2 family have not been characterized in cardiac development. Interestingly, the *Hes* and *Hey* families of transcriptional repressors are both direct targets of Notch signaling and play a role in the repression of cardiac differentiation (Campa *et al.* 2008), though this has yet to be analyzed with respect MEF2 transcriptional activity. On the other hand, the Notch and MEF2 interactions in skeletal muscle have been the subject of quite a bit of analysis. NICD has been shown to directly interact and inhibit the function of MEF2C, but not MEF2A, -B, or –D in skeletal myocytes (Wilson-Rawlins *et al.* 1999). The direct interaction of NICD inhibits the DNA-binding ability of MEF2C and appears to be associated with a divergent region of the MEF2C protein that isn't conserved in other MEF2 isoforms (Wilson-Rawlins *et al.* 1999).

Additionally, in the absence of Notch signaling, the Notch co-activator MAML1 exists in a complex with MEF2C and cooperates in the activation of MEF2C target gene expression (Shen *et al.* 2006). As is the case with NICD interaction, MAML1 interaction appears to be isolated to MEF2C and may occur through the same uncharacterized interaction domain that is missing in other MEF2 isoforms (Shen *et al.* 2006). Upon Notch activation, MAML1 is sequestered by the N1ICD/RBP-Jκ transcriptional complex and MEF2C mediated gene expression is further inhibited.

1.6 Statement of thesis rationale

The MEF2 family represents a core striated muscle transcription factor at the center of muscle differentiation and homeostasis. The purpose of this study is to provide an unbiased characterization of the complex interplay among the MEF2 family members in the context of global striated muscle gene regulation. While previous *in vitro* characterization fails to yield meaningful differences between the transcriptional activities of the MEF2 factors, *in vivo* loss-of-function analyses suggest distinct roles for each MEF2 factor in skeletal and cardiac muscle differentiation and homeostasis.

The primary goal of this study is to investigate the MEF2 family in much higher resolution than previously performed, and in so doing provide new understanding of the complex regulatory patterns that are required for a complex functional tissue to develop from precursor to terminally differentiated mature tissue. Additionally, further insight into the transcriptional regulation of muscle cellular processes by the MEF2 family will afford the field a new angle with which to understand striated muscle disease.

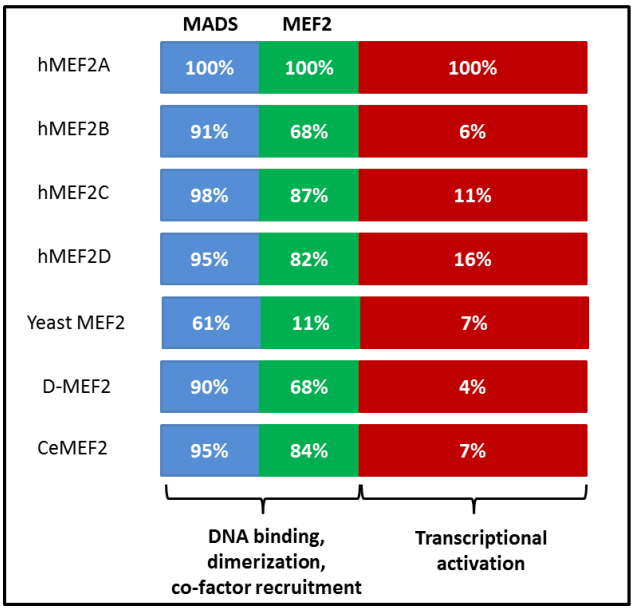

Figure 1.1 Comparison of MEF2 protein conservation. The mammalian family of MEF2 proteins shares high sequence similarity (~95%) in the N-terminal region containing the MADS box and MEF2 domains responsible for DNA-binding, dimerization, and co-factor recruitment. The amino acid sequences diverge considerably in the C-terminal transcriptional activation region. Additionally, yeast, *Drosophila* and *C. elegans* MEF2 homologs share considerable N-terminal conservation with the human MEF2 proteins. Adapted from (Potthoff *et al.* 2007).

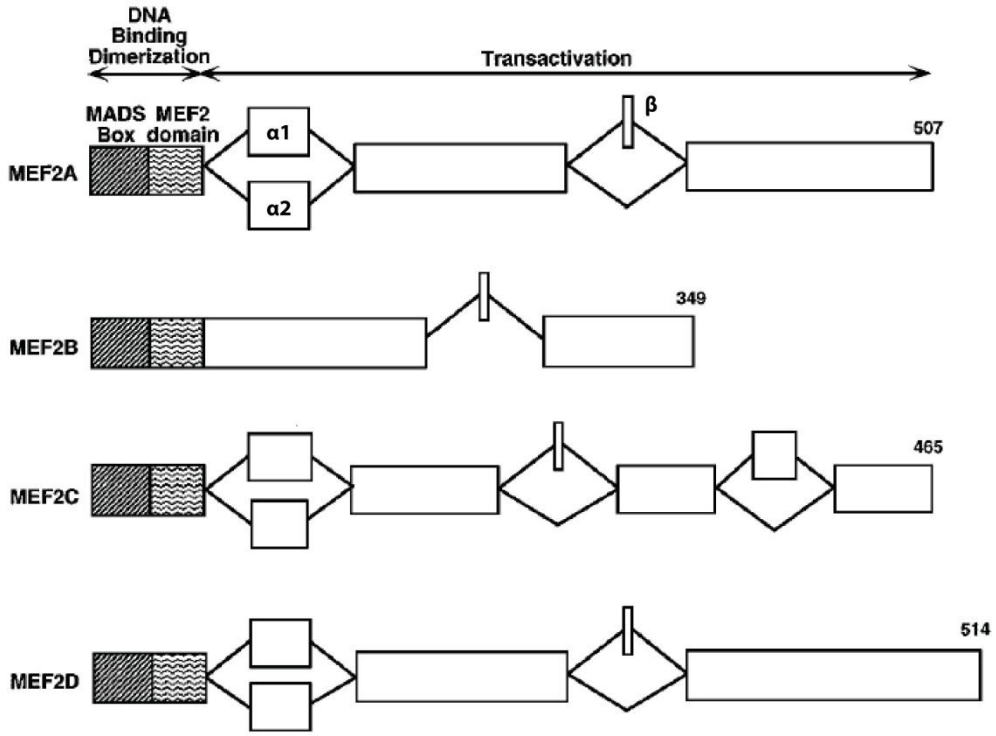

Figure 1.2 *Mef2* transcripts undergo multiple alternative splicing events. *Mef2a*, *-c*, and *–d* transcripts can undergo alternative splicing of an exon, denoted α, directly downstream of the MEF2 domain. Inclusion of the α_2 exon is associated with transcriptional activity in MEF2 target tissues. Additionally, all four *Mef2* transcripts undergo an alternative splicing event in a conserved C-terminal exon, denoted β, and inclusion of the β exon is associated with positive transcriptional activity (Zhu *et al.* 2005).

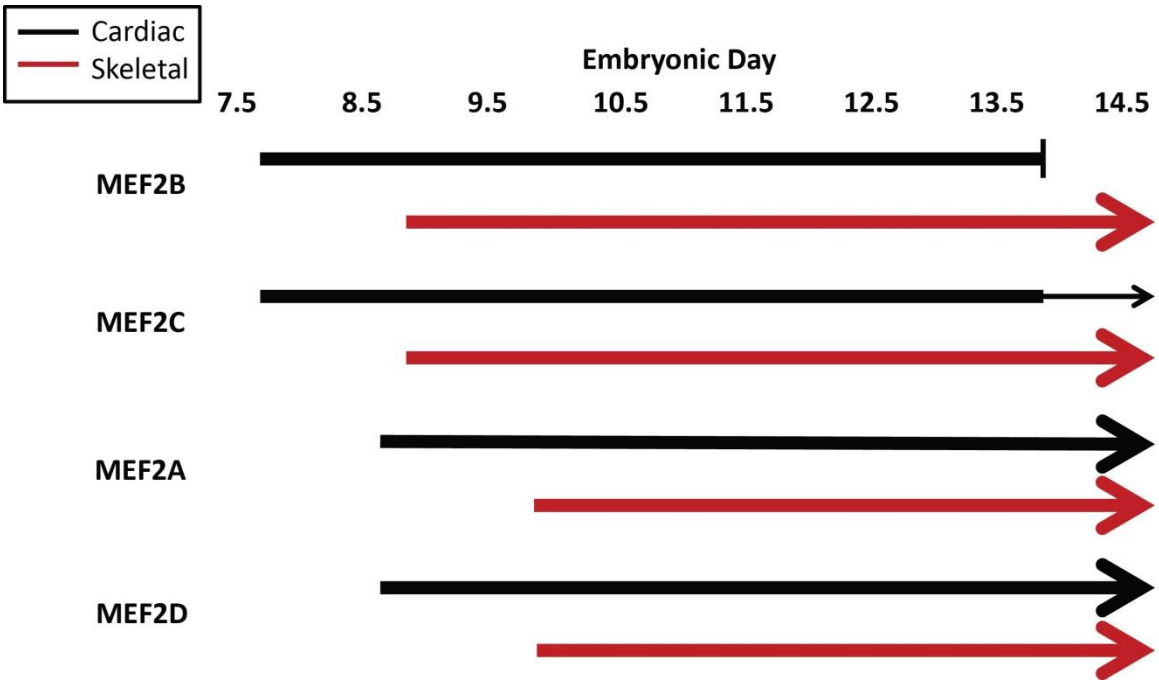

Figure 1.3 MEF2 factors display complex temporal expression in striated muscle. In mouse embryonic cardiac development, *Mef2b* and *–c* transcripts are observed first at embryonic day 7.5-8 (E7.5-8). *Mef2a* and *–d* transcripts appear about a day later at E9.0. Expression of the four *Mef2* transcripts persists until *Mef2b* transcripts drop to undetectable levels at approximately E14.0 and *Mef2c* levels drop concurrently. The expression pattern in mouse skeletal muscle is similar with the exception that all four *Mef2* isoform transcripts persist throughout development and into adulthood. Adapted from (Edmonson *et al.* 1994).

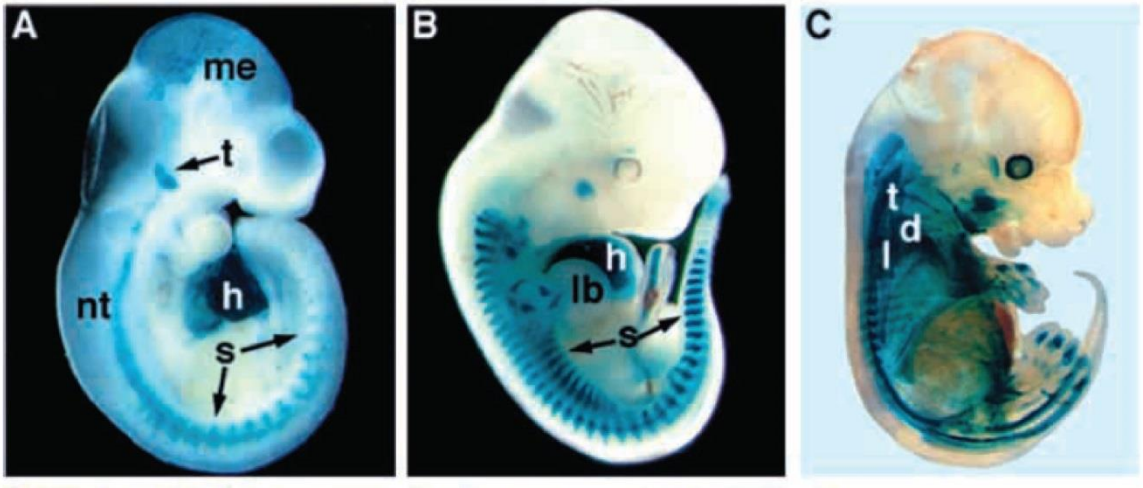

Figure 1.4 Expression of a 3x-*Des-MEF2-lacZ* reporter construct in the embryonic development of transgenic mice. Whole mount mouse embryos with X-gal staining at different embryonic time points. **A**, Mouse E9.5 embryos show early robust staining of MEF2 transcriptional activity in the heart (h), somites (s), neural tube (nt), mesencephalon (me), and trigeminal ganglia (t). **B**, Mouse E11.5 embryo shows persistent MEF2 activity in somites (s) and heart (h), and emergence of MEF2 activity in the developing limb buds (lb). **C**, Mouse E14.5 embryo shows MEF2 activity is expanded and persistent all the developing musculature of the embryo including the trapezius (t), lattisimus dorsi (l) and deltoid (d) muscles (Naya *et al.* 1999).

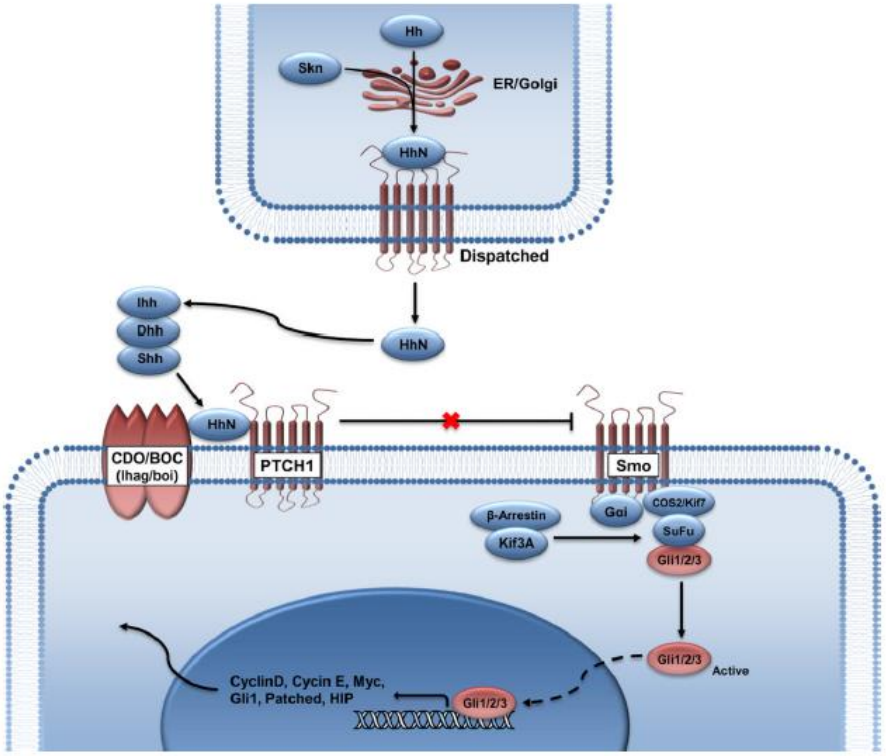

Figure 1.5 Hedgehog signaling pathway. Hedgehog (HH) signaling is a critical pathway in a wide array of mammalian tissues including skeletal and cardiac muscle Initiation of HH signaling is mediated by the processing and secretion of one of three mammalian hedgehog ligands: Sonic hedgehog (Shh), Indian hedgehog (Ihh), or Desert hedgehog (Dhh). Secreted HH ligands interact with the Patched-1 (PTCH1) transmembrane receptor to induce HH signal transduction in the target cell (Yu *et al.* 2012).

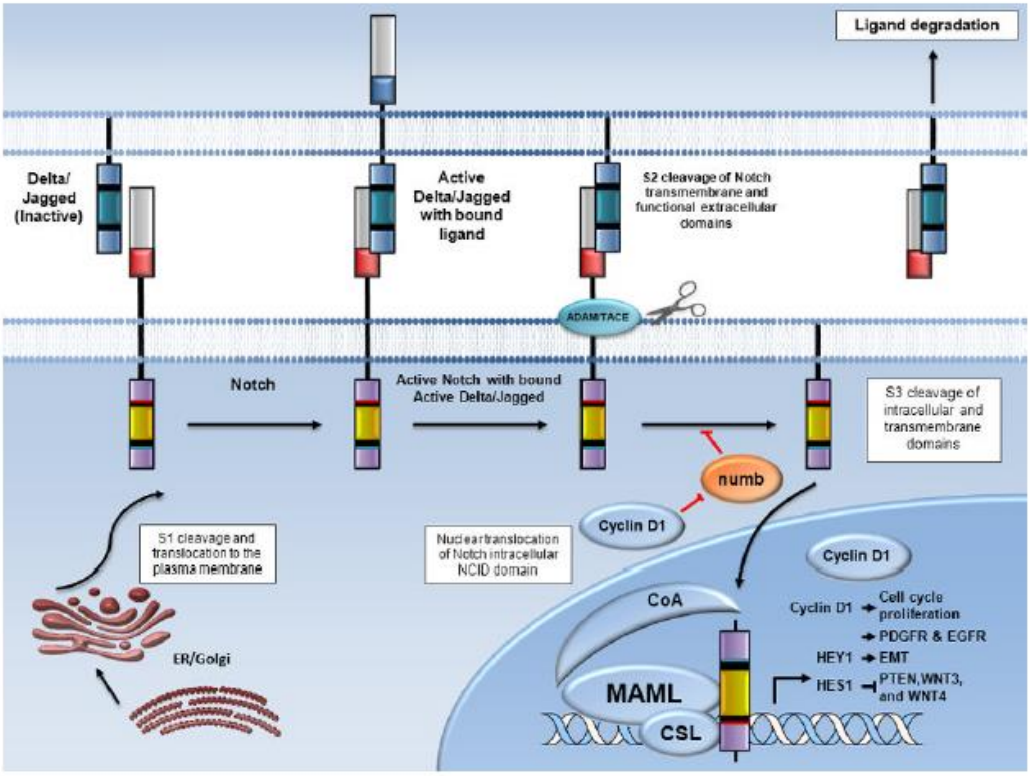

Figure 1.6 Notch signaling pathway. Notch signaling is mediated by four mammalian Notch receptors. Interaction of the extracellular receptor with ligands of the Delta-like and Jagged family induces cleavage of the intracellular domain. The released Notch intracellular domain (NICD) translocates into the nucleus where it interacts with the RBP-Jκ transcriptional activation complex to induce transcription of Notch target genes, including *Hey* and *Hes* families (Yu *et al.* 2012).

Model	MEF2 Isoform	Manipulation	Phenotype	Ref
Drosophila	**DMef2**	Global Loss-of-function (LoF)	Cardioblasts are specified, failure to differentiate	Lilly *et al.* 1994, 1995
C. elegans	**CeMef2**	Deletion	No observed phenotype	Lovato *et al.* 2015
D. rerio	***mef2aa***	Morpholino knockdown	Normal cardiac morphology Significant decrease in cardiac contractility	Lazic *et al.* 2011
		Morpholino knockdown (Bmp2)	Significant loss of Mef2a expression Decrease in cardiac contractility rescued by Mef2a overexpression	Hinits *et al.* 2007
	mef2ca	Morpholino knockdown	Delayed cardiomyocyte marker expression Cardiac development delayed, normal heart	Hinits *et al.* 2007
		Global LoF	Delayed cardiomyocyte marker expression Cardiac development delayed, normal heart	Hinits *et al.* 2007
	mef2cb	Morpholino knockdown	Secondary heart field defects Loss of cardiomyocytes in arterial poles Chamber shortening	Lazic *et al.* 2011
		Global LoF	No observed phenotype	Ticho *et al.* 1996
	mef2ca/cb	Global LoF	Pericardial edema Impaired cardiomyocyte differentation Impaired heart tube formation	Ticho *et al.* 1996
	All mef2	Morpholino knockdown	Loss of cardiomyocyte differentiation Lack of α-MHC expression	Ticho *et al.* 1996

Table 1.1 Compilation of MEF2 LoF phenotypes in invertebrates and Zebrafish.

Summary of cardiac-related phenotypes of MEF2 family transcription factor family misexpression in model systems with one, two, and three-chambered hearts. Global DMef2 LoF mutants yielded specified cardioblasts that failed to differentiate and mature into the dorsal vessel. Loss of CeMef2 expression had no observable phenotype. Loss of mef2 expression in *D. rerio* shows complicated transcriptional activity regulated by the mef2 family that appears to be focused around the mef2a and mef2c subfamilies. Adapted from (Desjardins *et al.* 2016).

Model	MEF2 Isoform	Manipulation	Phenotype	Ref
M. musculus	***Mef2A***	Global Loss-of-function (LoF)	80% **Perinatal lethality** Severe myofibrillary defects Dysregulated costamere gene expression	Naya *et al.* 2002, Ewen et al. 2011
			20% **Survival to adulthood** Mitochondrial deficiency Conduction abnormalities	Naya *et al.* 2002, Ewen et al. 2011
		Global overexpression	Dilated cardiomyopathy	Durham *et al.* 2006, van Oort *et al.* 2006, Xu *et al.* 2006
	Mef2C	Global LoF	Embryonic lethality Defective cardiac looping morphogenesis Vascular malformations	Lin *et al.* 1997, Lin *et al.* 1998, Bi *et al.* 1999
		CM-specific LoF @~E10.5	Viable embryo Normal cardiac development	Vong *et al.* 2005
		Double LoF (Mef2C/Nkx2.5)	Development of a single chamber heart Expression of atrial and secondary heart field markers	Vincentz *et al.* 2008
		SHF LoF	Outflow tract defects Overriding aorta and double outlet right ventricle	Barnes *et al.* 2016
		Cardiac overexpression	Dilated cardiomyopathy	Xu *et al.* 2006
	Mef2D	Global LoF	Viable, normal cardiac structure and function Attenuated hypertrophy and fibrosis in response to stress	Kim *et al.* 2008
		Global Mef2D overexpression	Atrial enlargement Extensive fibrosis	Kim *et al.* 2008
	All Mef2	Dominant Negative	***In vitro***: impaired cardiomycyte differentiation ***In vivo***: failure to form a heart (severe) thin-walled myocardium (mild)	Karamboulas *et al.* 2006
		Transgenic Dominant Negative	No observable phenotype	Kolodziejczyk *et al.* 1999, van Oort et al. 2006

Table 1.2 Compilation of MEF2 modulations in mouse models. Summary of cardiac-related phenotypes of MEF2 family transcription factor family modulations in mouse model systems (four chambered hearts). LoF phenotypes in mice are dependent on the MEF2 isoform being manipulated. Loss of MEF2A activity led to perinatal lethality with cardiac abnormalities, loss of MEF2C was embryonic lethal prior to E10.5 and appeared to be dispensable in the heart after E10.5. Loss of MEF2D activity had no overt cardiac phenotype but showed a blunted remodeling response to cardiac stress. Adapted from (Desjardins *et al.* 2016).

CHAPTER TWO: Materials and Methods

2.1 Recombinant DNA techniques

2.1.1 Transformation of DH5α *E.coli*

DH5α *E. coli* cells were made chemically competent for transformation with recombinant DNA as follows. *E. coli* were plated on Luria Broth (LB) Agar and inbuated overnight at 37°C. A single colony was isolated and used to inoculate 3 mL of LB and incubated overnight at 37°C in a shaking incubator. The 3 mL culture was then used to inoculate 200 mL of pre-warmed LB and allowed to grow at 37°C while shaking until early log phase. The culture was then centrifuged at 4000 rpm (Beckman centrifuge, JA-14 rotor) for 5 min at 4°C and the pellet was resuspended in 20 mL of chilled 10mM NaCl. Chilled $CaCl_2$ was added to a final volume of 100 mL and cells were centrifuged at 4000 rpm for 5 min at 4°C. The pellet was resuspended in 80 mL chilled 100 mM $CaCl_2$ and incubated on ice for 1 hr. Cell were centrifuged at 4000 rpm for 5 min at 4°C and resuspended in 20 mL of $CaCl_2$/glycerol solution (17 mL of chilled 100mM $CaCl_2$ + 3 mL glycerol). Cells were aliquoted (100µL) into 1.7 mL microcentrifuge tubes, and snap-frozen in liquid nitrogen. Long term storage was at -80°C.

2.1.2 Preparation of DNA

2.1.2.1 MiniPrep

For preliminary recombinant DNA analysis, 1.5 mL of a 3 mL transformed *E. coli* culture was transferred to a 1.7 mL microcentrifuge tube and centrifuged for 30 sec at 13500 rpm (Eppendof 5417C). Supernatant was discarded and pellet was resuspended in 100 µL of resuspension buffer (50 mM glucose, 10 mM EDTA pH 8, 25 mM Tris pH 8)

by vortexing. Bacterial cells were lysed by adding 200 µL of lysis solution (200 mM NaOH, 1% SDS) and mixed by inversion 10 times. Lysis reactions were incubated at room temperature for 4 min. Bacterial lysis was stopped with the addition of 150 µL of neutralization buffer (3M potassium acetate, 11.5% acetic acid) and mixed by inversion 10 times. Plasmid DNA was purified using phenol:chloroform extraction (see below) and pellets were allowed to air dry for 10 min before resuspension in 20 µL of de-ionized water (dH_2O) containing 40 µg/µL RNAse and incubated at room temperature for 30 min.

2.1.2.2 MidiPrep

For medium scale DNA preparations for cloning/recombinant DNA transfection use, NucleoBond® PC (ClonTech) columns were used with preparations made according to manufacturer's protocols.

2.1.2.3 Phenol/Chloroform extraction

An equal volume of 1:1 phenol/chloroform solution was added to nucleic acid sample to be purified. Samples were then vortexed and centrifuged for 1 min at 13500 rpm (Eppendorf 5417C). The aqueous upper phase containing plasmid DNA was transferred to a new 1.7 mL microcentrifuge tube and 2.5 volumes of ice cold 100% ethanol (~1 mL), $1/10^{th}$ volume 3M sodium acetate (pH 5.2), and 1 µL glycogen was added. Solution was mixed by inversion and incubated at -20°C for 30 min to precipitate the DNA. Solution was centrifuged at 13500 rpm for three min and DNA pellets were washed twice with 70% ethanol, with centrifugation at 13500 rpm for three min between

each wash. Supernatant was discarded and DNA pellets were dried for 10 min in inverted tubes.

2.1.3 Cloning

2.1.3.1 Preparation of DNA fragment

For routine cloning and sub-cloning a desired DNA fragment was produced via Polymerase Chain Reaction (PCR) amplification and electrophoresed on a 0.8% agarose gel containing ethidium bromide. DNA was visualized using UV light and fragment of interest was excised and gel extracted using the QIAquick gel extraction kit (QIAGEN) according to the manufacturer's protocol and resuspended in 30 µL of elution buffer provided with purification kit.

2.1.3.2 Restriction digest

Destination plasmid and DNA fragment were then digested with restriction endonucleases (New England Biolabs) to expose complimentary overhangs. Generally 1-5 µg of plasmid or up to 30 µL of insert were digested for 4 hr at 37°C. After digestion, the destination plasmid and DNA fragment were electrophoresed on a 0.8% agarose gel containing ethidium bromide. Bands were visualized and excised for gel extraction and phenol/chloroform extracted as described above. Purified digested destination vector and DNA fragment were ligated in a 20 µL consisting of a 1:5 vector to insert ratio, 1 µL T4 DNA ligase buffer, and 1 µL T4 DNA ligase and brought to final volume with dH_2O. Ligations were incubated at 16°C for 4 hr and maintained at 4°C overnight in a thermocycler.

2.1.3.3 PCR for cloning

The Expand Long Template PCR System (Roche) was used for cloning. Generally, 1 µg DNA was used in a 25 µL reaction containing 2.5 µL 10x PCR Buffer #2, 2 µL 2.5 mM dNTP mixture, 1 µL 25 µM primer mix, 0.5 µL Taq polymerase, and sterile dH_2O to a final volume of 25 µL. PCR reaction was performed in a thermocycler using a program determined by the size of the fragment and the characteristics of the primers. Generally, the cycle is designed with an initial incubation at 94°C for 4 min, followed by 94°C for 30 sec, 57-62°C (based on the melting temperature of the primer set) for 30 sec, and 68°C for 30 sec (time varies based on desired fragment size). Steps 2 through 4 are repeated 29 times, and the program ends with the final extension incubation at 68°C for 5 min. PCR reactions are then stored at -20°C.

2.1.4 Adenoviral amplification and purification

2.1.4.1 Generation of crude lysate

Adenoviral expression plasmids were digested with PacI overnight and phenol/chloroform extracted. Linearized plasmid was transfected into HEK293A seeded at a density of 5×10^5 cells/well in a 6-well dish. The next day the media was exchanged for fresh media and the following day cells were transferred to a 10 cm tissue culture plate containing 10 mL of media. Culture medium was changed every 2-3 days until cytopathic effect (CPE) was observed (usually 7-10 days post-transfection). Cells were allowed to develop approximately 80% CPE then were harvested into 15 mL conical tubes for preparation of crude lysate.

Crude lysate was created by incubating crude adenoviral cell solution at -80°C for 30 min, and then thawed at 37°C in a water bath for 15 min. This freeze/thaw cycle was repeated twice, and then the cell lysate was centrifuged at 3000 rpm for 15 min at room temperature. The resulting supernatant was aliquoted (1 mL) and stored at -80°C.

2.1.4.2 Adenoviral purification

Prior to transduction, HEK293A cells were plated and allowed to grow until approximately 80% confluent (about 3 x 10^6 cells per 10 cm dish). Upon reaching target confluency cells were transduced with either crude viral lysate (50-100 µL) or previously purified virus (0.1-0.2 µL) and incubated until CPE is visible. Cells were then harvested and stored in 50 mL conical tubes at -80°C until purification.

If frozen, cell suspensions are thawed at 37°C, and then pooled. Triton X-100 (or another non-ionic detergent) was added to a final concentration of 0.5% and cell suspension was incubated at room temperature on an orbital shaker for 10 min to induce lysis. Lysate was then centrifuged for 15 min at 20000xg (Beckman centrifuge, JA-14 rotor). Supernatant was transferred to a new flask and 0.5 volumes of precipitation solution (20% PEG8000, 2.5M NaCl) were added to supernatant. Precipitation was allowed to proceed overnight at 4°C on an orbital shaker.

The resulting precipitated virus was centrifuged for 15 min at 20000xg (Beckman centrifuge, JA-14 rotor) and supernatant was discarded. Resulting viral precipitate adhered to the walls of centrifuge bottle was resuspended in 1x phosphate-buffered saline (PBS) to a final volume of 4.5 mL. Resulting viral suspension was modified to a final density of 1.34 g/mL using cesium chloride salt and a final volume of approximately

5mL. The suspension was then loaded into an ultracentrifuge tube and centrifuged using the NVT-90 rotor at 70,000 rpms for at least 16 hr to create a cesium chloride density gradient. The densest viral band was extracted from the ultracentrifuge tube using a 21 gauge needle and transferred to a 1.7 mL microcentrifuge tube and kept on ice.

Purified virus was then desalted with two dialysis steps of no less than 250 mL of dialysis solution (10 mM Tris-HCl pH 8 autoclaved, 1 mM $MgCl_2$, and 10% glycerol) for at least 2 hr each on a stir plate at 4°C. Dialyzed virus was then removed from dialysis membrane and stored in 100 µL aliquots in cryovials at -80°C until titering.

2.1.4.3 Titering and storage of adenovirus

Viral titering is determined using the End-Point Dilution Assay. Briefly, one day prior to titer transduction HEK293A cells are seeded on a 96-well plate at a density of 10000 cells/well in 100 µL of media using a multi-channel pipettor. On the day of transduction, serial dilutions between 10^{-5} and 10^{-12}, one per row from A-H on the 96-well plate, were created using purified adenovirus and serum-free Dulbecco's Modified Eagle Medium (DMEM). The virus-containing media (100 µL) was added to columns 1-10 of rows A-H, and columns 11 and 12 were used as negative controls and 100 µL of serum-free media was added to each well in these columns. Plates were incubated in 37°C incubator for 10 days, and then each well was scored for CPE. The fraction of CPE-positive wells for each dilution was added together and this sum was used to calculate titer based on the Spearman-Karber method, where the viral titer equals $10^{X + 0.8}$ pfu/mL.

Once thawed, the 100 µL aliquots of purified virus were further aliquoted into 10 µL aliquots and each smaller aliquot was thawed only twice to ensure minimal loss of efficacy due to repeated freeze-thaw cycling.

2.2 Cell/Tissue culture

2.2.1 Maintenance of mammalian cell lines

Cos1, C2C12, HEK293A, and HEK293T cells were grown in DMEM containing 10% fetal bovine serum (FBS), 1% penicillin/streptomycin, and 1% L-glutamine and maintained in a humidified incubator at 37°C with 5% CO_2. Cells were passaged at approximately 75% confluency. First, growth media was aspirated and cells were washed once with 1x PBS, the 1x PBS was aspirated, and 0.25% Trypsin-EDTA was added to the cells and allowed to incubate at room temperature for 4 min. Media was added to plates and cells were detached and cell suspensions were plated at between 1:5 and 1:20.

2.2.2 Isolation of neonatal rat ventricular myocytes (NRVMs)

2.2.2.1 Ethics statement

Experimental procedures on animals used in this study were reviewed and approved by the Institutional Animal Care and Use Committee (IACUC) of Boston University (Protocol # 16-019). These studies were conducted in accordance with the principles of animal care and experimentation in the Guide For the Care and Use of Laboratory Animals.

2.2.2.2 Isolation

NRVMs were extracted from ten approximately two day old Sprague Dawley neonatal rats (Charles River Labs, Strain Code 400). Rats were sacrificed by decapitation

and hearts were exposed by incision down the sternum, and excised using forceps. Hearts were immediately placed in ice-cold Hank's Buffered Saline Solution (HBSS) until entire litter was dissected. After all hearts were collected, hearts were moved to a sterile tissue culture hood where the HBSS was aspirated and the hearts were deposited in a 60 mm dish containing 5 mL of fresh HBSS. Hearts were cleaned of blood, and atria and vessels were removed using fine scissors. The remaining ventricular region was transferred to a new 60 mm dish with 5 mL of HBSS. Ventricles were then cut into 3 or 4 fragments using single clean cuts to minimize tissue shearing. Once all the ventricles are processed, a 5 mL serological pipette was broken near its tip and the heart fragments were extracted from the HBSS and dispensed into a new 60 mm dish with 5 mL of HBSS with minimal transfer of old HBSS to the new 60 mm dish. This process is repeated twice more to wash the ventricles, then the ventricles are deposited in a glass bottle with 25 mL HBSS containing 0.6 mg/mL trypsin and incubated overnight at 4°C.

After overnight incubation in trypsin, ventricle fragments were treated with 10 mL of pre-warmed growth media, and incubated shaking at 37°C for 3 min to inactivate trypsin. Supernatant was aspirated and 10 mL of pre-warmed 10mg/mL collagenase II (Worthington Biochemical) in HBSS was added to isolate cardiomyocytes. Ventricle fragments were incubated in a shaking incubator for 6 min at 37°C at 125 rpm. The supernatant from this incubation was collected in a 50 mL conical vial and stored on ice until entire protocol is complete. This process is repeated seven more times for a total of eight collagenase digestion. The two 50 mL conical tubes containing the NRVM suspension were centrifuged at 1000 rpm for 4 min and the supernatant was carefully

aspirated making sure no to disturb the fragile cell pellet. Cell pellets were resuspended in 20 mL of pre-warmed growth media and centrifuged at 1000 rpm for 4 min. The supernatant was again removed and the cell pellets were resuspended in 10 mL of growth media for a total of 20 mL of NRVM suspension. This cell suspension was pre-plated onto a 10 cm dish for 1 h at 37°C to remove fibroblasts. Pre-plating was repeated once more with an incubation of 45 min – 1 hr to further enrich the NRVM population.

The cell suspension was then transferred to a new 50 mL conical tube and cell density was determined by making a 1:10 dilution of NRVM cell suspension and counting using a hemocytometer. Cells were plated in growth media at a density of 4 x 10^6 cell/ 10 cm dish on gelatinized plates (0.1% gelatin). After 24 hr in recovery, growth media was removed, NRVMs were washed with 1x sterile PBS and DMEM containing 0.1% Nutridoma-SP (Roche) was added to the dishes.

2.2.3 Polyethylamine (PEI) transfection

Transfections with PEI (Polysciences, Inc.) were performed at a 6:1 ratio of PEI to DNA. Transfections for reporter assays were performed on COS1 or HEK293T cells seed onto 6-well plates at a density of 75,000 to 100,000 cells/well. PEI was mixed with serum-free DMEM and incubated at room temperature for five min. This mixture was then added to DNA and incubated at room temperature for 15 min. The resulting complexes were added to the cells and cells were incubated for 48 hr prior to harvesting.

2.2.4 siRNA transfections

Rat siRNAs were acquired from Invitrogen. Transfections using an siRNA component were performed using a 1:3 ratio of Lipofectamine® RNAiMAX Reagent. For

a 6 well format, 90 pmol/well of siRNA was diluted into 150 µL/well of Opti-MEM® Medium (Gibco), and 9 µL/well of RNAiMAX reagent was diluted into 150 µL/well of Opti-MEM Medium. These two dilutions were then pooled and incubated for 5 min at room temperature, and 250 µL of the resulting mixture was added to each well.

2.2.5 Adenoviral transductions

Adenoviral shRNA constructs targeting *Mef2a, -b, -c, and -d* were transduced at an MOI of 25 and 50, for C2C12 myoblasts and NRVMs respectively. MEF2A, -C, and -D overexpression constructs were transduced at an MOI of 50 in C2C12 myoblasts and an MOI of 15 for NRVMs, with the exception of the MEF2A overexpression construct which was used at an MOI of 2.5. β-gal, MEF2A, -C, -D, and -VP16 overexpression constructs were generously provided by Jeff Molkentin (Children's Hospital, Cincinnati) and Ken Walsh (Boston University Medical School). The SHH-N overexpression vector was generously provided by Ronald G. Crystal (Cornell Medical Center) and used at an MOI of 25. N1ICD overexpression virus was generously provided by Igor Prudovsky (Maine Medical Center Research Institute) and was used at an MOI of 2.5. Transduced C2C12 cells were harvested for RNA 96 hr after transduction (3 days after induction of differentiation). NRVMs were harvested for RNA 48 hr after transduction, and viability assays were performed 72 h after transduction.

2.2.6 CellTiter-Blue® cell viability assay

NRVMs were cultured in 24-well plates at a cell density of $8x10^4$ cells/well and transduced with adenovirus 24 hr after seeding. NRVMs were cultured for 48 hr, then 20 µL of CellTiter Blue® reagent (Promega) was added to each well. Plates were incubated

for 16 h in a humidified 37°C incubator, and then 200 µL of media was extracted from each well and transferred to a 96-well dish. Fluorescence was measured at 560/590 nm using a Victor 3 plate reader (Perkin Elmer). Data were normalized to untreated control wells lacking NRVMs, and experiments were performed in biological triplicate.

2.2.7 Propidium iodide DNA quantification

DNA content was measured using propidium iodide staining and flow cytometry. NRVMs were plated at a cell density of $1x10^6$ cells/well onto 6-well plates. NRVMs were transduced and allowed to culture for 72 hr. Cultures were then scraped into their existing media to retain any cells that had already detached from the plates, and centrifuged at 1000 xg for 5 min at 4°C. Cell pellets were re-suspended in 3.33x PBS and ice cold 100% ethanol was added to suspension to a final volume of 1x PBS. Cells were stored for up to 2 weeks at 4°C.

On the day of flow cytometry analysis, permeabilized NRVMs were centrifuged at 1000 xg for 5 min at 4°C and washed once with 1x PBS. The NRVM cell pellet was then re-suspended in a freshly prepared propidium iodide staining solution (50 µg/mL propidium iodide + 2x PBS + 10 µg/mL RNase A) for 30 min at room temperature in the dark. Cells were then analyzed using a FASCalibur flow cytometer (488nm excitation/ 585 emission).

2.3 RNA Analysis techniques

2.3.1 Isolation of total RNA

Total RNA was isolated from samples using TRIzol® reagent (Invitrogen) according to the manufacturer's specifications. Briefly, cells were washed once with 1x

PBS, and an appropriate volume of TRIzol reagent was added directly to the well. Cells were scraped into the TRIzol, transferred to a 1.7 mL microcentrifuge tube and stored on ice until all well were collected. Cells were then incubated at room temperature for 5 min. RNA was isolated using chloroform phase separation per manufacturer's protocol, and RNA was washed once with 70% ethanol and allowed to dry inverted for 10 min. RNA was then re-suspended via pipetting into 30 µL of sterile dH_2O. RNA integrity was evaluated through gel electrophoresis with ethidium bromide and visualized using UV light. RNA concentrations were determined by measuring optical density of a 2 µL sample with a NanoDrop 1000 spectrophotometer (Thermo Scientific). Samples were kept on ice and stored at -80°C.

2.3.2 Transcriptional expression microarray

RNA quality for microarray analysis was evaluated using a Bioanalyzer® 2100 (Agilient). C2C12 cells were harvested 72 hr after induction of differentiation, and total RNA from *shLacZ*, *shMef2a*, *shMef2b*, *shMef2c*, and *shMef2d*-treated C2C12 cells (n=6, pooled to yield n=3 biological replicates, 15 arrays total, GEO accession number GSE63798) was harvested. Biological replicates were hybridized to the Mouse GeneChip® Gene 1.0 ST Array (Affymetrix). NRVMs were harvested 48 hr after transduction and total RNA from *shLacZ*, *shMef2a*, *shMef2c*, and *shMef2d*-treated NRVMs was hybridized to the Rat Gene 2.0 ST array (n=3 biological replicates, 12 total arrays, GEO accession number GSE92861). Array hybridization and analysis was performed by the Microarray Core at Boston University Medical Center. The technical quality of the microarrays was determined using relative log expression and normalized

unscaled standard error. Relative log expression and normalized unscaled standard error values greater than 0.1 and 1.05, respectively, are considered out of normal limits. All arrays had median values within the normal limits of these test. Microarray data was normalized using the Robust Multiarray average algorithm and were Log_2 transformed.

2.3.3. Quantitative real-time PCR (qRT-PCR)

2.3.3.1 cDNA synthesis

Total RNA extracted from cell culture was used to synthesize cDNA using reverse transcriptase (M-MLV) with random hexamers (Promega). qRT-PCR was performed in biological and technical triplicate using Power SYBR® Green Master Mix (Applied Biosystems) with the 7900HT Sequence Detection System (Applied Biosystems). List of qRT-PCR primers can be found in Tables 2.1-2.3. Data were analyzed using SDS 2.2.4 software (Ambion) and C_T values were compared between gene specific primers and reference gene controls. The C_T value for each transcript were averaged and subtracted from the average internal control (*Gapdh*) C_T value to determine the transcript Δ C_T of the control sample set. Fold changes between samples were calculated using the formula $F.C.=2^{-\Delta\Delta CT}$. Differences in relative gene expression were analyzed for significance using a Student's T-test, and a p-value of less than 0.05 was considered statistically significant.

2.3.3.3 Measuring intra-sample relative transcript expression

To assess the relative expression levels of different transcripts within the same sample, we first verified the efficacy of the primer pairs. This was done by performing a quantitative RT-PCR analysis on a series of serial two-fold dilutions of cDNA (at least 6

dilutions) synthesized from total NRVM RNA. Primers were considered 100% efficient if the slope of the C_T value vs. $\log_2$ scale of the dilutions yielded a slope of $|1|\pm0.1$. Primers that were 100% efficient can be compared to express the relative differences in transcript expression within a sample.

2.3.3.4 Primer design

qRT-PCR primers were designed using either Primer3 (Untergasser *et al.* 2012) or Primer-Blast (NCBI) with a product size between 50 and 200 bp with a primer crossing an exon-exon junction to ensure omission of genomic DNA contaminants. Additionally, primers were required to have at least 2 mismatches to unintended targets, a GC% between 40 and 60%, and self-complementarity and 3' self-complementarity score as low as possible, but not above 4. Unless specified, default parameters were used.

2.4 Protein techniques

2.4.1 Protein isolation

Plated cells were washed with 1x PBS and scraped into fresh 1x PBS. Cell suspension was centrifuged at 13,000 rpm for 10 min at 4°C. Supernatant was discarded and cells were Dounce homogenized in ELB (50 µM HEPES, 250 mM NaCl, 5 mM EDTA, 0.1% NP-40, 1 mM PMSF, 1 mM DTT, and 1x complete protease inhibitor [Roche Diagnostic]). Homogenized samples were placed on ice for 10 min, then centrifuged at 13,500 rpm for 10 min. Pellet was discarded and remaining supernatant was stored at -80°C.

2.4.2 Quantification of protein concentration using the Bradford assay

Protein concentration was determined using the Bradford assay. A standard curve of bovine serum albumin (BSA) was created between 1 mg/mL and 0.2 mg/mL. 10 µL of each standard and all proteins samples to be measured was transferred to a 96-well plate and 200 µL of 1x Bio-Rad Bradford Protein Assay Dye (Bio-Rad Laboratories) was added to each well. Samples were allowed to incubate for 5 min at room temperature, then absorbance was measured at 595nm and the standard curve was used to determine the concentration of unknown protein lysate.

2.4.3 Western blotting

2.4.3.1 Protocol

Between 10 and 20 µg of proteins was mixed with SDS loading buffer and electrophoresed on a polyacrylamide gel composed of a lower separating gel (10% acrylamide, 375 nM Tris-HCl pH 8.8, 0.1% SDS) and an upper stacking gel (5% acrylamide, 125 mM Tris-HCl pH 6.8, 0.1% SDS). Protein samples were electrophoresed at 190 volts in 1x SDS running buffer (25 mM Tris-HCl, 190 mM glycine, 0.1% SDS) for approximately 45 min. After electrophoresis, stacking gel was excised and discarded. The separating gel was equilibrated for 10 min in 1x transfer buffer (20mM Tris-HCl, 150mM glycine, 20% methanol). Proteins were transferred to an Immuno-blot PVDF membrane (Bio-Rad Laboratories) by electroblotting overnight at the lowest setting (~20-50 mA). After transfer, the protein blot was blocked in the appropriate blocking buffer (5% nonfat dry Carnation milk in 1x TBS, or 5% BSA in 1x TBS/0.1% Tween-20) for 1h at room temperature or overnight at 4°C. Membranes were then incubated for 1 hr with

appropriate primary antibody in fresh blocking solution. The membrane was washed three times for 5 min in 1x TBS/0.1% Tween-20 then incubated with the appropriate secondary antibody conjugated to HRP in 1x TBS/0.1% Tween-20 for 30 min at room temperature. The membrane was then washed again three times for 5 min in 1x TBS/0.1% Tween-20 and treated with Western Lighting Chemiluminescent Reagent (Perkin-Elmer) for 1 min. Protein was visualized through exposure to X-ray film for between 5 min and 30 sec.

2.4.3.2 Antibodies used

Antibodies used for Western blotting included: anti-GAPDH (1:1000, Santa Cruz), anti-MEF2 (1:1000, Santa Cruz), anti-MEF2C (1:1000, Sparrow Biosciences), anti-MEF2D (1:1000, BD Biosciences), anti-FLAG (1:10,000, Sigma Aldrich). Blots were incubated with HRP-conjugated secondary antibodies (1:10,000, Sigma Aldrich).

2.4.4 Co-immunoprecipitation

Transfected cells were harvested 36-48 hr post-transfection in modified AT buffer (20% glycerol, 1% Triton X-100, 20 mM HEPES pH 7.9, 1 mM EDTA, 150 mM NaCl, 1 mM DTT, 1 µg/mL PMSF, and 1:25 complete protease inhibitor [Roche]). Approximately 35 µL of Protein G sepharose beads (GE Healthcare) and 1 µg of anti-Myc antibody was added and incubated with AT buffer precursors (modified AT buffer excluding DTT, PMSF, and protease inhibitor). The beads, protein, and antibodies were incubated rotating at 4°C overnight. The next day, samples were boiled and loaded onto an 8% acrylamide gel. Normal Western blot procedures (as described above) were performed.

2.4.5 Cleaved caspase 3 activity assay

NRVMs were seeded at a cell density of 1 x 10^6 cells/well and total protein lysate was collected as described above. Protein lysates were then treated with a fluorogenic caspase-3 substrate, Ac-DEVD-7-amido-4-methylcoumarin (BD Biosciences) to a final concentration of 50 µM. Lysates were then incubated at 37°C for 1 hr. Fluorescence was measured at 440/460 nm using a Victor3 plate reader (Perkin Elmer). Data were normalized to total protein concentration of the lysate as determined by Bradford assay.

2.4.6 Luciferase activity assay

Cells were harvested for luciferase assays 48 h after transfection. Cells were washed once with 1x PBS, then lysed in 1x Passive Lysis Buffer (Promega) by shaking for 15 min at room temperature. Lysates were mixed by pipetting and transferred to a 1.7 mL microcentrifuge tube. Firefly luciferase activity was measured by transferring 10 µL of protein lysate to a new 1.7 mL microcentrifuge tube and mixed with 50 µL luciferase activity reagent (Promega). Samples were mixed by pipetting and readings were measured on a luminometer. Luciferase readings were normalized to β-gal activity to control for transfection efficiency.

2.4.7 β-galactosidase activity assay

Cells were harvested for luciferase activity as described above. β-galactosidase activity assay was performed using the J.H. Miller method, by incubating whole cell protein lysate with a reaction mixture of 15 µL Z Buffer (60 mM $Na_2HPO_4.7H_2O$, 40 mM $NaH_2PO_4.H_2O$, 10 mM KCl, 1 mM $MgSO_4$, 50 mM β-mercaptoethanol) + 16.5 µL ONPG (8 mg/mL), and brought to a final concentration of 150 uL with dH_2O. Samples

were incubated in a 37°C water bath until yellow color is noticeable. The reaction was then quenched by adding 250 µL Na_2CO_3. Absorbance was measured at 415 nm and values were used to normalize luciferase readings.

2.4.8 Immunocytochemistry

NRVMs were cultured on acid-etched coverslips and transduced with the appropriate shRNA adenoviruses for 48 h. Cells were then washed with 1x PBS and fixed in freshly prepared 4% paraformaldehyde. Cells were then blocked with Mouse on Mouse Blocking solution (Vector Labs) for one hr at room temperature. Cells were incubated with primary antibody diluted in antibody dilution buffer (1x PBS, 1% BSA, 0.3% Triton X-100) overnight at 4°C. The following day, cells were washed three times for 5 min with 1x PBS. Cells were then incubated with fluorochrome-conjugated secondary antibody diluted in antibody dilution buffer for two hr at room temperature in the dark. Cells were washed three times for 5 min in 1x PBS and mounted on slides with VECTASHIELD Mounting Medium with DAPI (Vector Labs). Slides were sealed with a thin layer of nail polish and stored at 4°C in the dark. Slides were imaged with an Olumpus DSU scanning confocal microscope. α-actinin antibody was used as primary antibody (1:500, Sigma), secondary antibody was Alexa fluor 568 donkey anti-mouse H+L (1:500, Invitrogen).

2.5 Computational and bioinformatics analysis

2.5.1 Construction of differentially expressed gene sets

Significant dysregulation of gene expression was determined using a one-way analysis of variance and the Benjamini-Hochberg false discovery rate correction was then

applied to obtain corrected *q*-values, and a *q* threshold of less than 0.05 was used to determine significant dysregulation. Tukey's honest significant difference *post hoc* test was used to identify significantly dysregulated genes and correct for multiple testing errors across all intergroup comparisons. A corrected *q* value of less than 0.05 was used to determine statistically significant gene dysregulation among treatment groups.

2.5.2 Functional genomic analysis

Statistically distinct gene sets sensitive to individual MEF2 isoforms were analyzed using three independent analysis algorithms. Gene Ontology term analysis (Ashburner *et al.* 2000) and Kyoto Encyclopedia of Genes and Genomes (KEGG) (Kanehisa *et al.* 2017) were performed using the DAVID bioinformatics database with default parameters and entries were considered statistically significant if the p-value was less than 0.05. Ingenuity Pathway Analysis (Qiagen Bioinformatics) was used to determine the canonical cellular pathways associated with each gene set. Parameters for the IPA analysis were Reference Set: Ingenuity Knowledge Base (Genes Only); Relationship to include: Direct and indirect; pathways considered statistically significant if p-value was less than 0.05.

2.5.3 Regulatory region sequence determination

2.5.4 Consensus binding site variance

MEF2-binding site comparisons were performed by identifying putative MEF2-binding sites in the proximal promoter regions (5 kb upstream of putative transcriptional start site) of gene sets preferentially-sensitive to each MEF2 isoform using the FIMO tool from the MEME suite (Grant *et al.* 2011). Identification was performed by scoring 10 bp

motifs against the MEF2 motif stored in the JASPAR database (MA0052.1) using a *p*-value threshold of less than 0.0001. The output position-weight matrices were then used to compile a sequence logo using the WebLogo (Doerks *et al.* 2002) applet.

2.5.5 Candidate Co-regulatory Proteins

Transcription factor-binding motif enrichment analysis was performed on the proximal promoter region of genes preferentially sensitive to each MEF2 isoform using MatInspector from the Genomatix software suite (Quandt *et al.* 1995). A default background composed of a cross-section of genomic promoter sequences was used to discriminate between enriched features and non-specific promoter regions. The resulting transcription factor motifs were then sorted by Z-score, and motifs with a Z score greater than 2.0 were considered significantly enriched (Ho Sui *et al.* 2005). Additional data for each enriched motif was extracted from the Genomatix Matbase and NCBI databases. Paired enriched motif analysis was performed for proximal promoter regions of antagonistically regulated genes. The analysis is similar to described above but restrains the search for motifs to within 50bp of a putative MEF2 binding site to enrich for potential direct interaction partners.

Gene	Forward	Reverse
Cdkn1c	5’ CCAATGCGAACGACTTCTTCGC	5’ AACTAACTCATCTCAGACGTTTGCGC
Sept4	5’ TACACTCATGGTGGCAGGAGAATCTG	5’ CACTCTGTGTTGTTGACTGCATCC
Hspb7	5’ GCTGAGAAGCTGGCAGCTGATG	5’ ATCTCAGTCCGGAAGGTCTGCTG
Myom1	5’ CTACTCTGGACGGCAAGTGCAC	5’ GTGGTCCGTTTGGAGGTTGC
Stc2	5’ CTGCAGAACACAGCGGAGATCC	5’ CTGGGCATCGAATTTTCCAGCGT
Tex16	5’ CTTCTTGCCCTTTCAAGGTGT	5’ TACCTGTTTGGAGTCTGAGCTGAA
Selp	5’ TACACAGCCTCCTGCCAGGA	5’ CTGAAGGTGCACTGTGAGTTGAAGG
C1ql1	5’ GGTCACCAACCTAGGCAACAACTAC	5’ CTCCATCCAGCTTGATGAAGACCTC
Bace2	5’ ACTCAGAGAGCTCCAGCACATACC	5’ GCCAAAGCAGCATAAGCAAGTCC
Pi16	5’ CTGCAGATGAGGTGGGATG	5’ GCCGTGCTGAAATTGTAATACTC
Themis	5’ CTACGGACGACCTTTTTGAAAT	5’ CTAAGATCCTCGAAGCCTGGTA
Glipr1	5’ ACTCAGGTTGTTTGGGCAGACAG	5’ TGCAGAGACTGTTGAGACACTTGTCA
Cpa4	5’ GTACACGCAAAGCCAGAACC	5’ CCATGGTACACTTCAGAGCAAG
Fam78a	5’ AGCAGGGCATGTCTAGCTGG	5’ CACGTGGTGAAGCTCTGGTC
Ppp1r3	5’ GCTAGACTTGATGATAAACCAACGG	5’ CCCATGAACAAGTCAGTGTTGA

Table 2.1 List of mouse quantitative RT-PCR Primers used in Chapter Three.

Gene	Forward	Reverse
Gapdh	5'-TGGCAAGTGGAGATTGTTGCC	5'-AAGATGGTGATGGGCTTCCCG
Mef2a	5'-GAACTCAGTGTGCTCTGTGACTGTGAG	5'-GCCAGTGCTTGGTGGTCTCT
Mef2b	5'-GAAAGAAAGCCGCTCTGCACAG	5'-ACCTTCTGGCCCCTCCTCCATA
Mef2c	5'-CAGGGACGAGAGAGAGAAGAAAC	5'-CAATCTTTGCCTGCTGATCATTAG
Mef2d	5'-CTTTCCTCTCTGGCACTAAGGAC	5'-CCAGTCTATAACTCTGCATCATC
Dnm3	5'-TAACCACATCCGTGAGCGAG	5'-GCGGAAGATTGGTTCCCTGA
Ccl5	5'-GCTTTGCCTACCTCTCCCTC	5'-TCCTTCGAGTGACAAAGACGA
Filip1	5'-GCAGGAGCGAGAGAGGTTGA	5'-CATCAGGGCGAAGGACTTGA
Lrrc39	5'-CACGGAGAACAGAAGACCAAG	5'-CATGATGTCTTCCACAAGCAAA
Cirbp	5'-AGACTACTATGCCAGCCGGA	5'GGACGCAGAGGGCTTTTACT
Adamtsl2	5'-CTCACAAGGCAAGGACCAGAC	5'-CCACTTCAACGCCATCGTAG
Cdh8	5'-GGAGCCCGACCTGAGAAAT	5'-TCTAAGCAGCTTTTCCAAGACCA
Mdga2	5'-CTCATCGTGCAGTATCCCCC	5'-ACGCCATTCGTAAGTCAGCA
Kit	5'TTTAAAGGTAACAGCAAAGAGCAA	5'-GTGACCACGAAGCCAATGAG
Sept4	5'-GGACTGAAGCTGGGGATGAC	5'-CCGATCCCGGTACAAGTCAG
Upk1b	5'-CAGCCAGTCCAGTGGGAAAT	5'-GGCGATCCCACACATACCAA
Pten	5'-ACTGCAGAGTTGCACAGTATCCTT	5'-GCCTCTGACTGGGAATAGTTACTCC
Mcm3	5'-AACCCGTTCCAAGGATGTCTTTGAG	5'-GGTTTCCTGTCTGTGGTGACG
Mcm5	5'-GGACATGATGCTGGCCAAACATGT	5'-GGCTGCAGTTTCATCTTGCTGAGG
Mcm6	5'-GACTTCCTGGAAGAGTTCCAGGG	5'-CGATCCTGGAGGAAGTGAGCTC
Pcna	5'-CGTGAACCTCACCAGCATGTCC	5'-CCAAGTTGCTCAACGTCTAAGTCCA
Ccne1	5'-CCAGGATAGCAGTCAGCCTTGG	5'-TGCTCTCATCCTCGCCTGC
Ccne2	5'-AATTGTTGGCCACCTGTACTGTCTG	5'-ACTTCACAGACCTCTAAAAGCCAGTCT
E2f3	5'-AGGAGCGAGAGATGAGAAAGG	5'-GTGGTGAGGATCTGGATGTACG
Myh7	5'-GGAAGAACCTACTGCGACTGCAGGACC	5'-TGTTTCAAAGGCTCCAGGTCTCAGGGC
Myl2	5'-GAAGGCCGACTATGTCCGGG	5'-TGGGGATGGAGAACAGGCTA
Myom1	5'-GAGAAAAATCGGGCTCGGGT	5'-GCAGGTGAGATTGAGTGCCT
Myom2	5-AAGCCTCTTTGTCTCCCGAA	5'-TCCCAGAAAGATGAGGAGTACC
Ttn	5-CACCACCAGTCCCAGAAGTT	5'-AGACTGCTTCCTTCCGTTCA
Ptch1	5'-AAGTGTTGCCCCAAACTCCA	5'-AACAGGCGTAGGCAAGCATC
Gli1	5'-CTGGTCTGCCCTTTTGCCAC	5'-GAAAGAGTGACCCCTCAGTGCAG
Gli2	5'-TCACCATCCATAAGCGGAGC	5'-GTTGCTCCTGTGTCAGTCCA
Gli3	5'-TTCCTCCATTACACGTGCCT	5'-GTGCAAGGAGCGGATGTAGT
Hey2	5'-AGGGTGTCCGTAGCTCTTCT	5'-ACTGTGCCCCGGAGTAATTGT
Hes1	5'-AGCACAGAAAGTCATCAAAGCC	5'-CTTGGAATGCCGGGAGCTAT

Table 2.2 List of rat quantitative RT-PCR primers used in Chapter Four.

Gene	Forward	Reverse
Egr1	CACCTGACCACAGAGTCCTT	ACAAGGCCACTGACTAGGCT
Ank2	AGATTACTGTGCAGCATAACAGG	TGGTTGTAAAGGAAACACACTCA
Dmd	CGAGACCCAAACCACTTGTTG	GCGGAGAACCTGACATTATTCA
Dysbind	TGGGCAGTGTGAGTTAGAAAGA	TGCTCTGTATCGAGTTCAGCTT
Fhl2	AGCAGCCCATTGGAACCAAG	CTCCTGTGGTGATAGGCTTTTT
Lamb2	GAACTTCGCTTGGGCCTACTT	GGTGGCTGGATAGCAGCTT
Obscn	AATTTGCTGGTGGTCGTGAGAGAGCC	AATTGCCTGCCTTGAACAGAGAGCT
Pdlim1	TCGATGGGAAGATACCAGCA	TCTGTTCAGACCTGGATACTGTG
Pdlim5	AGCGTCAAGTCACCTAGCTG	TTGCCCCGCTGGAATGTGTT
Sgca	ATCGAGACGTTTTGACACCACTA	CCTTAATGTATACCCCTTCCTTCC
Sgcb	ATCGTCCTCCTGTTTATCCTGG	GTGGAACTCCATGCTATCACAC
Sgcg	TCACCGAGGGCACTCACATA	CGAGCAGGAGAAGAACGAATAGG
Tcap	GATGCGCCTGGGTATCCTC	GATCGAGACAGGGTACGGC
Xirp2	TGAGACCATCGCGGCTAAGA	GTGTCGGTATTCCATCATCTCC

Table 2.3 List of rat quantitative RT-PCR primers used in Chapter Five.

CHAPTER THREE: MEF2 transcription factors regulate distinct gene programs in mammalian skeletal muscle differentiation

Parts of this research were originally presented in the Journal of Biological Chemistry. Estrella, NL. **Desjardins, CA**. Nocco, SE. Clark, AL. Maksimenko, Y. Naya, FJ. MEF2 transcription factors regulate distinct gene programs in mammalian skeletal muscle differentiation *J Biol Chem.*2015; 290:1256-1268.

3.1 Introduction

Skeletal muscle development is characterized by the complex coordination of a diverse group of gene regulatory networks to attain the complex contractile structures required for its appropriate functioning. These events require the regulation of vast gene programs mediated by a set of core transcription factors. The MEF2 family of transcription factors plays a critical role in the processes of myogenesis and muscle homeostasis (Black *et al.* 1998, Sandmann *et al.* 2006, Potthoff *et al.* 2007). MEF2 exists as a single gene in invertebrate genomes, and plays a critical role in myogenic specification in *Drosophila* (Lilly *et al.* 1994). The MEF2 family has diverged through evolution into a four member family composed of MEF2A through –D in mammals (Edmonson *et al.* 1994). The expansion of the MEF2 gene family has added complexity to its regulatory role in skeletal muscle development. Early *in vitro* analysis of the MEF2 family suggested that all four family members shared transcriptional activity (Gossett *et al.* 1989, Pollock *et al.* 1991, Yu *et al.* 1992), and were able to recognize and bind the

same consensus sequence in DNA. While the *in vitro* data suggested a high degree of redundant function, *in vivo* loss of function mouse models revealed drastically different mutant phenotypes. Loss of MEF2B (Black *et al.* 1998) or MEF2D (Kim *et al.* 2008) expression appears to have little effect on skeletal myogenesis and homeostasis. On the other hand, mice lacking MEF2A exhibited impaired regenerative capacity after injury (Snyder *et al.* 2013), and mice bearing a conditional skeletal muscle depletion of MEF2C developed normally, but sustained rapid loss of skeletal muscle tissue perinatally (Potthoff *et al.* 2007), suggesting a role for MEF2A and –C in myofiber homeostasis.

While *in vivo* data suggests distinct regulatory roles not shared by every MEF2 factor, previously efforts have typically focused on a single MEF2 factor, and extrapolated shared effects to the entire family. Here we present a comprehensive transcriptomic analysis of the four mammalian MEF2 factors in the C2C12 cell culture model of skeletal muscle differentiation. We first observed a myotube fusion defect upon the depletion of MEF2A that is not shared by depletion of the other family members. Additionally, overexpression of the MEF2 family members was unable to rescue the fusion defect, but a constitutively active fusion, MEF2-VP16, was sufficient to rescue appropriate differentiation. These results support our hypothesis that the MEF2 family regulates distinct but overlapping gene regulatory networks. We proceeded with an analysis of transcriptome effects of depletion of individual MEF2 factors and observed a surprising lack of overlap in the genes sensitive to loss of each MEF2 family member. Upon further bioinformatics analysis these genes played roles in very different pathways. While the molecular mechanism through which this differential regulation can occur is

not obvious, we determined that it is unlikely to be MEF2 isoform binding site preferences and have determined a subset of enriched transcription factor binding sites that might help mediate differential regulation of genes by the MEF2 family.

3.2 Acute depletion of MEF2 isoforms in skeletal myoblasts

Adenoviral shRNA transduction was used to assess the effects of targeted MEF2 depletion on gross morphological features of C2C12 myoblast differentiation. The mammalian MEF2 factors display different temporal expression during C2C12 differentiation (Ramachandran *et al.* 2008, Snyder *et al.* 2013); therefore our analysis was restricted to 3 days post-induction of differentiation, a time point at which all four MEF2 isoforms are known to be expressed in normal development. Briefly, C2C12 myoblasts were transduced, then differentiated for three days, then evaluated for gross morphological defects in MEF2 depletion. As previously reported, depletion of MEF2A resulted in impaired myotube formation (Figure 3.1 A). Interestingly, depletion of MEF2B, -C, and –D failed to yield a gross morphological defect. Myosin heavy chain (MHC) was used as a protein marker for skeletal myofiber differentiation, and we observed a decrease in MHC expression only in the *Mef2a*-deficient myotubes (Figure 3.1 B-C). These results support the hypothesis that MEF2A is required for myoblast differentiation, and other MEF2 isoforms are dispensable for this process. We then assessed whether overexpression of MEF2C, -D, or a constitutively-active MEF2-VP16 was sufficient to restore myotube formation in the MEF2A-depleted myoblasts. Transduction of MEF2C and -D overexpression constructs failed to rescue the myotube formation defect in the MEF2A-depleted myoblasts (Figure 3.2). Interestingly,

overexpression of the constitutively-active MEF2-VP16 construct was sufficient to restore normal differentiation to MEF2A-deficient myoblasts (Figure 3.2). These data support the hypothesis that individual MEF2 isoforms play distinct regulatory roles in skeletal myoblast differentiation. Specifically, MEF2A is required for appropriate myotube formation, and other MEF2 isoforms are not required for this process. Additionally, overexpression of a constitutively-active MEF2 construct was sufficient to rescue the defect, but not overexpression of MEF2C or -D.

3.3 Transcriptomic analysis reveals that MEF2 isoforms regulate distinct but overlapping gene sets.

The emergence of a MEF2A-specific function in myoblast differentiation suggests that the individual MEF2 family members may play distinct regulatory roles in skeletal muscle. To elucidate other potential roles for individual MEF2 isoforms, we performed global gene expression analysis of myoblasts for each MEF2-depletion. Briefly, microarray analysis was performed on C2C12 myotubes depleted of individual MEF2 proteins (n=3 arrays for each shRNA), and dysregulation was determined by one-way analysis of variance using the Benjamini-Hochberg false discovery rate correction with a threshold q value of 0.05. The statistical analysis yielded 7685 significantly dysregulated genes across all MEF2 isoform depletions when compared to negative shLacZ-treated myoblasts (Figure 3.3). Interestingly, approximately 50% of all dysregulated genes were shown to be sensitive to MEF2A depletion, suggesting that MEF2A plays a prominent role in the transcriptional coordination of skeletal muscle cells. Additionally, MEF2B and -C depletions are responsible for the dysregulation of

approximately 14 and 13% of genes, respectively, and MEF2D depletion had strikingly few dysregulated genes (~1.5%, 110 genes, Figure 3.3). Dysregulation on the microarray was validated by quantitative RT-PCR analysis of a subset of the most dysregulated genes (both up- and down-regulated) from each MEF2 depletion experiment. The majority of genes validated in this manner displayed the expected dysregulation (Figure 3.4).

We began by identifying genes sensitive to a single MEF2 isoform. Preferentially sensitive genes were defined as genes whose dysregulation by depletion of one MEF2 isoform was significantly different than dysregulation by depletion of the other three MEF2 isoforms using Tukey's honest significant difference *post hoc* test. Based on this statistical testing, a subset of genes dysregulated by each MEF2 isoform was clearly found to be significantly more sensitive to a specific MEF2 isoform than to other members of the family. As shown in Figure 3.3A, these non-overlapping cohorts included 3248 genes (81% of total dysregulated by MEF2A), 126 genes (12%) for MEF2B, 101 genes (10%) for MEF2C, and 28 genes (25%) for MEF2D. Additionally, this analysis revealed that 75-90% of genes dysregulated in MEF2B, -C, and -D depletion were dysregulated in one or more other MEF2 depletions. Finally, only 21 of 7685 genes (<0.003%) were in all of the MEF2 factor depletion cohorts. These results suggest that only a small fraction of MEF2-sensitive genes in C2C12 cells are sensitive to all four MEF2 factors, but many can be regulated by two or more factors, likely in homo- and heterodimeric combinations.

3.4 Genes sensitive to depletion of each MEF2 factor show complicated regulatory patterns

We next closely examined the subset of genes that was dysregulated by depletion of all MEF2 factor. Because this subset of genes is sensitive to all MEF2 isoforms, we hypothesized that, based on their largely indistinguishable transcriptional activities *in vitro*, these genes would be similarly regulated by each isoform and provide a logical starting point to mechanistically dissect MEF2-dependent gene regulation in C2C12 cells. Analysis of the pattern of dysregulation of these 21 genes revealed that only five of the 24 potential regulatory patterns are represented (Figure 3.5). Interestingly, genes that were downregulated in MEF2A or MEF2D depletion and upregulated in MEF2B and MEF2C depletion were the most prevalent group (14 genes, 66.67%). In contrast to our hypothesis, no genes were upregulated with the loss of each MEF2 factor, and only one gene, *Dpy19l1* (*Dumpy19-like-1*), was downregulated in every MEF2 depletion. *Dpy19l1* is an apparent ortholog of a *C. elegans* gene, *dpy19,* which encodes for a transmembrane protein with C-mannosyltransferase activity involved in neuroblast migration (Watanabe *et al.* 2011, Buettner *et al.* 2013). *Dpy19* may also function upstream muscle development genes in worms, making it an exciting MEF2-dependent gene for further investigation (WormBase). Our analysis of the commonly dysregulated genes among all MEF2 depletions reveals complex intrafamily regulatory mechanisms that go beyond the *in vitro* transcriptional capacity of the MEF2 family described in the literature.

3.5 Identification of functional pathways in MEF2 depletion sensitive gene sets

The emergence of significant gene sets preferentially sensitive to individual MEF2 factor depletion and the paucity of shared dysregulated genes led us to investigate the functional roles played by these disparate gene sets in C2C12 cells. A survey of functional pathways represented in these gene sets was performed using three bioinformatics algorithms: Ingenuity Pathway Analysis (IPA), Gene Ontology (GO), and Kyoto Encyclopedia of Genes (KEGG).

Analysis of functional pathways using IPA reveals that genes preferentially sensitive to individual MEF2 knockdowns operate in vastly different cellular processes (Table 3.1). Roles distinct to genes preferentially sensitive to MEF2A depletion include calcium signaling, Germ cell-Sertoli cell junction signaling, and actin cytoskeletal signaling. It is interesting the two pathways most closely related to skeletal muscle functioning (calcium signaling, actin cytoskeleton signaling) are in the cohort of genes preferentially sensitive to MEF2A depletion. Genes preferentially sensitive to MEF2B are associated with hepatic fibrosis, ovarian cancer signaling, and human stem cell pluripotency, whereas genes preferentially sensitive to MEF2C are involved in control of the G_1/S cell cycle checkpoint, eicosanoid signaling, and estrogen-mediated S phase entry. Due to the dearth of genes preferentially sensitive to MEF2D depletion in C2C12 cells, only two pathways, JAK-2 and hypoxic response signaling, were statistically significant, but other pathways that may be distinct to MEF2D sensitive genes, including RhoA signaling and AMPK signaling, appear to suggest that MEF2D may have a distinct role in mediating signal processing in skeletal muscle cells.

In addition to functions that are distinct to each MEF2 isoform, several pathways are shared among multiple MEF2 gene cohorts even though the dysregulated genes differ and are preferentially sensitive to only a single MEF2 isoform depletion (Table 3.1). These include canonical pathways related to cancer, which are shared by MEF2A (molecular mechanisms of cancer) and MEF2C (ovarian cancer signaling), and Rho signaling shared by MEF2A (Rho family GTPases) and MEF2D (RhoA Signaling). These results likely reflect regulation of distinct proteins by individual MEF2 factors that play a role in the same pathway.

IPA was also performed on the subset of 21 genes sensitive to depletion of individual MEF2 factors (Table 3.1). Three of the top five canonical pathways appear to have skeletal muscle relevance. Integrin and FAK signaling have been shown to play critical roles in adhesion and signaling at the myofiber membrane (Mayer 2003), and calpain proteases are calcium-regulated protease important for skeletal muscle homeostasis (Sorimachi *et al.* 2012).

Investigation of enriched GO terms associated with each preferentially regulated gene set yielded muscle specific terms in the MEF2A regulated set (Table 3.2), including heart development, muscle cell differentiation, and striated muscle differentiation, as well as several actin cytoskeletal GO terms. Genes preferentially regulated by MEF2B were predominately associated with development of the vasculature, including blood vessel morphogenesis/development, and angiogenesis, but also contained the muscle organ development group. Genes preferentially regulated by MEF2C play a role in many metabolic processes including metabolism of various fatty acids, but surprisingly did not

contain any muscle specific pathways. Finally genes preferentially regulated by MEF2D had far fewer associated GO terms, likely due to far fewer dysregulated genes in MEF2D depletion, but there was a surprising uniformity of GO terms involved in the cell cycle (Table 3.2). When the KEGG algorithm was used to analyze the preferentially regulated gene sets, MEF2A regulated genes were associated with cancer and included several pathways involved in cardiac dysfunction (Hypterophic cardiomyopathy and Arrhythmogenic right ventricular cardiomyopathy) (Table 3.3). Far fewer KEGG pathways were associated with the remaining MEF2 factors, but MEF2B and -C gene sets both played a role in cancer pathways as well, and the MEF2D sensitive gene set played a role in RNA degradation (Table 3.3). Extensive bioinformatics analysis of the gene sets preferentially sensitive to a single MEF2 factor reveals largely distinct roles for each MEF2 isoform in C2C12 cells. Additionally, there was considerable variation in the enriched processes depending on which algorithm was used, suggesting that a more extensive analysis is necessary to understand the full breadth of the pathways associated with MEF2 in skeletal muscle cells.

3.6 Consensus binding site analysis

Functional pathway analysis confirmed our hypothesis that genes preferentially sensitive to individual MEF2 isoform depletion regulate many distinct cellular pathways. We began our mechanistic analysis of this differential sensitivity by investigating variations in MEF2 DNA-binding sites within 5kb of the putative transcriptional start site of genes preferentially sensitive to each MEF2 isoform. The proximal promoter sequence was extracted, and FIMO analysis was used to identify potential MEF2 binding sites.

Sequences were considered putative MEF2 binding-sites if they were significantly similar to the JASPAR consensus MEF2 binding site ($CTA(A/T)_4TAG$) with a p-value $<10^{-4}$. This statistical criterion led to the analysis of 3814 putative MEF2A binding sites, 152 putative MEF2B binding sites, 137 putative MEF2C binding sites, and 36 putative MEF2D binding sites (Figure 3.6). Composite sequence logos of each group of preferentially sensitive MEF2 binding sites yielded the same MEF2 DNA binding site, which is not distinct from the JASPAR consensus sequence for MEF2 DNA-binding (Figure 3.6). These results suggest that preferential transcriptional regulation of these gene sets is unlikely to be mediated by variations in the binding preference of the MEF2 isoforms.

3.7 Candidate co-regulatory factors using *de novo* motif analysis

The lack of a measurable variance in the MEF2 binding site between gene sets preferentially sensitive to individual MEF2 isoforms suggests that the differential transcriptional potential of each MEF2 factor might be mediated by interacting co-regulatory factors. We hypothesized that an analysis of co-regulatory binding sites in the proximal regulatory region of genes preferentially sensitive to individual MEF2 factors will reveal distinct candidate binding partners which may explain the observed regulatory effects. We performed transcription factor binding site enrichment analysis (Genomatix) to compile a list of distinct co-regulatory proteins which may mediate the MEF2-specific regulation of these gene sets. We considered a binding site with an enrichment score of >2 to be considered significantly enriched in these analyses.

We focused our initial analysis on the frequency with which enriched binding sites were shared between genes that were preferentially sensitive to different MEF2 factors (Figure 3.7A). As expected, the vast majority of binding sites was present in genes from different preferentially sensitive cohorts. These likely represent members of core regulatory families and transcriptional machinery. Specifically, we observed that 43% of binding sites were present in genes in all four MEF2-specific cohorts, 32% were shared by at least 3 preferentially sensitive cohorts, and 18% of binding sites were observed in two preferentially sensitive cohorts. The remaining 7% of enriched binding sites represent the potential co-regulatory factors that may explain the preferentially regulatory effect of an individual MEF2 factor for its distinct cohort. These enriched binding sites were then parsed into MEF2 factor pairwise, three-way, and completely shared cohorts (Figure 3.7B). Interestingly, we observed many enriched binding sites shared between genes preferentially sensitive to MEF2A and genes preferentially sensitive to MEF2B, -C, and -D, but we observed no enriched binding sites that were only shared between MEF2B, -C, and -D in all conformations. These data suggest that in addition to the distinct enriched binding sites we were investigating, there may exist a common set of co-regulatory factors, and MEF2A may play a more prominent role in transcriptional regulation than the other four factors in C2C12 cells.

We also examined this data from the perspective of each MEF2 factor and uncovered interesting patterns. Specifically, genes preferentially sensitive to MEF2A had a far greater number of unique co-regulatory binding sites (15, representing 14% of all binding sites enriched in the MEF2A cohort, Figure 3.7). Additionally, distinct binding

sites are rare in MEF2B (1, 1.43%) and MEF2D (2, 5%), and no binding site was found to be enriched only in the MEF2C-sensitive gene cohort. It is obvious from these data that while the presence of a single co-regulatory factor may explain some of the distinct transcriptional regulation between MEF2 family members, it is unlikely to be the explanation for all differential transcriptional activity.

We then compiled a list of candidate co-regulatory factors that may help explain our interesting transcriptional regulation difference between MEF2 family members (Table 3.4). As mentioned previously, a binding site was only considered enriched if the Z-score (enrichment score) exceeded 2.0. The majority of candidate proteins are members of the C2H2 zinc finger or homeodomain transcription factor superfamilies (Doerks *et al.* 2002, Svingen *et al.* 2006, Liu *et al.* 2008). On the other hand, this analysis did reveal a subset of specific factors that are associated with genes preferentially regulated by individual MEF2 factors (Table 3.4). Through *de novo* enriched binding site analysis of regulatory regions preferentially sensitive to individual the MEF2 factors, we believe we have uncovered candidate co-regulatory transcription factors that may partially mediate the differential regulatory control of muscle genes within the MEF2 family.

3.8 Discussion

Here we present a comprehensive analysis of the regulatory patterns of a family of core striated muscle transcription factors. Previous *in vitro* MEF2 studies have focused on dissecting single members of the family, but failed to consider the concurrent and diverse roles that other MEF2 isoforms might be playing in skeletal muscle tissue. Based

on the variety of phenotypes revealed in *in vivo* global loss-of-function mouse models, we hypothesized that individual MEF2 isoforms were responsible for regulating diverse functions in skeletal muscle.

Interestingly, *in vitro* MEF2 factor depletion experiments uncovered a required role for MEF2A in C2C12 myotube formation. Other MEF2 factors were dispensable for this pathway, but overexpression of a constitutively-active MEF2-VP16 fusion construct was sufficient to rescue myotube fusion. These results support a previously described role for MEF2A in skeletal muscle regeneration (Snyder *et al.* 2013). Global MEF2A KO was associated with an impaired regenerative capacity after muscle injury. Here we show that the defect may be associated with impaired myoblast differentiation and myotube fusion. These observations are encouraging because they validate the use of the C2C12 *in vitro* model as a means to further dissect the gross morphological phenotypes that we observe *in vivo*.

The fusion defect provided evidence that the MEF2 family members may regulate distinct transcriptional programs in skeletal muscle cells. These findings motivated us to perform a comparative transcriptomic analysis of genes dysregulated by individual MEF2 depletion in C2C12 cells. This analysis yielded a surprising paucity of overlap in the genes dysregulated by each MEF2 factor (Figure 3.3). While we are certain that each overlapping regulatory group has interesting transcriptional regulation, we focused our initial analyses on the gene cohorts preferentially-sensitive to individual MEF2 factor ablation (i.e. genes that were only significantly dysregulated in the loss of MEF2A, but not -B, -C, and -D), and the gene cohort that are sensitive to loss of each MEF2 factor

individually. We hypothesized that the gene sets preferentially sensitive to individual MEF2 factors would reveal differently regulated cellular pathways, and in addition, may provide information critical to our understanding of how a family of highly related transcription factors can regulate transcriptional activity in so diverse a manner.

We first wanted to understand the cellular pathways that are regulated by these preferentially-dysregulated gene cohorts. We felt that a single algorithm might be insufficient to capture the interesting gene interactions in these cohorts, so we performed IPA, GO term, and KEGG pathway analyses with the hope of understanding the breadth of pathways that were represented in each gene set. Considering MEF2's role in striated muscle development and differentiation, we were initially surprised by the lack of prominent muscle-specific pathways in these analyses. Upon inspection of the more classically muscle-associated genes, we observed that these genes were, in fact, dysregulated in these knockdown experiments, they were most often dysregulated in multiple MEF2 depletions, suggesting that intrafamily regulatory relationships influence the regulation of these genes. Additionally, the MEF2A-senstive gene cohort did yield several GO terms associated with striated muscle gene programs (Table 3.2) including heart development, striated muscle cell differentiation, and actin cytoskeleton organization. The emergence of these pathways suggests that MEF2A may be a focal point for the regulation of canonical muscle specific pathways.

In parallel to these analyses, we began analyzing the genes that were preferentially sensitive to the individual depletion of every MEF2 factor. This group is of particular interest because it may represent a group where all the MEF2 factors play a

relevant regulatory role. This group is a departure from the canonical thinking about MEF2, which suggests a high degree of redundancy in transcriptional regulation by the MEF2 family, yet we observed a small subset of genes that might portray quite the opposite, a total lack of ability of MEF2 factors to compensate for each other in the regulation of these genes. The gene cohort was first parsed into groups based on the shared direction of dysregulation in individual MEF2 depletions. Constructing these pattern based sets yielded a surprising set of enriched regulatory patterns (Figure 3.5). Of the 24 possible regulatory combinations, we only observed 5 patterns that were represented in the gene sets. Notably, two thirds of all the genes in this cohort (14 genes) are downregulated in MEF2A and –D depletion, and upregulated in MEF2B and -C depletion, suggesting a distinct regulatory pattern where members of the MEF2 family regulate gene expression in opposite directions. Additionally, only a single gene, *DumPY-19-like-1* (*Dpy19l1*), was dysregulated in the same direction by individual MEF2 depletions. While *ceMEF2* depletion itself has no obvious phenotype in *C. elegans* (ref), *Dpy19l1*, is a gene that has a putative role in regulation of muscle development (Watanabe *et al.* 2011, Buettner *et al.* 2013).

We proceeded through an extensive literature search to determine the cellular function of the candidate cofactors and potentially further highlight key candidates for further investigation (Table 3.4). Four of the enriched binding sites are bound by transcription factors that play a role in skeletal muscle differentiation. In the MEF2A-sensitive cohort, *distal*-les homeobox factors *Dlx1-6* were among the most enriched factors. Dlx factors play a pivotal role in craniofacial development, and while a muscle

specific role for Dlx factors has yet to be characterized, a closely related cousin, Msx1, is associated with maintenance of an undifferentiated state during the developmental migration of skeletal muscle precursors (Bendall *et al.* 2000). Zfhx3/Atbf1, another enriched binding site in the MEF2A-sensitive cohort is a well characterized inhibitor of myogenic differentiation whose primary function is to inhibit binding of pro-myogenic bHLH factors by occupying E-box binding sites (Berry *et al.* 2001). Additionally, one splice variant, Zfhx3-B, as a transcriptional activator and promotes myogenic differentiation (Berry *et al.* 2001).

The two families of transcription factors that bind the enriched sites in MEF2D-sensitive genes regions also play roles in myogenic differentiation. Specifically Meis1 and Pknox2 are members of a small transcription factor family that function as pioneer transcription factors in skeletal muscle to stabilize MyoD/E12 DNA-binding on suboptimal E-box sites (Knoepfler *et al.* 1999, Heidt *et al.* 2007, Grade *et al.* 2009). Finally, Gtf2ird1/Gtf3 is the second transcription factor family associated with enriched binding sites in MEF2D-sensitive regulatory regions. This factor shares high similarity to TFII-1, potentially playing an important role in the integration of muscle-specific transcriptional signaling and the general transcriptional apparatus (O'Mahoney *et al.* 1998). Interestingly, the human ortholog of Gtf3 is found in a region that is deleted in Williams-Beuren syndrome, a disease that is associated with muscle weakness and atrophy (Tassabehji *et al.* 1999). Of the genes localized to this deleted region, Gtf3 is the only one associated with skeletal function, supporting our analysis that this transcription factor may play an important role in skeletal muscle (Tassabehji *et al.* 1999). Through *de*

novo enriched binding site analysis of regulatory regions preferentially sensitive to individual MEF2 factors; we believe we've uncovered candidate co-regulatory transcription factors that may partially mediate the differential regulatory control of muscle genes within the MEF2 family.

Unfortunately, our analysis did not uncover any enriched transcription factor binding sites yielding candidates that might explain the MEF2C preferentially sensitive gene set. We suspect that this may be due to issues arising from not being able to determine which of the dysregulated genes direct MEF2 targets are, and which secondary effects are. Since this is the case, it is possible that either MEF2C sensitive regulation is caused by some unique combination of cofactors, or that we lack the analytical resolution to truly assess what may be a very small number of unique co-regulatory transcription factor reactions in the case of MEF2C.

This study reveals complex isoform-specific transcriptional regulatory networks focused on the mammalian MEF2 transcription factors in C2C12 differentiation. While we acknowledge that the *in vitro* C2C12 model is distinct from primary skeletal myogenesis, we believe that the patterns we have observed will shed additional light on the complicated coordination of myogenesis in mammalian skeletal muscle tissue. Additionally, our comprehensive computational analyses introduce a new level of understanding of the intrafamily dynamics of the MEF2 factors, and reveal that reductionist analysis of these factors in isolation fails to appropriately encompass the features of this transcription factor family.

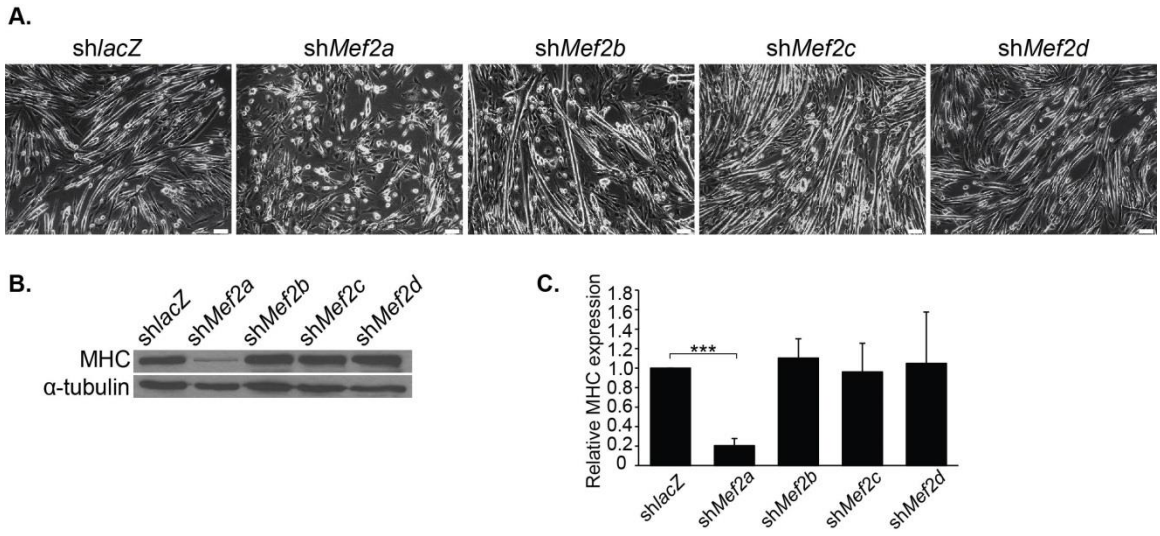

Figure 3.1 Depletion of *Mef2a*, but not *-b*, *-c*, or *-d* transcript caused a myotube fusion defect. C2C12 myoblasts were transduced with *Mef2* shRNA adenovirus then allowed to differentiate for three days. **A**, Bright field microscopy of differentiating myotubes in each *Mef2* shRNA treatment. Only depletion of *Mef2a* caused a noticeable phenotype. **B**, Loss of myotube fusions is concurrent with decreased Myosin heavy chain (MHC) protein expression. **C**, Quantification of MHC protein expression in *Mef2* shRNA-treated myotubes reveals a significant reduction in MHC expression only in *Mef2a*-depleted C2C12 myotubes. Data are means (n=3) ± S.E.M. (error bars). *, $p<0.05$; ** $p<0.01$; *** $p<0.001$.

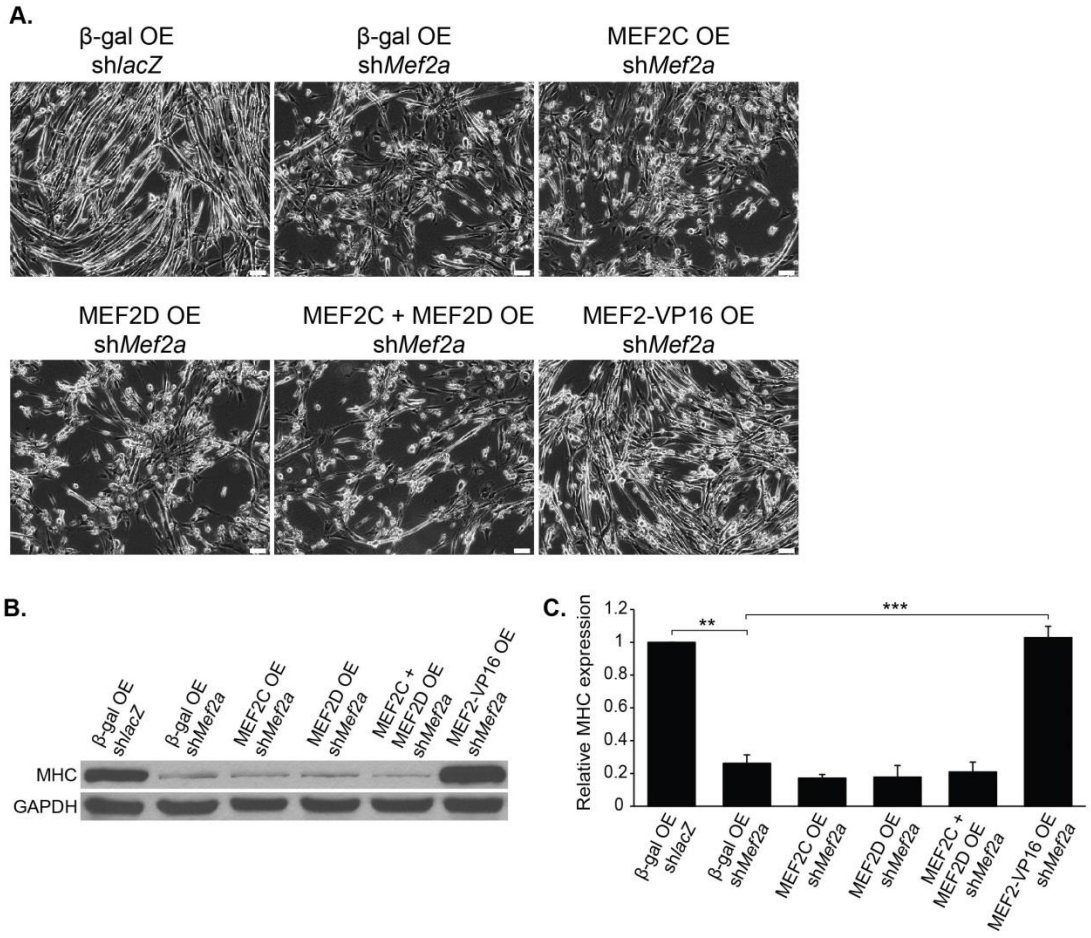
A.
β-gal OE
sh*lacZ*
β-gal OE
sh*Mef2a*
MEF2C OE
sh*Mef2a*
MEF2D OE
sh*Mef2a*
MEF2C + MEF2D OE
sh*Mef2a*
MEF2-VP16 OE
sh*Mef2a*
B.
β-gal OE shlacZ
β-gal OE shMef2a
MEF2C OE shMef2a
MEF2D OE shMef2a
MEF2C + MEF2D OE shMef2a
MEF2-VP16 OE shMef2a
MHC
GAPDH
C.
Relative MHC expression
1.2
1
0.8
0.6
0.4
0.2
0
**
***
β-gal OE shlacZ
β-gal OE shMef2a
MEF2C OE shMef2a
MEF2D OE shMef2a
MEF2C + MEF2D OE shMef2a
MEF2-VP16 OE shMef2a

Figure 3.2 Overexpression of a constitutively-active MEF2 construct rescues myotube fusion. *Mef2a* shRNA adenovirus was co-transduced with MEF2 overexpression adenoviruses in C2C12 myoblasts. Myoblasts were then induced to differentiate for three days and myotube fusion was assessed. **A**, Bright-field microscopy of transduced C2C12 reveals restored myotube fusion with MEF2-VP16 overexpression in *Mef2a*-depleted C2C12 cells. **B**, A representative immunoblot shows restoration of Myosin heavy chain (MHC, a marker of myocyte differentiation) in MEF2-VP16 overexpression. **C**, Quantification of MHC protein expression in C2C12 cells shows restored MHC expression only in the MEF2-VP16 treatment. Data are means (n=3) ± S.E.M. (error bars). *, $p<0.05$; ** $p<0.01$; *** $p<0.001$.

A.

MEF2 Isoform	Dysregulated Genes	% of total
MEF2A	4020	52.31
MEF2B	1057	13.75
MEF2C	967	12.58
MEF2D	110	1.43
Total	7685	

B.

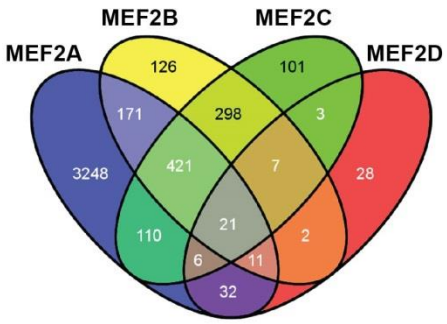

Figure 3.3 Comparative analysis of MEF2 knockdown gene sets. Comparative microarrays were performed in triplicate for each *Mef2* shRNA virus and dysregulation was compared to the *shLacZ* negative control. Microarray analysis reveals that C2C12 cells are differentially sensitive to depletion of the MEF2 isoforms. **A**, A summary of the significantly dysregulated ($p<0.05$) genes sensitive to the depletion of each MEF2 isoform shows that over 50% of genes dysregulated by MEF2 depletion are sensitive to the loss of MEF2A. **B**, a composite Venn diagram incorporating all overlapping gene sets as determined by Tukey's honest significant difference *post-hoc* test ($q<0.05$).

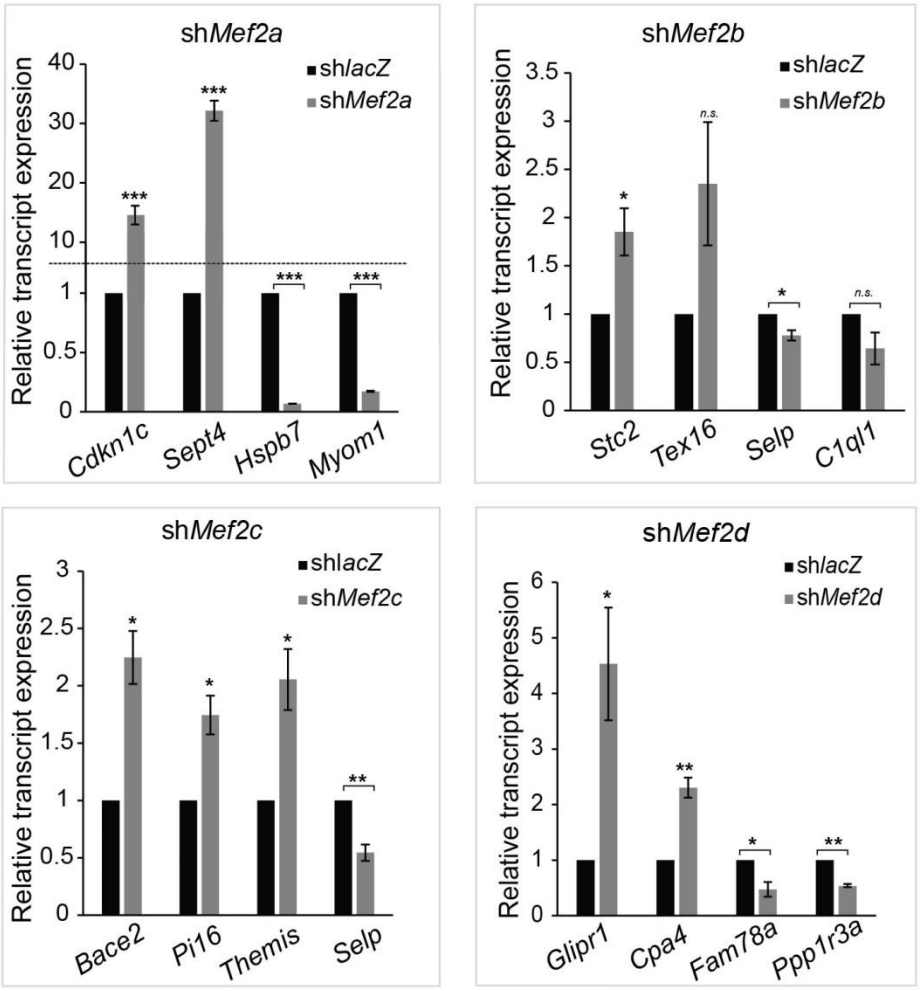
shMef2a
shlacZ
shMef2a
Relative transcript expression
40
30
20
10
1
0.5
0
***
***
***
***
Cdkn1c
Sept4
Hspb7
Myom1
shMef2b
shlacZ
shMef2b
Relative transcript expression
3.5
3
2.5
2
1.5
1
0.5
0
*
n.s.
*
n.s.
Stc2
Tex16
Selp
C1ql1
shMef2c
shlacZ
shMef2c
Relative transcript expression
3
2.5
2
1.5
1
0.5
0
*
*
*
**
Bace2
Pi16
Themis
Selp
shMef2d
shlacZ
shMef2d
Relative transcript expression
6
5
4
3
2
1
0
*
**
*
**
Glipr1
Cpa4
Fam78a
Ppp1r3a

Figure 3.4 Quantitative RT-PCR validation of microarray gene dysregulation. A subset of genes dysregulated (up- and downregulated) in each MEF2 isoform depletion was quantified using RT-PCR. *Cdkn1c, cyclin-dependent kinase inhibitor 1c; Sept4, septin 4;Hspb7, heat shock protein family member 7(cardiovascular); Myom1, myomesin 1; Stc2, stanniocalcin 2; Tex16, testis expressed gene 16; Selp, selectin (platelet); C1ql1, complement component 1, q subcomponent-like-1; Bace2, beta-site APP-cleaving enzyme 2; Pi16, peptidase inhibitor 16; Themis, thymocyte selection associated; Selp, selectin (platelet); Glipr1, GLI pathogenesis-related 1 like 1; Cpa4, carboxypeptidase A4; Fam78a, family with sequence similarity 78, member A; Ppp1r3a, protein phosphatase 1, regulatory (inhibitor) subunit 3a*. Data are means (n=3) ± S.E.M. (error bars). *, $p<0.05$; ** $p<0.01$; *** $p<0.001$.

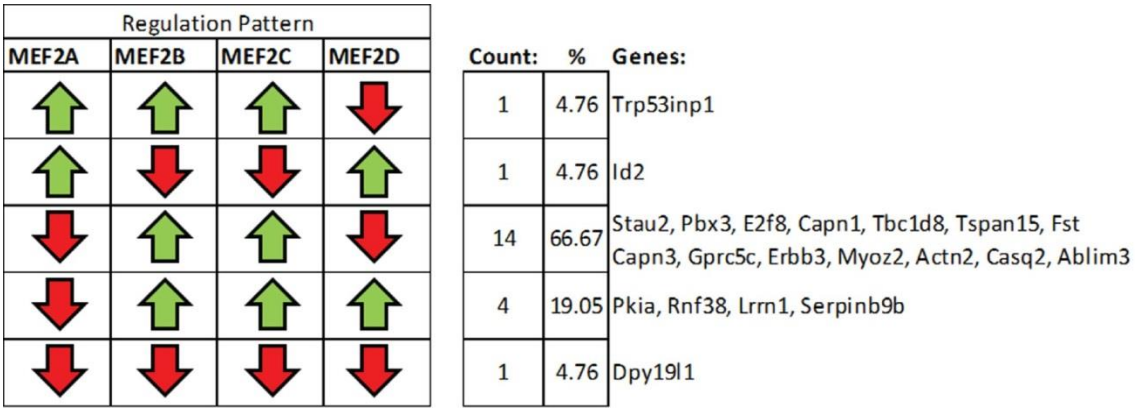

Figure 3.5 Regulatory patterns of genes sensitive to the depletion of each MEF2 isoform. Only 21 genes were dysregulated upon the depletion of each MEF2 isoform. These genes were parsed into groups based on the direction of dysregulation upon depletion of each MEF2 isoform. Only five of the possible patterns of dysregulation are represented, and nearly 67% of genes were downregulated in the loss of MEF2A or -D, and upregulated in the loss of MEF2C, or –D. Additionally, only a single gene, *Dpy19l1 (DumPY19-like 1),* is downregulated in each MEF2 factor depletion.

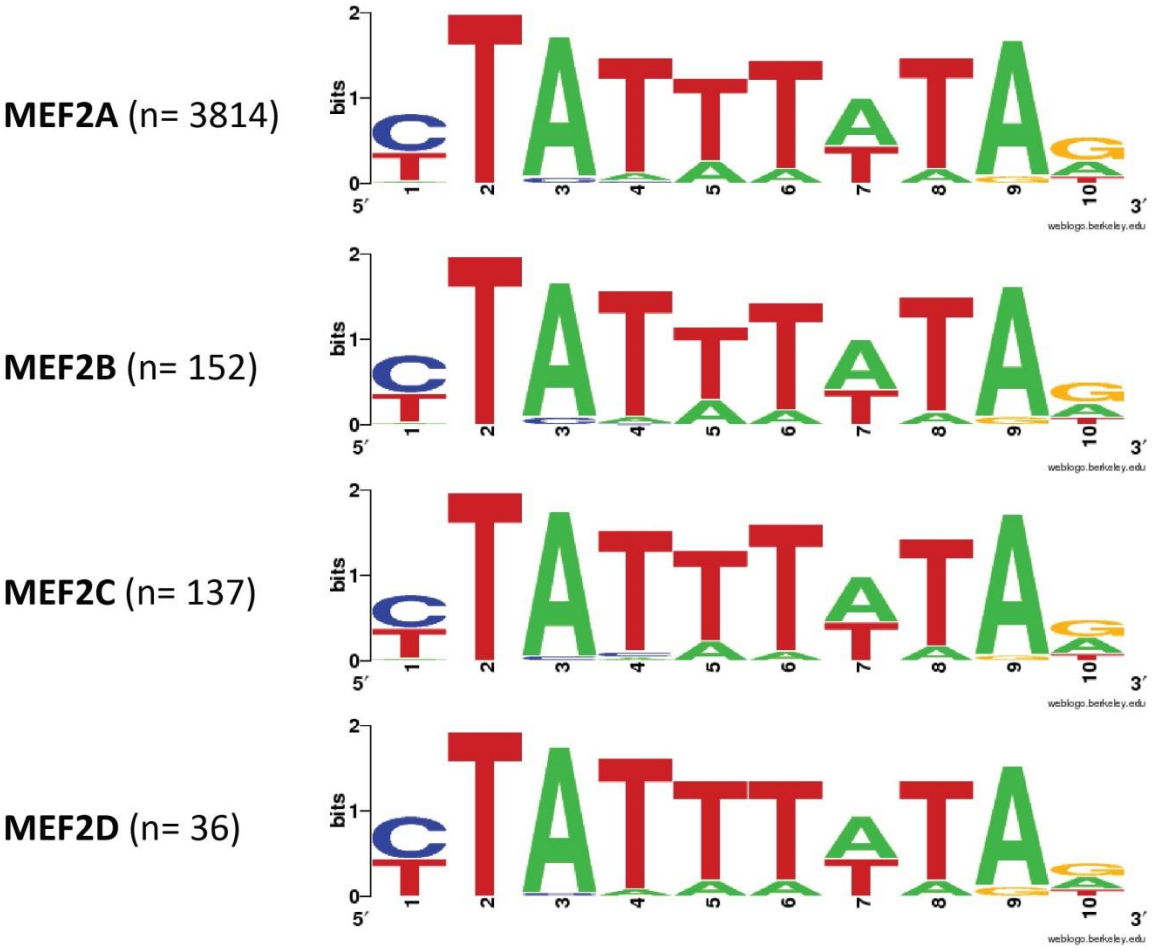

Figure 3.6 Putative MEF2 binding sites from gene preferentially sensitive to individual MEF2 factor depletion. FIMO (MEME suite) analysis extracted putative MEF2 binding sites from the proximal 5kb upstream region of the transcriptional start site of each gene dysregulated in MEF2 depletion. The analysis identified 3814 potential sites in MEF2A-sensitive genes, 152 sites in MEF2B sensitive genes, 137 sites in MEF2C sensitive genes, and 36 sites in MEF2D sensitive genes. These sites were compiled into position-weight matrices describing binding sites associated with preferential sensitivity to loss of a single MEF2 factor, and sequence logos were built.

A.

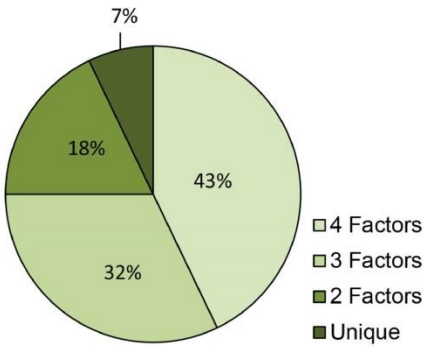

B.

MEF2A

Overlap	# of TFBS	%
Unique	15	14.15
2 Factors	31	29.25
3 Factors	30	28.30
4 Factors	30	28.30
Total	106	

MEF2C

Overlap	#	%
Unique	0	0.00
2 Factors	15	20.27
3 Factors	29	39.19
4 Factors	30	40.54
Total	74	

MEF2B

Overlap	#	%
Unique	1	1.43
2 Factors	13	18.57
3 Factors	26	37.14
4 Factors	30	42.86
Total	70	

MEF2D

Overlap	#	%
Unique	2	5.00
2 Factors	3	7.50
3 Factors	5	12.50
4 Factors	30	75.00
Total	40	

Figure 3.7 Identification of distinct transcription factor binding sites associated with each MEF2 knockdown gene set. Transcription factor binding site enrichment analysis (Genomatix) was performed on the proximal 5kb upstream region of genes preferentially sensitive to the depletion of a single MEF2 factor. A binding site was considered enriched if it had a Z-score > 2.0. **A**, Nearly 43% of enriched binding sites were shared by all four gene sets, 32% were shared by three MEF2 gene sets, 18% were shared by two, and only 7% were unique to genes dysregulated by depletion of a specific MEF2 isoform. **B**, Binding sites were parsed based on their presence in genes dysregulated by individual MEF2 factors. MEF2A showed the greatest number of distinct TF binding sites (14%), and MEF2C lacked any unique binding sites.

Canonical Pathway	p-value	Ratio
MEF2A		
Molecular Mechanisms of Cancer	2.40E-08	92/387 (0.238)
Calcium Signaling	2.26E-07	55/217 (0.253)
Germ Cell-Sertoli Cell Junction Signaling	6.20E-06	46/169 (0.272)
Actin Cytoskeletal Signaling	1.63E-05	57/242 (0.236)
Signaling by Rho Family GTPases	1.96E-05	60/262 (0.229)
MEF2B		
Hepatic Fibrosis/Hepatic Stellate Cell Activation	1.31E-03	5/155 (0.032)
Ovarian Cancer Signaling	7.57E-03	4/152 (0.026)
Human Embryonic Stem Cell Pluripotency	7.77E-03	4/161 (0.025)
Ceramide Signaling	1.13E-02	3/91 (0.033)
Apoptosis Signaling	1.47E-02	3/100 (0.03)
MEF2C		
Cell Cycle: G1/S Checkpoint Regulation	3.14E-03	3/68 (0.044)
Eicosanoid Signaling	3.14E-03	3/85 (0.035)
Molecular Mechanisms of Cancer	5.49E-03	6/387 (0.016)
Estrogen-mediated S-phase Entry	5.48E-03	2/28 (0.071)
Sulfate Activation for Sulfonation	9.42E-03	1/8 (0.125)
MEF2D		
Role of JAK2 in Hormone-like Cytokine Signaling	4.03E-02	1/37 (0.027)
Hypoxia Signaling in the Cardiovascular System	7.69E-02	1/68 (0.015)
RhoA Signaling	1.32E-01	1/122 (0.008)
Artherosclerosis Signaling	1.37E-01	1/138 (0.007)
AMPK Signaling	1.50E-01	1/180
All MEF2		
Regulation of Cellular Mechanics by Calpain Protease	3.20E-05	3/73 (0.041)
nNOS Signaling in Neurons	1.20E-03	2/52 (0.038)
Integrin Signaling	1.24E-03	3/208 (0.014)
Amyloid Processing	1.41E-03	2/61 (0.033)
FAK Signaling	4.05E-03	2/106 (0.019)

Table 3.1 IPA canonical pathway analysis of gene sets preferentially sensitive to MEF2 factor depletion. Each preferentially sensitive gene set, and the set of 21 genes sensitive to every MEF2 isoform were analyzed using the Ingenuity Pathway Analysis algorithm. The top five most significantly dysregulated canonical pathways are provided. All the canonical pathways were considered significantly sensitive to specific MEF2 factor depletion ($p<0.05$) with the exception of MEF2D-sensitive canonical pathways. The table also provides the ratio of genes dysregulated in each canonical pathway against the total number of genes in each pathway.

GO Term	Count	%	p-value
MEF2A			
GO:0006793~phosphorus metabolic process	215	6.65	2.10E-11
GO:0006796~phosphate metabolic process	215	6.65	2.10E-11
GO:0016310~phosphorylation	183	5.66	8.30E-11
GO:0006468~protein amino acid phosphorylation	167	5.16	8.92E-11
GO:0046907~intracellular transport	119	3.68	1.83E-09
GO:0007049~cell cycle	144	4.45	1.63E-06
GO:0030029~actin filament-based process	54	1.67	2.72E-06
GO:0008104~protein localization	170	5.26	2.94E-06
GO:0016568~chromatin modification	66	2.04	6.43E-06
GO:0007507~heart development	63	1.95	7.53E-06
GO:0042692~muscle cell differentiation	39	1.21	1.02E-05
GO:0006665~sphingolipid metabolic process	25	0.77	1.71E-05
GO:0015031~protein transport	146	4.51	2.28E-05
GO:0006643~membrane lipid metabolic process	25	0.77	3.17E-05
GO:0045184~establishment of protein localization	146	4.51	3.41E-05
GO:0051146~striated muscle cell differentiation	31	0.96	3.84E-05
GO:0034613~cellular protein localization	76	2.35	4.71E-05
GO:0030036~actin cytoskeleton organization	48	1.48	4.75E-05
GO:0006886~intracellular protein transport	71	2.20	5.73E-05
GO:0070727~cellular macromolecule localization	76	2.35	5.97E-05
MEF2B			
GO:0048514~blood vessel morphogenesis	9	7.14	3.85E-05
GO:0001568~blood vessel development	9	7.14	1.66E-04
GO:0001944~vasculature development	9	7.14	1.96E-04
GO:0007389~pattern specification process	9	7.14	4.62E-04
GO:0060688~regulation of morphogenesis of a branching structure	4	3.17	5.27E-04
GO:0001763~morphogenesis of a branching structure	6	4.76	1.23E-03
GO:0042471~ear morphogenesis	5	3.97	1.42E-03
GO:0001525~angiogenesis	6	4.76	1.62E-03
GO:0048706~embryonic skeletal system development	5	3.97	1.96E-03
GO:0048598~embryonic morphogenesis	9	7.14	2.09E-03
GO:0008284~positive regulation of cell proliferation	8	6.35	2.27E-03
GO:0001501~skeletal system development	8	6.35	2.32E-03

GO:0003002~regionalization	7	5.56	2.49E-03
GO:0030878~thyroid gland development	3	2.38	3.51E-03
GO:0042474~middle ear morphogenesis	3	2.38	3.51E-03
GO:0048562~embryonic organ morphogenesis	6	4.76	3.71E-03
GO:0043583~ear development	5	3.97	4.43E-03
GO:0048568~embryonic organ development	7	5.56	4.47E-03
GO:0007517~muscle organ development	6	4.76	5.41E-03
GO:0043009~chordate embryonic development	9	7.14	5.49E-03
MEF2C			
GO:0046456~icosanoid biosynthetic process	3	3.03	6.27E-03
GO:0006636~unsaturated fatty acid biosynthetic process	3	3.03	6.73E-03
GO:0006690~icosanoid metabolic process	3	3.03	9.82E-03
GO:0033559~unsaturated fatty acid metabolic process	3	3.03	1.10E-02
GO:0030097~hemopoiesis	5	5.05	2.47E-02
GO:0002063~chondrocyte development	2	2.02	3.48E-02
GO:0048534~hemopoietic or lymphoid organ development	5	5.05	3.54E-02
GO:0010558~negative regulation of macromolecule biosynthetic process	6	6.06	3.69E-02
GO:0001501~skeletal system development	5	5.05	3.70E-02
GO:0008610~lipid biosynthetic process	5	5.05	3.70E-02
GO:0031327~negative regulation of cellular biosynthetic process	6	6.06	4.09E-02
GO:0002520~immune system development	5	5.05	4.11E-02
GO:0009890~negative regulation of biosynthetic process	6	6.06	4.23E-02
GO:0045892~negative regulation of transcription, DNA-dependent	5	5.05	4.69E-02
GO:0007242~intracellular signaling cascade	9	9.09	4.69E-02
GO:0006631~fatty acid metabolic process	4	4.04	4.77E-02
GO:0051253~negative regulation of RNA metabolic process	5	5.05	4.78E-02
GO:0006633~fatty acid biosynthetic process	3	3.03	4.97E-02
MEF2D			
GO:0022402~cell cycle process	5	17.86	1.22E-03
GO:0000279~M phase	4	14.29	4.90E-03

GO:0007049~cell cycle	5	17.86	6.03E-03
GO:0022403~cell cycle phase	4	14.29	7.37E-03
GO:0000087~M phase of mitotic cell cycle	3	10.71	2.40E-02
GO:0000278~mitotic cell cycle	3	10.71	3.66E-02

Table 3.2 Gene Ontology (GO) term analysis of gene sets preferentially sensitive to MEF2 factor depletion. GO term analysis was performed using the DAVID bioinformatics database. This table presents the top 20 dysregulated GO terms sensitive to specific MEF2 factor depletion. The table also includes the number of genes dysregulated (Count), percentage of the pathway dysregulated (%), a p-value showing statistically dysregulated pathways (p-value; $p<0.05$ was considered significant).

KEGG Pathway	Count	%	p-value
MEF2A			
mmu04142:Lysosome	43	1.33	5.91E-08
mmu04115:p53 signaling pathway	25	0.77	5.47E-05
mmu04520:Adherens junction	25	0.77	3.02E-04
mmu05410:Hypertrophic cardiomyopathy (HCM)	26	0.80	6.24E-04
mmu05212:Pancreatic cancer	23	0.71	8.81E-04
mmu04710:Circadian rhythm	8	0.25	1.50E-03
mmu04810:Regulation of actin cytoskeleton	51	1.58	1.78E-03
mmu05210:Colorectal cancer	25	0.77	2.13E-03
mmu00310:Lysine degradation	15	0.46	2.37E-03
mmu00051:Fructose and mannose metabolism	14	0.43	2.52E-03
mmu05414:Dilated cardiomyopathy	26	0.80	2.59E-03
mmu04010:MAPK signaling pathway	59	1.82	2.84E-03
mmu00600:Sphingolipid metabolism	15	0.46	3.06E-03
mmu04722:Neurotrophin signaling pathway	33	1.02	3.99E-03
mmu00604:Glycosphingolipid biosynthesis	8	0.25	4.24E-03
mmu03030:DNA replication	13	0.40	4.60E-03
mmu04540:Gap junction	24	0.74	4.69E-03
mmu05200:Pathways in cancer	68	2.10	5.49E-03
mmu05211:Renal cell carcinoma	20	0.62	8.19E-03
mmu05412:Arrhythmogenic right ventricular cardiomyopathy (ARVC)	21	0.65	8.35E-03
MEF2B			
mmu05200:Pathways in cancer	6	4.76	3.55E-02
mmu04920:Adipocytokine signaling pathway	3	2.38	5.62E-02
mmu03320:PPAR signaling pathway	3	2.38	7.51E-02
MEF2C			
mmu04630:Jak-STAT signaling pathway	5	5.05	5.17E-03
mmu00590:Arachidonic acid metabolism	3	3.03	5.75E-02
mmu05222:Small cell lung cancer	3	3.03	5.99E-02
mmu05200:Pathways in cancer	5	5.05	6.22E-02
MEF2D			
mmu03018:RNA degradation	2	7.14	7.10E-02

Table 3.3 KEGG pathway analysis of gene sets preferentially sensitive to MEF2 factor depletion. KEGG pathway analysis was performed using the DAVID bioinformatics database. This table presents the top 20 dysregulated KEGG pathways sensitive to specific MEF2 factor depletion. The table also includes the number of genes dysregulated (Count), percentage of the pathway dysregulated (%), a p-value showing statistically dysregulated pathways (p-value; $p<0.05$ was considered significant).

TF Module	Module Description	Z-Score	Known Factor	Binding Domain	Function
Mef2a					
V$SF1F	Vertebrate steroidogenic factor	13.53	Nr5a1	C4 zinc finger domain	Essential for embryonic sex determination
V$DLXF	Distal-less homeodomain transcription factors	12.93	Dlx1 through 6	homeodomain	Repressor, important of embryonic development (shared function)
V$IKZF	Ikaros family zinc finger 5	10.16	Ikzf5	C2H2 zinc finger domain	Repressor, lymphocyte development
V$BARB	Barbiturate-inducible element box	9.68	Not characterized	Not characterized	
V$ZF05	C2H2 zinc finger transcription factor 5	9.49	Zfp410	C2H2 zinc finger domain	ECM remodeling
V$IKRS	Ikaros zinc finger family	8.8	Ikzf1 through 4	C2H2 zinc finger domain	Repressor, lymphocyte development (shared function)
V$THAP	THAP domain containing protein	6.72	Thap1	THAP domain	Cell cycle progression dow nstream of Rb-E2F signaling
V$HEAT	Heat shock factors	6.34	Hsf1, Hsf2, Hsf4	HSF-HTH	Heat-sensitive activator, embryonic development
V$ATBF	AT-binding transcription factor	6.15	Zfhx3	C2H2 zinc finger domain, C2HC zinc finger domain, homeodomain	Repressor, promotes neuronal and myogenic differentiation
V$OVOL	OVO homolog-like transcription factor	6.15	Ovol1, Ovol2	C2H2 zinc finger domain	Ovol1: repressor, contributes to epithelial development. Ovol2: repressor, embryonic cardiovascular development
V$GTBX	GT box	4.38	Zfp628	C2H2 zinc finger domain	Uncharacterized transcriptional regulator
V$PTF1	Pancreas transcription factor 1, heterotrimeric transcription factor	4.33	Ptf1a, Rbpj, Rbpjl	bHLH	Ptf1a: involved in pancreatic and neuronal development. Rbpj: involved in cardiac and hematopoeitic development. Rbpjl: uncharacterized transcriptional regulator.
V$RU49	Zinc finger transcription factor RU49, zinc finger proliferation 1 - Zipro1	3.4	Zscan21	C2H2 zinc finger domain	Uncharacterized transcriptional regulator
V$HZIP	Homeodomain-leucine zipper transcription factors	2.21	Homez	homeodomain	Uncharacterized transcriptional regulator
V$CHOP	C/EBP homologous protein (CHOP)	2.12	Ddit3	bZIP	Stress sensitive transcriptional regulator, negative regulator of myogenic differentiation.
Mef2b					
V$BTBF	BTB/POZ (broad complex, TramTrack, Bric-a-brac/pox viruses and zinc fingers)	2.56	Zbtb33	BTB-POZ C2H2 zinc fingers	Repressor of Wnt target genes. Activator of an unrelated set of genes.
Mef2c					
Mef2d					
V$TALE	TALE homeodomain class recognizing TG motifs	3.94	Meis1, Meis2, Meis3, Pknox1,Pknox2, Tgif1, Tgif2	TALE class homeodomain	Meis1: angiogenic and hematopoeitic development. Meis2: mammalian eye/neuronal development. Meis3: activator, dow nstream of PKB signaling. Pknox1: activator, hematopoeitic and angiogenic development. Pknox2: associated w ith actin cytoskeleton. Tgif1: Dow nstream of TGF-β signaling, embryonic development. Tgif2: uncharacterized regulator dow nstream of TGF-β signaling.
V$DICE	Dow nstream Immunoglobulin Control Element, critical for B cell activity and specificity	2.31	Gtf2i, Gtf2ird1	GTF2I repeat domain	Gtf2i: embryonic development, negative regulator of angiogenesis. Gtf2ird1: modulates cell cycle progression, skeletal muscle differentiation.

Table 3.4 List of candidate co-regulatory factors from transcription factor binding site enrichment analysis. The Genomatix transcription factor binding site enrichment analysis revealed a subset of co-regulatory proteins distinct to gene sets preferentially sensitive to only a single MEF2 factor depletion. Here we present these candidate co-factors with a brief description of their family, the enrichment score (Z-score >2 considered enriched), the family members known to bind the enriched binding site, the binding domain of these proteins, and finally a brief literature search description of the of the function of each candidate co-factor, focusing on any roles played in skeletal or cardiac muscle. Interestingly, genes preferentially sensitive to MEF2C depletion did not have any unique enriched TF binding sites.

CHAPTER FOUR: Antagonistic regulation of cell cycle and differentiation gene programs in neonatal cardiomyocytes by homologous MEF2 transcription factors

Parts of this research are in revision for a submission to the Journal of Biological Chemistry (1/10/17).

4.1 Introduction

Cardiac development involves precise integration of specification, proliferation, and differentiation gene programs in cardiomyocytes and non-muscle cell types (Srivastava 2006, Vincent *et al.* 2010, Paige *et al.* 2015). The gene regulatory network that drives heart organogenesis is controlled by a core of evolutionarily conserved cardiac transcription factors (TFs) (Olson 2006, Waardenberg *et al.* 2014). MEF2 is a key member of this core group whose activity is essential for cardiac development in numerous animal species (Potthoff *et al.* 2007, Desjardins *et al.* 2016). Vertebrates have evolved multiple isoforms of MEF2 (MEF2A, B, C, and D), thereby broadening the gene regulatory potential of this cardiac TF and adding additional layers of complexity to the transcriptional circuitry of cardiac organogenesis. The diverse regulatory roles of MEF2 in the heart are exemplified by the distinct array of cardiovascular phenotypes associated with knockout or inhibition of individual MEF2 genes in vertebrate model systems (Lin *et al.* 1997, Naya *et al.* 2002, Wang *et al.* 2005, Kim *et al.* 2008, Hinits *et al.* 2012, Guo *et al.* 2014). While there is no doubt that MEF2 is required for differentiation and regulates structural genes in muscle (Black *et al.* 1998, Estrella *et al.* 2014), the repertoire of gene programs controlled by this family in

cardiomyocytes is largely unknown. Based on the range of cellular processes mediated by MEF2 isoforms in other specialized cell types such as neurons, the regulatory potential of this core cardiac TF has not been fully realized in cardiomyocytes.

The perinatal period is a critical time for proper cardiac maturation during which differentiated cardiomyocytes with persistent proliferative capacity are programmed to permanently exit the cell cycle (Pasumarthi 2002, Ahuja *et al.* 2007, Zacchigna *et al.* 2014). Cardiomyocyte quiescence will prevent further growth of the heart through cell division, instead promoting growth by increases in cardiomyocyte size. Perhaps not coincidentally, it is also the time during which the mammalian heart begins to lose its ability to regenerate (Porrello *et al.* 2011, Foglia *et al.* 2016). Neonatal cardiomyocytes also undergo radical switches in metabolic pathways and contractile protein isoforms to fully commit to the mature differentiated phenotype (Murphy 1996, Murray *et al.* 2014). We understand surprisingly little about the mechanisms by which cell cycle exit and terminal differentiation are coordinated considering the importance of precisely executing these processes for adult cardiomyocyte homeostasis and function.

We have previously reported that neonatal cardiomyocyte homeostasis is dependent on MEF2. Cytoarchitectural (costamere/muscle focal adhesion) and cell cycle gene programs in neonatal cardiomyocytes were shown to be regulated by MEF2A and D protein isoforms, respectively (Ewen *et al.* 2011, Estrella *et al.* 2015). Interestingly, defects in these distinct gene programs both led to severely impaired cardiomyocyte survival. Based on the importance of MEF2 for cardiomyocyte survival we wanted to

explore the global gene programs that mediate this process further by performing an unbiased gene expression pathway analysis of all MEF2 protein isoforms.

The gene regulatory function of MEF2 isoforms has typically been studied individually. Here we present a comprehensive morphological and genome-wide transcriptomic analysis on the three major cardiac MEF2 isoforms, MEF2A, C, and D, in neonatal cardiomyocytes under identical conditions. MEF2A and D but not MEF2C were found to be essential for cardiomyocyte survival. Consistent with these differential effects on survival, a detailed computational analysis uncovered distinct roles for these protein isoforms in cell cycle and structural gene regulation. The results of this study reveal an entirely unexpected antagonistic regulatory role among MEF2 isoforms and have provided a mechanistic understanding of the intricate transcriptional relationships among homologous proteins in a core cardiac transcription factor family.

4.2 Quantification of relative *Mef2* transcript expression in NRVMs

While expression of *Mef2* transcripts has been qualitatively examined in mouse cardiac development (Edmonson *et al.* 1994), the relative expression of the four mammalian *Mef2* transcripts has never been quantified specifically in cardiomyocytes. Using quantitative RT-PCR, we found that *Mef2a* is the most abundant isoform in neonatal rat ventricular myocytes (NRVMs) (Table 4.1). *Mef2c* and -*d* displayed similar expression levels and were 22- to 25-fold lower than *Mef2a*, respectively. *Mef2b* transcripts were largely undetectable in NRVMs, expressed at levels 350-fold lower than that of *Mef2a*. Based on these results, MEF2A, C, and D were deemed to be the

predominant MEF2 isoforms expressed in NRVMs and our analysis is restricted to these three MEF2 factors.

4.3 Neonatal cardiomyocyte survival is dependent on MEF2A and –D but not –C

NRVMs were transduced with MEF2 isoform-specific shRNA adenoviruses and examined three days post-transduction. Analysis of MEF2 expression in each of the isoform knockdowns revealed efficient inhibition of the respective MEF2 isoform (Figure 4.1). We have previously demonstrated the isoform-specificity of these shRNAs and did not observe cross-reactivity with other MEF2 proteins (Estrella *et al.* 2015). Interestingly, we observed downregulation of *Mef2d* in *Mef2a* deficient NRVMs, and a reciprocal downregulation of *Mef2a* in *Mef2d* NRVMs (Figure 4.1). In contrast, *Mef2c* deficiency did not affect endogenous expression of *Mef2a* or -*d*. Finally, with the exception of an upregulation of *Mef2c* in *Mef2d* deficient NRVMs, there was no compensatory upregulation of *Mef2* isoforms in response to our acute ablation of individual MEF2 isoform expression using these vectors. Given the previously described specificity of these shRNAs, we conclude that the reciprocal downregulation of *Mef2a* and *–d* transcripts is likely to be transcriptional co-regulation within the MEF2 family in NRVMs.

Previous studies have described distinct *in vivo* loss of function phenotypes for mammalian MEF2 family members (Lin *et al.* 1997, Naya *et al.* 2002, Kim *et al.* 2008). We evaluated whether acute *Mef2* isoform knockdown caused distinct morphological defects in NRVMs. Knockdown of *Mef2a* resulted in reduced cardiomyocyte number (Figure 4.2), decreased viability (Figure 4.3A), and increased cleaved caspase-3 activity,

an indicator of programmed cell death (Figure 4.3B). *Mef2d* knockdown also resulted in a significant reduction in cardiomyocyte viability and increase in caspase-3 activity (Figure 4.2, 4.3). By contrast, *Mef2c* knockdown did not impair NRVM survival. These results indicate that MEF2A and MEF2D are necessary for neonatal cardiomyocyte survival, and MEF2C is not.

To determine whether MEF2 proteins function redundantly in cardiomyocyte survival we performed double and triple MEF2 isoform knockdowns. Pairwise knockdowns of *Mef2* isoforms did not modulate the previously observed impaired viability phenotype (Figure 4.3), and an effect of *Mef2c* knockdown did not emerge in combination with *Mef2a* knockdown, *Mef2d* knockdown, or *Mef2a/d* knockdown NRVMs (Figure 4.2, 4.3). These results demonstrate that MEF2C is dispensable for NRVM survival and does not have a role masked by the presence of MEF2A or -D in normal NRVM survival. However, while MEF2A and -D appear to both be required for NRVM survival, *Mef2a*-deficiency led to earlier loss of NRVM survival with adverse effects on viability observable at 48 hr (data not shown).

4.4 MEF2 overexpression in MEF2A-depleted NRVMs

To determine if overexpression of any MEF2 isoform is sufficient to rescue the *Mef2a* deficient loss of NRVM viability, we overexpressed MEF2A, C, D, and MEF2-VP16, a constitutive MEF2 activator, in *Mef2a*-deficient myocytes. Overexpression of MEF2A, D, or MEF2-VP16 abrogated the loss of cardiomyocytes and significantly decreased cleaved caspase-3 activity in *Mef2a*-deficient NRVMs (Figure 4.4 and 4.5). By

contrast, overexpression of MEF2C failed to prevent cardiomyocyte loss and did not significantly reduce cleaved caspase-3 activity in *Mef2a* knockdown NRVMs.

Based on this intriguing isoform-specific difference we bolstered our analysis by measuring DNA degradation using propidium iodide staining followed by flow cytometry. As shown in Figure 4.6, *shLacZ* control NRVMs contain a population of cells with diploid (2n) through tetraploid (4n) DNA content portraying the known heterogeneity of mono- and binucleated neonatal myocytes (Figure 4.6A, left panel). *Mef2a* knockdown resulted in a significant redistribution of this DNA content profile, with the emergence of a peak representing, myocytes containing sub-2n DNA content (Figure 4.6A, right panel), consistent with elevated DNA fragmentation observed in apoptosis.

We subsequently evaluated the ability of MEF2 isoforms to reduce the sub-2n fragmented DNA fraction and restore normal DNA content in *Mef2a*-deficient NRVMs. Overexpression of all MEF2 isoforms promoted similar effects on the sub-2n population. MEF2A, C, and MEF2-VP-16 significantly reduced the number of myocytes with this irregular sub-2n DNA content (Figure 4.6B, right set of bars), and MEF2D overexpression also reduced the sub-2n myocyte population but this difference did not reach statistical significance. These results demonstrate that overexpression of MEF2 isoforms is sufficient to diminish DNA fragmentation in *Mef2a*-deficient NRVMs. Interestingly, while MEF2C overexpression failed to rescue cell viability and reduce cleaved caspase-3 activity in MEF2A depleted NRVMs, it had a favorable effect on genomic DNA integrity. These results suggest that MEF2C is distinct from other MEF2

isoforms in that its apparent compensatory activity is restricted to a late stage in the apoptotic pathway, while being unable to modulate earlier steps, or ultimately affect survival.

Further analysis of the DNA content profile revealed previously uncharacterized effects of MEF2 isoform overexpression on the cardiomyocyte genome. MEF2A overexpression in *Mef2a*-deficient NRVMs resulted in a significant reduction in the sub-2n population and a modest increase in myocytes harboring 2n, 2n-4n, and 4n DNA content (Figure 4.6C). These increases likely represent the myocyte population that was rescued from apoptotic DNA fragmentation by MEF2A overexpression. A similar effect and profile was observed for MEF2-VP16. By contrast, MEF2D overexpression in *Mef2a* deficiency resulted in significantly more myocytes with 2n compared to MEF2A overexpression and fewer cells containing 2n-4n and 4n DNA content. Curiously, MEF2C overexpression in the MEF2A depleted background displayed a profile quite distinct from MEF2A, D, and MEF2-VP16. This population displayed a significant decrease in diploid (2n) NRVMs and a significant increase in myocytes with 2n-4n and 4n DNA content. By thoroughly analyzing the DNA content profile of *Mef2a* deficient NRVMs overexpressing various MEF2 proteins we have demonstrated that, despite their ability to rescue DNA fragmentation (sub-2n), these isoforms elicited differing effects on the genomic DNA content.

4.5 Genome-wide transcriptomics and comparative analysis of individual MEF2 knockdowns in NRVMs

The contrasting effect of MEF2A, C, and D on cardiomyocyte survival and DNA content suggested distinct regulatory functions of these isoforms despite their largely indistinguishable transcriptional activities *in vitro.* This hypothesis is also supported by previously characterized distinct *in vivo* loss-of-function phenotypes. Thus, we performed global gene expression profiling to determine what sets of genes and cellular processes are regulated by individual MEF2 proteins in neonatal cardiomyocytes.

Transcriptomic analysis of NRVMs depleted of individual MEF2 proteins resulted in overlapping but largely distinct dysregulated gene sets. Using stringent statistical criteria (see Chapter Two), the most striking effect on gene expression in NRVMs was observed in MEF2A knockdown. As shown in Figure 4.7A, knockdown of *Mef2a* revealed 3,197 significantly dysregulated genes, representing 43% of the total number of dysregulated genes. Knockdown of *Mef2c* and *Mef2d* resulted in only 471 and 786 dysregulated genes, or 6.4 and 10.6% of the total, respectively. In terms of overlapping dysregulated genes, MEF2A and D gene sets had 20% of the genes in common, which was the highest percent of all the MEF2 isoform comparisons (Figure 4.7B). This was followed by 9% of commonly dysregulated genes between MEF2A and C. The lowest overlap was observed in the genes shared between MEF2C and D, representing 2.8% of the total. Finally, only 8.2% of the dysregulated genes were shared in all three MEF2 isoform knockdowns (Figure 4.7B).

These dysregulated gene expression levels were subsequently validated by qRT-PCR analysis on a subset of the top dysregulated genes, top two upregulated and down-regulated genes, from each individual MEF2 knockdown. As shown in Figure 4.8, the vast majority of genes in each MEF2 isoform gene set examined displayed the expected dysregulation.

4.6 Classification of cellular processes in MEF2 knockdown gene sets

To gain insight into the distinct roles of the MEF2 family in NRVMs, the dysregulated, non-overlapping genes in each subgroup were categorized into cellular processes using Ingenuity Pathway Analysis (IPA).

IPA of MEF2 isoform-sensitive gene sets revealed vastly different cellular processes in the preferentially dysregulated target genes from each MEF2 knockdown (Table 4.2). Many genes distinctly sensitive to MEF2A play roles in cell-cell junction signaling and cancer pathways. By contrast, genes preferentially regulated by MEF2C are involved in energy production in mitochondria. And genes regulated by MEF2D are involved in cellular growth (HIPPO pathway) and survival (PI-3 kinase signaling). Finally, the group of genes sensitive to all three MEF2 isoforms functions in multiple aspects of the cell cycle including DNA replication and DNA damage checkpoints. Notably, this overlapping category did not have pathways in common with any of the significantly enriched processes in the individual MEF2 gene sets. These results reveal the breadth of cellular processes under MEF2 control and suggest that these gene programs have evolved sophisticated transcriptional mechanisms to differentiate among MEF2 isoforms in cardiomyocytes.

4.7 Complex and antagonistic patterns of dysregulated gene expression among MEF2 family members.

The emergence of a common cell cycle gene program regulated by all MEF2 isoforms piqued our interest as this could potentially explain the effects on cardiomyocyte survival and genomic DNA content. Because this subset of genes is sensitive to all MEF2 isoforms, we hypothesized that, based on their largely indistinguishable transcriptional activities *in vitro*, these genes would be similarly regulated by each isoform and provide a logical starting point to mechanistically dissect MEF2-dependent gene regulation in cardiomyocytes.

Remarkably, analysis of the dysregulated patterns of the 610 common genes revealed that the vast majority of these genes were not similarly affected by knockdown of specific MEF2 isoforms (Figure 4.9). These comparisons revealed four distinct groups based on similarity of dysregulation in all three MEF2 knockdowns or combinations of two MEF2 isoforms, e.g. Shared, MEF2A/D, MEF2A/C, and MEF2C/D. Strikingly, only about one-third of the MEF2 isoform-sensitive genes were dysregulated in the same direction (Shared), but nearly two-thirds of the genes were differentially affected and showed the opposite dysregulation in at least one MEF2 isoform knockdown (Figure 4.9, right). Of these, the most predominant pattern of was the similarity in gene dysregulation by *Mef2a* and *-d* knockdown and the opposite dysregulation by *Mef2c* knockdown as shown in the MEF2A/D row (48%; Figure 4.9). These patterns suggest that a subset of pathways in cardiomyocytes dependent on all MEF2 isoforms are not regulated similarly,

extending the notion of isoform-specific regulation to genes functioning in common cellular processes.

Given the unexpected and disparate effects of dysregulation within the common group we performed IPA on those genes within the various regulatory patterns to obtain a comprehensive analysis of the types of cellular processes for each pattern. As shown in Table 4.3, the pathways for each regulatory pattern were dramatically different. Genes regulated in the same manner by all three MEF2 isoforms (Shared; all up- or all downregulated) have been shown to function primarily in fibrosis and amino acid biosynthesis. Those genes regulated in the same manner by MEF2A and C (A/C) and MEF2C and D (C/D) isoform pairs, play a role in signal transduction but the specific ligand-receptor pathway for each of these groups was quite distinct. The most enriched pathway identified in the A/C pattern of regulation belonged to ephrin signaling, a critical pathway in cell positioning and guidance in development. The genes present in the C/D regulatory pattern were enriched for cytokine and interferon pathways. The most intriguing result, however, was obtained for the genes exhibiting the MEF2A and D (A/D) regulatory pattern, where genes were similarly affected by *Mef2a* and *-d* knockdown but displayed the opposite dysregulation by *Mef2c* knockdown. Pathway analysis of this particular cohort, which had the largest collection of genes, revealed the cell cycle as the most significantly enriched pathway. This helps to explain the enrichment of the cell cycle program in our analysis of the 610 overlapping group of genes. Moreover, these data suggest a previously undescribed role for MEF2A and C protein isoforms in cell cycle control in cardiomyocytes, and independently confirm our

previous observations of MEF2D-dependent regulation of the cell cycle (Estrella *et al.* 2015)

Based on this interesting finding we next validated the expression of select cell cycle genes in the individual MEF2 isoform knockdowns. These genes have been shown to function in DNA replication and checkpoint control. As shown in Figure 4.10, both MEF2A and D inhibition resulted in the upregulation of the cell cycle genes *Mcm3, -5, -6, cyclin E,* and *Pcna*. Upregulation of the cell cycle program did not lead to increased proliferation but rather cell cycle re-entry followed by programmed cell death, and is entirely consistent with our previous characterization of MEF2D depleted NRVMs (Estrella *et al.* 2015). By contrast, *Mef2c* knockdown resulted in downregulation of cell cycle gene expression (Figure 4.10).

Given that cell cycle and differentiation programs are often competing forces in the cell, we complemented this analysis by examining the expression of representative sarcomere genes which are established markers of differentiated cardiomyocytes. Expression of the sarcomere genes *myosin heavy chain 7 (Myh7), myosin light chain 2 (Myl2), myomesin 1 and 2, and titin,* in MEF2A and D depleted NRVMs was significantly downregulated whereas these genes were upregulated in MEF2C-depleted cells (Figure 4.11). These data reveal a previously unappreciated mechanism of MEF2-dependent gene regulation in cardiomyocytes, one in which MEF2 protein isoforms antagonistically regulate gene programs despite their similar transcriptional activities *in vitro*. Specifically, MEF2A and -D are required for repression of cell cycle genes, and

activation of a subset of sarcomeric markers, and MEF2C plays an antagonistic role by activating cell cycle genes and repressing sarcomeric markers of differentiation.

4.8 Identification of distinct transcription factor modules associated with MEF2-dependent cell cycle and sarcomere genes

Given the lack of evidence demonstrating differences in DNA consensus sequence preferences of MEF2 isoforms, we hypothesized that the antagonistic regulatory patterns resulted from specific interactions with transcriptional coregulators. Therefore, upstream regulatory regions were computationally analyzed for discrete transcription factor (TF) modules harboring a MEF2 binding site within 50 base pairs of a predicted TF binding site. To identify these TF modules enriched in cell cycle genes, we performed module-based motif enrichment analysis (Genomatix). Modules were considered significantly enriched in a set of promoters if the z-score was greater than 2. As shown in Table 4.4, although similar TF modules were found to be overrepresented in both cell cycle and sarcomere genes the vast majority were unique to each gene set. Regarding the similar TF modules between the two groups, the basic helix-loop-helix (bHLH) proteins (or E-box binding factors) such as HAND, Twist, and Mesp play prominent and diverse roles in cardiogenesis such as specification, proliferation, and differentiation (Bondue *et al.* 2010, Conway *et al.* 2010, VanDusen *et al.* 2012), thus it is not surprising to find them overrepresented in both gene categories. Similarly, the MADS box factor SRF and the steroid receptor RXR which have pleiotropic gene regulatory functions (Niu *et al.* 2007, Evans *et al.* 2014), were enriched in TF modules within the regulatory regions of both cell cycle and sarcomere genes. Analysis of the largely unique

modules revealed transcriptional regulators that function downstream of Notch and Hedgehog signaling. These evolutionarily conserved signal transduction pathways emerged as the most interesting candidates because of their important role not only in developmental gene regulation but also in cardiogenesis (Rochais *et al.* 2009, de la Pompa *et al.* 2012). These upstream signals could be the linchpin to establish isoform selectivity in the MEF2-dependent regulation of cell cycle and sarcomere gene programs in cardiomyocytes in cardiac development.

4.9 Notch and Hedgehog signaling coordinate MEF2 isoform-specific regulation of cell cycle and differentiation programs.

To determine whether Notch and/or Hedgehog signaling modulate MEF2-dependent gene regulation in a program-specific fashion we initially evaluated the ability of NRVMs to respond to these pathways by examining the expression of their known downstream target genes, some of which are mediators of these signals. As shown in Figure 4.12, transduction of NRVMs with adenoviruses overexpressing constitutively active Sonic hedgehog (SHH-N) and the Notch intracellular domain (N1ICD) induced expression of the GLI (*Gli1-3*) and vertebrate enhancer of split (*Hey2* and *Hes1*) TFs, respectively.

Overexpression of SHH-N was found to diminish the upregulation of cell cycle gene expression in NRVMs that were depleted of MEF2A and -D (Figure 4.13, left). SHH-N alone also had a repressive effect on cell cycle gene expression. In contrast, SHH-N had no significant effect on the expression of sarcomere genes either in the presence or absence of MEF2A and -D (Figure 4.13, right).

Conversely, constitutive Notch activity further upregulated cell cycle gene expression in both MEF2A and D-depleted NRVMs (Figure 4.14, left). Notch alone had a modest effect on the expression of cell cycle genes. These data suggest that presence of MEF2A or -D represses the ability of Notch signaling to activate cell cycle gene expression. Additionally, Notch was sufficient to activate sarcomere genes, but this activation required the presence of MEF2A or -D (Figure 4.14, right). As depicted in the model in Figure 4.15, the ability of the Hedgehog signaling pathway to modulate MEF2A and D-dependent gene regulation is restricted to the cell cycle program. By contrast, Notch modulates the MEF2A and D-dependent cell cycle and sarcomere programs in NRVMs but in a reciprocal fashion.

4.10 Discussion

The mechanisms of coordinating cell cycle and differentiation programs in cardiomyocytes remain poorly understood. Here, we have used acute isoform-specific knockdown of the mammalian MEF2 proteins to demonstrate that protein isoforms of this evolutionarily conserved, core cardiac transcription factor have distinct regulatory roles in neonatal cardiomyocytes. Interestingly, we have also uncovered a previously uncharacterized antagonistic regulatory role between individual members of the MEF2 family in the regulation of cell cycle and differentiation gene programs. These disparate roles are most evident in cardiomyocyte survival, where a differential requirement of specific MEF2 isoforms is observed for this process. These results reveal a mechanism whereby two mutually exclusive regulatory pathways can function simultaneously to promote proper development and growth of the heart.

To our knowledge MEF2 represents the first transcription factor to have a dual and antagonistic function in the regulation of both cell cycle and differentiation (sarcomere) gene programs in cardiomyocytes. The forkhead box transcription factor family was previously demonstrated to have antagonistic roles in neonatal cardiomyocyte cell cycle withdrawal and proliferation (Sengupta *et al.* 2013). However, the opposing function of two family members, FoxO and FoxM1, was restricted to the cell cycle program. These TFs were shown to coordinate the regulation of cell cycle activators and inhibitors depending on nutrient availability or growth factor levels. FoxO was demonstrated to prevent neonatal cardiomyocyte proliferation through direct negative regulation of *IGF1* whereas FoxM1 positively regulated this growth factor gene. In addition, these differential regulatory effects were mediated upstream by the activation status of AMPK. Since differentiation genes were not examined in that study it is unknown whether the forkhead TFs regulate this gene program in an antagonistic fashion.

Another example of antagonistic transcriptional regulation is found in the relationship between Irx3 and Irx5. These two transcription factors share redundant functions during the development of the mammalian heart, but appear to play divergent roles in adult cardiac electrophysiology (Gabori *et al.* 2012). Single knockouts of each Irx factor leads to a loss in appropriate depolarization gradient, but double knockouts restore the appropriate polarization gradient. These results suggest that Irx5 is required to repress the function of Irx3 in specific regions of the adult heart, and provides an additional example of homologous cardiac transcription factors playing an antagonistic relationship that is required for normal cardiac homeostasis.

We have shown that MEF2A and MEF2D were able to rescue loss of cardiomyocyte viability in the context of *Mef2a*-deficiency. Interestingly, MEF2C overexpression in MEF2A depleted NRVMs failed to rescue viability and cleaved caspase 3 activation, but was capable of reducing apoptotic DNA degradation. Ultimately, MEF2C overexpression had no effect on survival, suggesting that MEF2C activity is not functionally redundant with and cannot compensate for MEF2A in the more proximal events of programmed cell death.

We have previously described canonical pathways in the common set of dysregulated genes in individual MEF2 knockdowns in skeletal myoblasts (Estrella *et al.* 2015). Because striated muscle cell types share many gene programs we compared the co-regulated MEF2 pathways between skeletal myoblasts and cardiomyocytes. Overall, there was no obvious overlap in the pathways regulated by all MEF2 isoforms between skeletal and cardiac myocytes. The co-regulated MEF2 pathways in skeletal myoblasts were dominated by signal transduction cascades whereas the co-regulated pathways in cardiomyocytes were predominately associated with cell cycle control. These comparisons reveal that distinct gene programs in these highly related cell types have evolved to largely distinct roles for MEF2 in genes transcriptionally co-regulated by all family members in skeletal and cardiac muscle.

Comparison of pathways preferentially sensitive to individual MEF2 knockdowns in skeletal myoblast with our present data in cardiomyocytes shows distinct roles for MEF2 isoforms in these related striated muscle cell types. Specifically, comparison of gene sets preferentially sensitive to MEF2A in cardiomyocytes and skeletal myoblasts

revealed only two pathways, Molecular Mechanisms of Cancer and Germ Cell-Sertoli Cell Junction Signaling, were shared in both muscle cell types. The remaining pathways in NRVMs and skeletal myoblasts dependent on MEF2A did not have any obvious functional relationships to each other. A recently published study investigated the overlap of MEF2A binding in skeletal myoblasts and cardiomyocytes using ChIP-exo (Wales *et al.* 2014). While many of their enriched GO terms were distinct from our canonical pathways analysis, induction of apoptosis and cell death were among the enriched pathways in cardiomyocytes. These results support our observations that MEF2A is required for cardiomyocyte survival.

Interestingly, several cell cycle pathways (G1/S Checkpoint Regulation and Estrogen-mediated S-phase Entry) were shown to be significantly enriched in MEF2C depleted skeletal myoblasts. This is in stark contrast to the enrichment of this gene program in MEF2A and D depleted cardiomyocytes. The most significantly enriched canonical pathways preferentially dysregulated by *Mef2c* knockdown in NRVMs are associated with energy metabolism, suggesting a distinct role for MEF2C in cardiomyocyte metabolism that is not shared in skeletal muscle.

Knockdown of *Mef2d* displayed the most disparate effect on pathway enrichment in both striated muscle cell types. There was very little overlap between specific pathways preferentially dysregulated in skeletal and cardiac myocytes. For this MEF2 isoform, cytokine, hypoxia, and AMPK signaling were enriched in skeletal myoblasts whereas HIPPO, PI-3kinase, and neuregulin pathways were sensitive to MEF2D in NRVMs. The majority of pathways preferentially dysregulated by *Mef2d* knockdown in

both models are generally associated with signal transduction, suggesting a distinct role for MEF2D in integrating cell signaling in both muscle cell types.

The presence of canonical MEF2 binding sites in both cell cycle and sarcomere gene sets suggested that differential regulation might be mediated by program exclusive co-regulators. Indeed, we observed a lack of significant overlap in overrepresented transcription factor binding sites between the cell cycle and sarcomere genes. Among the most significantly enriched binding sites in cell cycle and sarcomere genes belonged to the TFs that mediate Hedgehog and Notch signaling, respectively. These predictions were validated by the ability of these upstream signals to modulate MEF2-dependent gene regulation.

The Hedgehog signaling pathway has an early role in patterning of the developing heart (Rochais *et al.* 2009). Curiously, the Hedgehog signaling pathway has been shown to intersect with MEF2C in cardiomyocyte differentiation. That particular study showed that the Gli transcription factor regulates *Mef2c* expression to promote cardiogenesis (Voronova *et al.* 2012). In that study it was shown that the Gli transcription factor regulates *Mef2c* gene expression to promote cardiogenesis. Our present report suggests that Hedgehog signaling can cooperate with MEF2 to modulate cell cycle gene expression.

Notch has been shown to play an important role in cardiac morphogenesis in multiple cell lineages in the heart including cardiomyocytes (de la Pompa *et al.* 2012). In addition, previous studies have shown that the Notch signaling pathway modulates MEF2 activity in mammalian skeletal myoblasts (Wilson-Rawlins *et al.* 1999, Shen *et al.* 2006).

Notch also synergizes with MEF2 to promote proliferation in fly development (Pallavi *et al.* 2012). Although a specific function for Notch has not been ascribed to sarcomere gene regulation it has been shown to promote cell cycle re-entry of neonatal cardiomyocytes (Campa *et al.* 2008). Our present data suggest that Notch induction of proliferative markers is repressed by MEF2A and -D, introducing a potential mechanism for the loss of proliferative capacity observed in those studies. These results suggest a fundamental regulatory mechanism centered on the relative abundance of MEF2A, -C, and –D that mediates quiescence and terminal differentiation in cardiomyocytes.

We have demonstrated that protein isoforms of the mammalian MEF2 transcription factor family antagonistically regulate cell cycle and differentiation gene programs in neonatal cardiomyocytes. Moreover, the ability of MEF2A and D to regulate disparate gene programs is modulated by Hedgehog and Notch signaling. These results introduce the possibility of a fundamental mechanism that determines the differentiation state of cardiomyocytes based on the relative expression levels of a core cardiac transcription factor family with respect to each other. In the future it would be interesting to determine whether the TFs that function downstream of Notch and Hedgehog physically interact with MEF2 proteins to antagonistically regulate the cell cycle and differentiation.

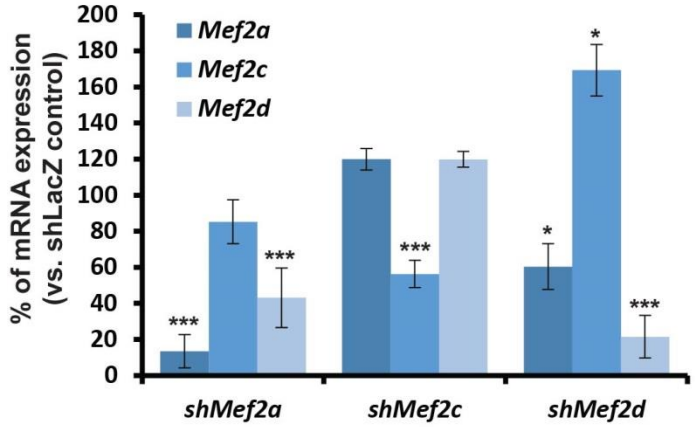

Figure 4.1 *Mef2* shRNA adenoviral transduction efficiently and specifically depletes targeted *Mef2* transcripts. Neonatal cardiomyocytes were transduced with *Mef2* shRNA adenovirus for 48 hr, and *Mef2* transcripts were measured. Quantitative RT-PCR analysis of specific shRNA knockdown efficiency shows significant knockdown of targeted *Mef2* transcripts in neonatal cardiomyocytes. Data are means (n=3) ± S.E.M. (error bars). *, $p<0.05$; ** $p<0.01$; *** $p<0.001$.

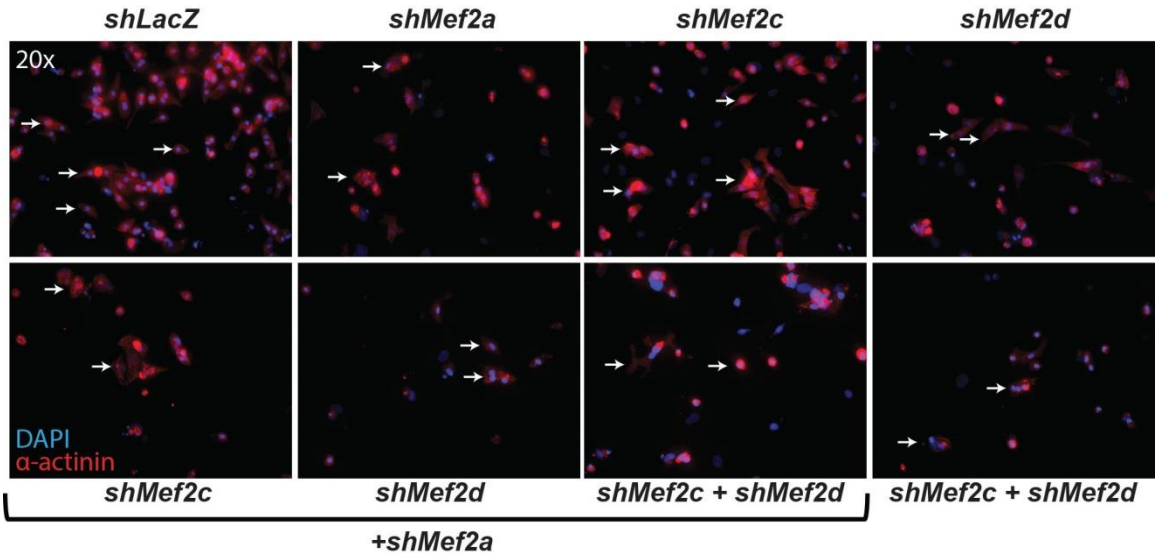

Figure 4.2 Neonatal cardiomyocyte survival is dependent on MEF2A and –D, but not MEF2C. Neonatal cardiomyocytes were transduced with *Mef2* shRNA adenovirus for 48 hr then fixed for immunocytochemistry. Immunofluorescent images of neonatal cardiomyocytes treated with combinations of *Mef2* shRNAs shows a decrease in cell numbers in cultures treated with *Mef2a* and *–d* shRNA, but not *Mef2c* shRNA alone. Neonatal cardiomyocytes are characterized by α-actinin immunoreactivity (red) and counterstained with DAPI (blue). White arrows depict examples of typical cardiomyocyte morphology.

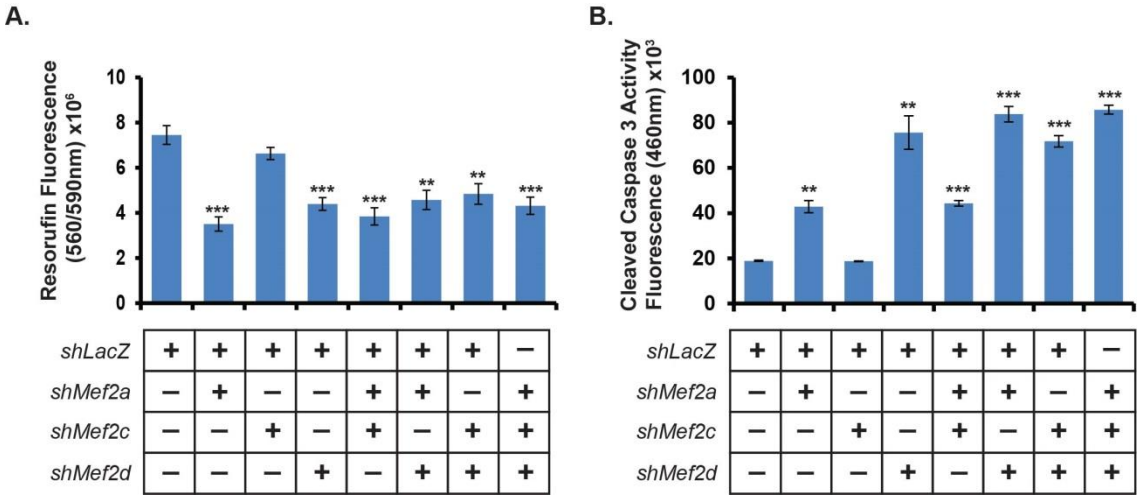

Figure 4.3 *Mef2a* and *–d*, but not *Mef2c* knockdown causes a decrease in cell viability and an increase in Caspase 3 activity. A, Viability of neonatal cardiomyocytes treated with *Mef2a* shRNA was measured using CellTiter Blue viability assay. *Mef2a* and *–d* depleted myocytes show a significant loss of viability that is not observed in *Mef2c* depleted cardiomyocytes. **B**, Ac-DEVD-AMC is an activated Caspase 3 substrate that produces fluorescence upon cleavage. Neonatal cardiomyocytes were treated with *Mef2* shRNA then lysates were incubated with Ac-DEVD-AMC to measure cleaved Caspase 3 activity. *Mef2a* and *–d* depleted myocytes show a significant increase in Caspase 3 activity that is not observed in *Mef2c* depleted cardiomyocytes. Data are means (n=3) ± S.E.M. (error bars). *, $p<0.05$; ** $p<0.01$; *** $p<0.001$.

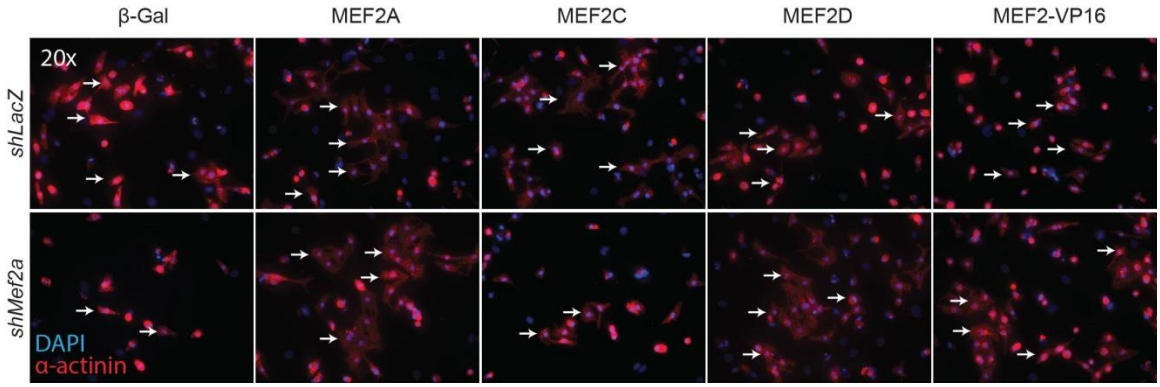

Figure 4.4 Overexpression of MEF2A, -D, and MEF2-VP16 reduces loss of cell viability caused by MEF2A knockdown. Neonatal cardiomyocytes were co-transduced with *Mef2a* shRNA and a MEF2 overexpression adenovirus for 48 hr, and then fixed for immunocytochemistry. Immunofluorescent images of NRVMs co-transduced with *Mef2a* shRNA and a MEF2 overexpression virus show that overexpression of MEF2A, -D, and a constitutively-active MEF2-VP16 increases the number of α-actinin positives cells. MEF2C overexpression did not appear to rescue the number of α-actinin positives cells. Neonatal cardiomyocytes are characterized by α-actinin immunoreactivity (red) and counterstained with DAPI (blue). White arrows depict examples of typical cardiomyocyte morphology.

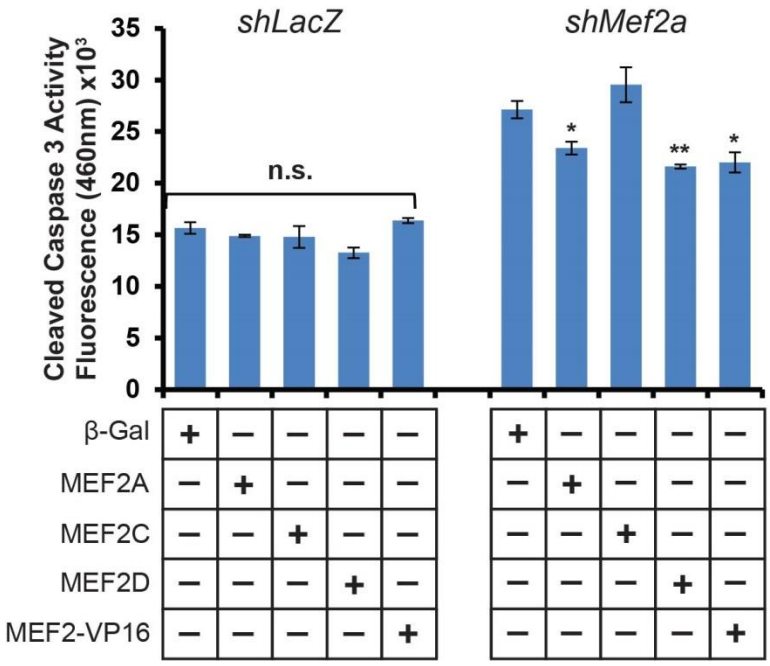

Figure 4.5 Overexpression of MEF2A, -D, and –VP16 reduces caspase 3 activity in *Mef2a*-deficient neonatal cardiomyocytes. Ac-DEVD-AMC is an activated caspase 3 substrate that produces fluorescence upon cleavage. Neonatal cardiomyocytes were treated with *Mef2* shRNA then lysates were incubated with Ac-DEVD-AMC to measure cleaved caspase 3 activity. Overexpression of MEF2A, -D, and MEF2-VP16, but not MEF2C leads to a reduction in activated caspase 3 in *Mef2a*-deficient neonatal cardiomyocytes. Data are means (n=3) ± S.E.M. (error bars). *, $p<0.05$; ** $p<0.01$; *** $p<0.001$.

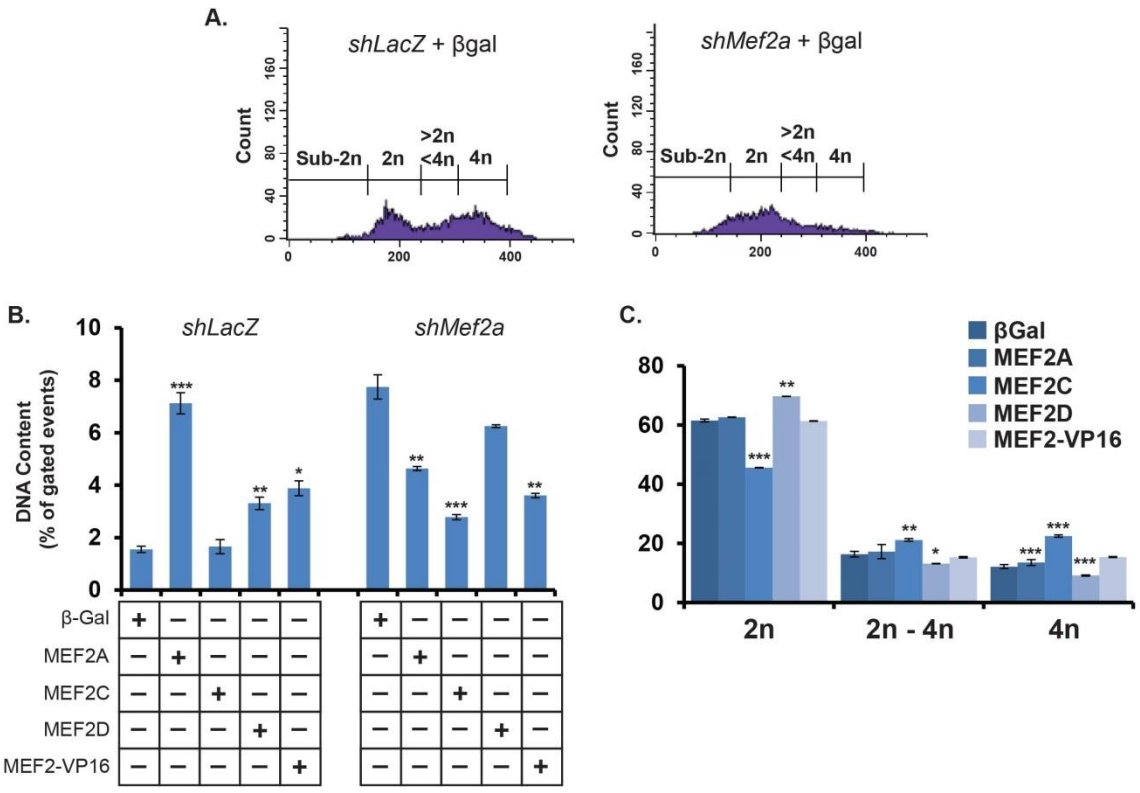

Figure 4.6 Measurement of DNA content using propidium iodide staining. Neonatal cardiomyocytes where co-transduced with *Mef2a* shRNA and an overexpression virus for 48hr. Cardiomyocytes were then fixed and stained with propidium iodide, and flow cytometry was performed to determine DNA content. **A**, Propidium iodide stained flow cytometry shows the emergence of a significant cell population with sub-2n DNA content in *Mef2a* shRNA treated-NRVMs. **B**, Quantification of flow cytometry cell populations measuring DNA content shows an increase in cells with sub-2n DNA content upon treatment with *Mef2a* shRNA, and a reduction of this group upon overexpression of MEF2 constructs. **C**, Measurement of neonatal cardiomyocytes containing 2n, 2n-4n, and 4n DNA content. Data are means (n=3) ± S.E.M. (error bars). *, $p<0.05$; ** $p<0.01$; *** $p<0.001$.

A.

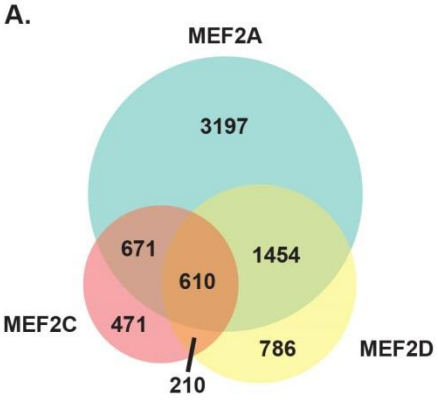

B.

MEF2 Knockdown	Dysregulated Genes	% of Total
MEF2A	3197	43.2
MEF2C	471	6.37
MEF2D	786	10.6
MEF2A + MEF2C	671	9.1
MEF2A + MEF2D	1454	19.7
MEF2C + MEF2D	210	2.8
All MEF2	610	8.2

Figure 4.7 Comparative analyses of MEF2 isoform-specific transcriptomes. Neonatal cardiomyocytes were transduced with *Mef2* shRNA for 48 hr, and then microarrays were performed to measure relative gene expression vs. *shLacZ* (negative control, n=3 arrays for each shRNA). **A**, Genes dysregulated in individual *Mef2* isoform knockdowns were grouped into statistically related gene cohorts. A composite Venn diagram incorporating all overlapping gene sets (as determined by the Tukey's HSD *post hoc* test , $p<0.05$). **B**, A summary of total significantly dysregulated ($p<0.05$) genes in each *Mef2* isoform shRNA knockdown reveals that 43% of genes are sensitive to *Mef2a* knockdown, 6% are sensitive to *Mef2c* knockdown, and 10% are sensitive to *Mef2d* knockdown.

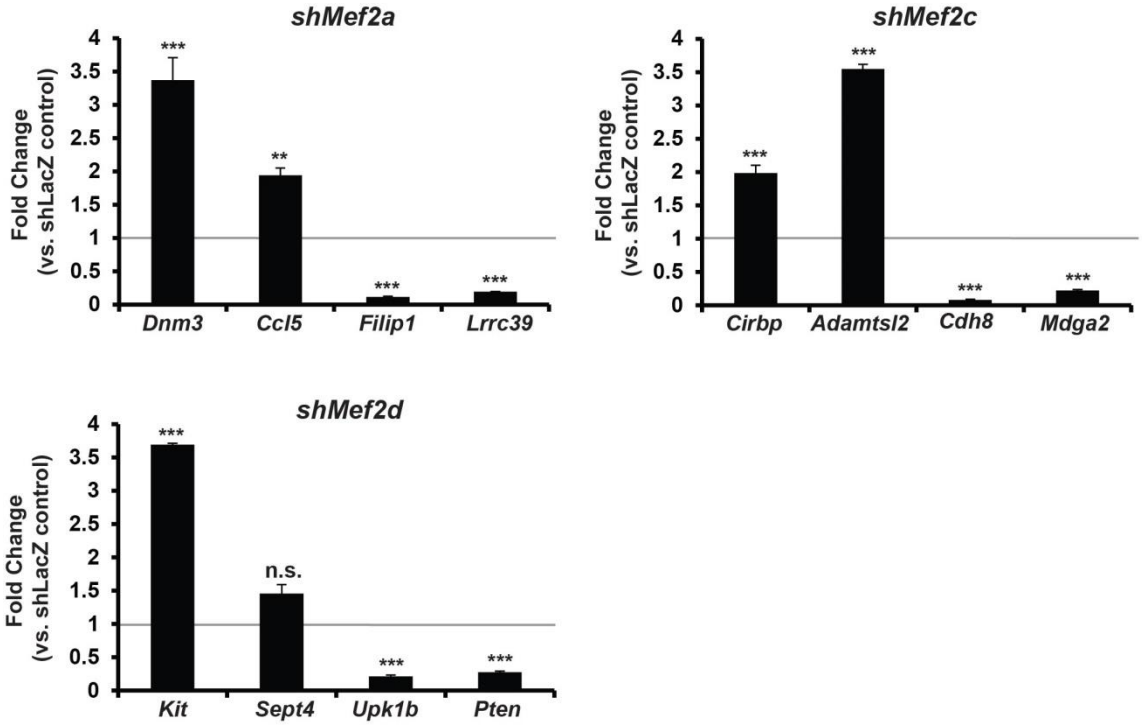

Figure 4.8 Validation of microarray gene dysregulation. Quantitative RT-PCR analysis of a subset of genes preferentially dysregulated in an individual *Mef2* shRNA knockdown microarray. *Dnm3*, dynamin 3; *Ccl5*, chemokine (C-C motif) ligand 5; *Filip1*, filamin A interacting protein 1; *Lrrc39*, leucine rich repeat containing 39; *Cirbp*, cold inducible RNA binding protein; *Adamtsl2*, ADAMTS-like 2; *Cdh8*, cadherin 8; *Mdga2*, MAM domain containing glycosylphosphatidylinositol anchor 2; *Kit*, v-kit Hardy-Zuckerman 4 feline sarcoma viral oncogene; *Sept4*, septin 4; *Upk1b*, uroplakin 1B; *Pten*, Phosphatase and tensin homolog. Gray line represents no dysregulation, data are means (n=3) ± S.E.M. (error bars). *, $p<0.05$; ** $p<0.01$; *** $p<0.001$.

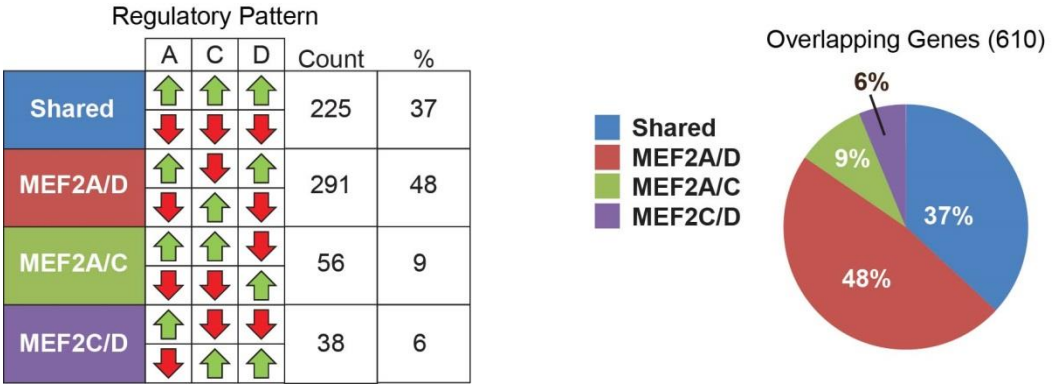

Figure 4.9 Distinct regulatory patterns of overlapping genes sensitive to all MEF2 isoforms. Distribution of genes dysregulated in each individual knockdown based on pattern of dysregulation across all knockdowns. Genes dysregulated in the same direction in each *Mef2* knockdown represent 37% of overlapping genes, genes dysregulated in the same direction by *Mef2a* and *-d* knockdown represent 48% of overlapping genes, genes dysregulated in the same direction by *Mef2a* and *-c* knockdown and *Mef2c* and *-d* knockdown represent 9 and 6% of overlapping genes, respectively.

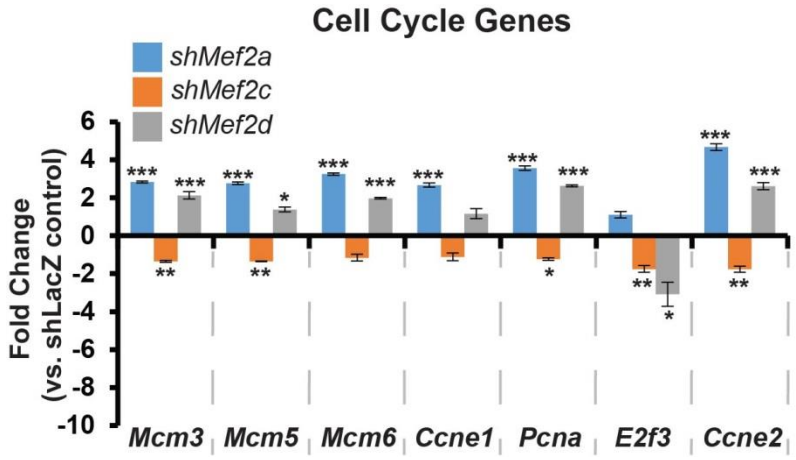

Figure 4.10 Cell cycle related genes dysregulated in *Mef2* isoform knockdown. Quantitative RT-PCR analysis of a subset of cell cycle related genes show upregulation upon the knockdown of *Mef2a* and *-d*, and downregulation in *Mef2c* knockdown. *Mcm3*, minichromosome maintenance component 3; *Mcm5*, minichromosome maintenance component 5; *Mcm6*, minichromosome maintenance component 6; *Ccne1*, cyclin e1; *Pcna*, proliferating cell nuclear antigen; *E2f3*, E2F transcription factor 3; *Ccne2*, cyclin e2. Data are means (n=9) ± S.E.M. (error bars). *, $p<0.05$; ** $p<0.01$; *** $p<0.001$.

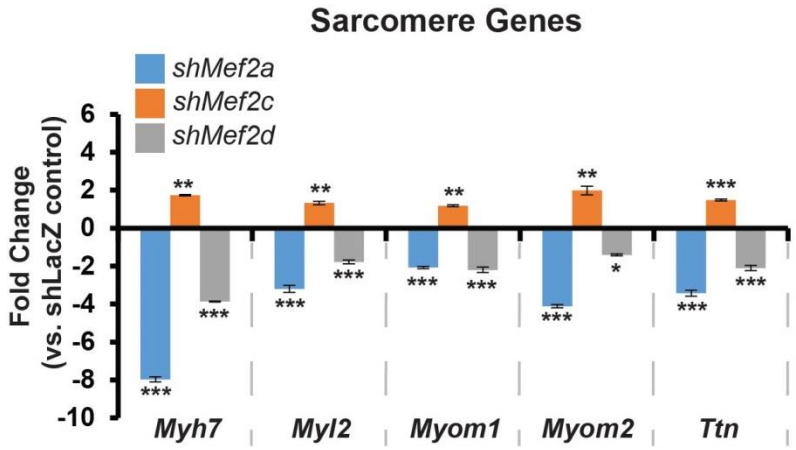

Figure 4.11 Sarcomere related genes dysregulated in *Mef2* isoform knockdown. Quantitative RT-PCR analysis of a subset of sarcomere related genes show downregulation upon the knockdown of *Mef2a* and *-d* and upregulation in the knockdown of *Mef2c*. *Myh7*, myosin heavy chain 7, cardiac muscle, beta; *Myl2*, myosin light polypeptide 2, regulatory, cardiac, slow; *Myom1*, myomesin 1; *Myom2*, myomesin 2; *Ttn*, titin. Data are means (n=9) ± S.E.M. (error bars). *, $p<0.05$; ** $p<0.01$; *** $p<0.001$.

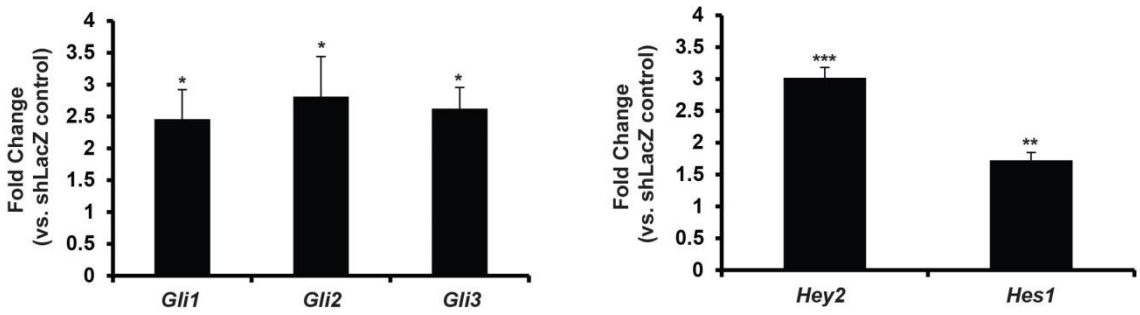

Figure 4.12 Adenoviral overexpression of SHHN and N1ICD activate downstream markers. Transduction with constructs overexpressing the N-terminal SHH protein (SHH-N, left panel) or the Notch 1-intracellular domain (N1ICD, right panel) leads to efficient induction of downstream transcripts. *Gli1*, GLI family zinc finger 1; *Gli2*, GLI family zinc finger 2; *Gli3*, GLI family zinc finger 3; *Hey2*, hairy/enhancer-of-split related with YRPW motif 2; *Hes1*, hairy and enhancer of split 1. Data are means (n=9) ± S.E.M. (error bars). *, $p<0.05$; ** $p<0.01$; *** $p<0.001$.

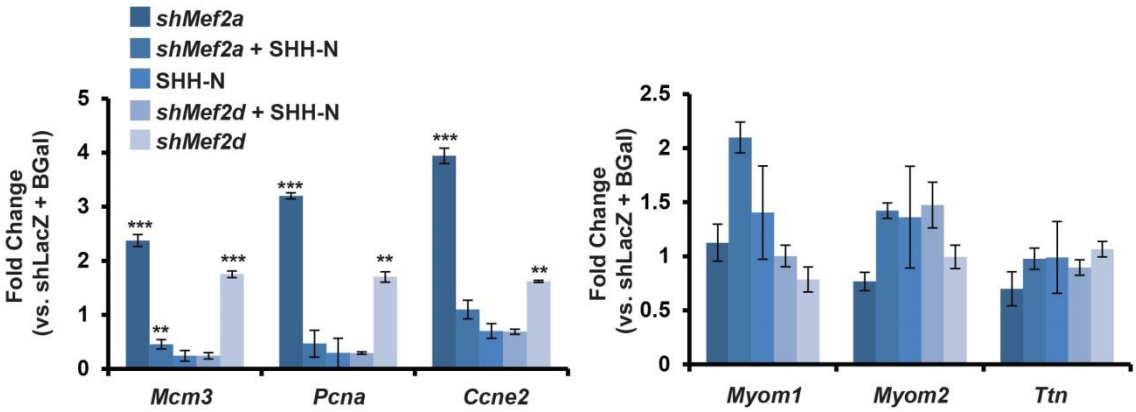

Figure 4.13 SHHN overexpression represses cell cycle genes. Quantitative RT-PCR analysis of a subset of cell cycle (left) and differentiation (right) transcripts in *Mef2a* shRNA alone, *Mef2a* shRNA and SHH-N, SHH-N overexpression alone, shRNA and SHH-N, and *Mef2d* shRNA alone (bars left to right) treatments. Data are means (n=3) ± S.E.M. (error bars). *, $p<0.05$; ** $p<0.01$; *** $p<0.001$ vs. SHH-N or N1ICD treatment alone.

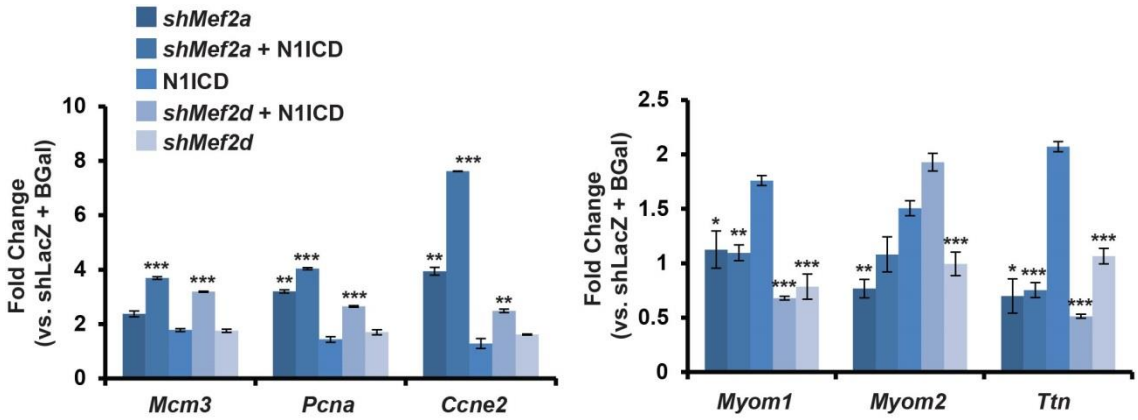

Figure 4.14 N1ICD overexpression represses cell cycle genes. Quantitative RT-PCR analysis of a subset of cell cycle (left) and differentiation (right) transcripts in *Mef2a* shRNA alone, *Mef2a* shRNA and N1ICD, N1ICD overexpression alone, shRNA and N1ICD, and *Mef2d* shRNA alone (bars left to right) treatments. Data are means (n=3) ± S.E.M. (error bars). *, $p<0.05$; ** $p<0.01$; *** $p<0.001$ vs. SHH-N or N1ICD treatment alone.

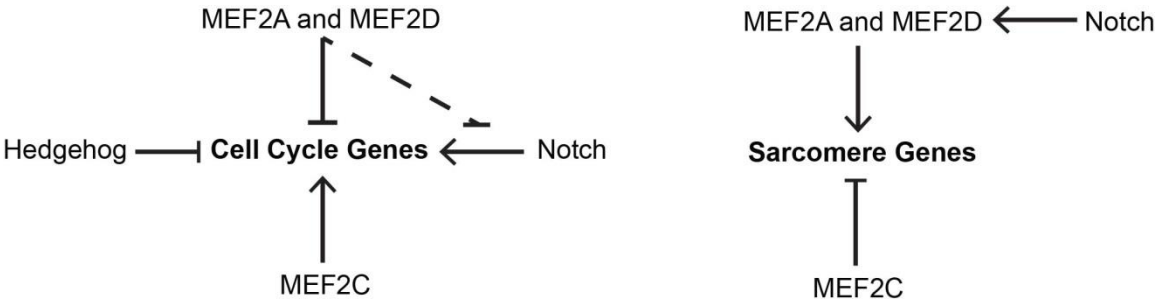

Figure 4.15 Model of MEF2A and –D regulation of Notch and Hedgehog signaling. A compilation of the observed interactions of signaling and MEF2 expression modulations on the antagonistically regulated cell cycle and sarcomere gene sets reveals a putative role in MEF2A and –D in Notch-mediated signaling.

Transcript	Fold Difference	SEM	*p* value
Mef2a	1		
Mef2b	-351	±1.3	2.73E-05
Mef2c	-22	±1.2	8.35E-05
Mef2d	-25	±1.1	1.63E-06

Table 4.1 Relative transcript expression of the *Mef2* family in NRVMs. Quantitative reverse-transcriptase-PCR analysis of relative expression of *Mef2* isoform transcripts in untreated NRVMs shows *Mef2a* transcripts are the most abundant, with *Mef2b* transcripts expressed at a 350-fold lower level, and *Mef2c* and *–d* expression at approximately 20-fold lower levels. Data are means (n=3) ± S.E.M. (error bars). *, $p<0.05$; ** $p<0.01$; *** $p<0.001$.

Canonical Pathway	*p* value	Ratio
MEF2A		
Germ Cell-Sertoli Cell Junction Signaling	1.07E-08	50/160 (0.312)
Molecular Mechanisms of Cancer	1.81E-08	90/365 (0.247)
14-3-3-mediated Signaling	1.98E-07	38/117 (0.325)
Protein Ubiquitination Pathway	2.13E-07	66/255 (0.259)
Death Receptor Pathway	3.13E-07	32/92 (0.348)
MEF2C		
Mitochondrial Dysfunction	1.96E-07	13/171 (0.076)
TCA Cycle II (Eukaryotic)	2.17E-05	4/23 (0.174)
Fatt Acid-oxidation III (Unsatuared, Odd Number)	2.40E-05	2/3 (0.667)
Oxidative Phosphorylation	3.05E-05	8/109 (0.073)
Methylmalonyl Pathway	3.67E-05	2/4 (0.50)
MEF2D		
HIPPO Signaling	2.08E-04	11/86 (0.128)
PI3k Signaling in B Lymphocytes	5.78E-04	13/128 (0.102)
Neuregulin Signaling	1.03E-03	10/88 (0.114)
Proline Degradation	1.23E-03	2/2 (1.00)
Fc Receptor-mediated Phagocytosis in Macrophages and Monocytes	1.57E-03	10/93 (0.108)
All MEF2		
Cell Cycle Control of Chromosomal Replication	0.000000499	8/27 (0.296)
Hepatic Fibross/ Hepatic Stellate Cell Activation	4.47E-05	17/198 (0.086)
Antiproliferative Role of TOB in T Cell Signaling	6.70E-05	6/26 (0.231)
Cell Cycle : G1/S Checkpoint Regulation	6.94E-05	9/64 (0.141)
Factors Promoting Cardiogenesis in Vertebrates	2.52E-04	10/92 (0.109)

Table 4.2 Canonical pathways associated with genes preferentially dysregulated in individual *Mef2* shRNA treatments. IPA of canonical pathways preferentially dysregulated by *Mef2* shRNA treatment. Analyzed gene set represents genes that were only statistically dysregulated in knockdown of a single MEF2 factor. The top five most significantly regulated canonical pathways are presented with the number of genes dysregulated in relation to the accepted number of genes associated with each canonical pathway (ratio).

Canonical Pathway	*p* value	Ratio
Shared		
Hepatic Fibrosis/Hepatic Stellate Cell Activation	5.23E-04	8/183 (0.044)
Phenylalanine Degradation I (Aerobic)	5.80E-04	2/4 (0.50)
Serine Biosynthesis	9.75E-04	2/5 (0.40)
Superpathway of Serine and Glycine Biosynthesis I	2.02E-03	2/7 (0.286)
Antiproliferative Role of TOB in T Cell Signaling	2.16E-03	3/26 (0.115)
MEF2A/D		
Cell Cycle Control of Chromosomal Replication	1.64E-09	8/27 (0.296)
Role of CHK proteins in Cell Cycle Checkpoint Control	8.27E-06	7/55 (0.127)
Factors Promoting Cardiogenesis in Vertebrates	3.24E-05	8/92 (0.087)
GADD45 Signaling	1.03E-04	4/19 (0.210)
DNA damage-induced 14-3-3 Signaling	1.03E-04	4/19 (0.210)
MEF2A/C		
Ephrin Receptor Signaling	9.52E-03	3/174 (0.017)
Glycerol-3-phosphate Shuttle	1.00E-02	1/4 (0.250)
Melatonin Degradation II	1.00E-02	1/4 (0.250)
Ephrin B Signaling	1.45E-02	2/73 (0.027)
Glycerol Degradation I	1.50E-02	1/6 (0.167)
MEF2C/D		
Type I Diabetes Mellitus Signaling	1.01E-03	3/110 (0.027)
Role of JAK2 in Hormone-like Signaling	1.70E-03	2/34 (0.059)
Role of Pattern Recognition Receptors in Recognition of Bacteria and Viruses	1.91E-03	3/137 (0.022)
Interferon Signaling	1.91E-03	2/36 (0.056)
Activation of IRF by Cystolic Pattern Recognition Receptors	5.57E-03	2/62 (0.032)

Table 4.3 Pathway analysis of regulatory patterns of genes dysregulated in each MEF2 knockdown. IPA® canonical pathway analysis of genes dysregulated in the same direction in each treatment (Shared), pathways dysregulated in the same direction by *Mef2a* and *–c* treatment or *Mef2c* and *–d* treatment (MEF2A/C and MEF2C/D), or in the same direction by *Mef2a* and *–d* treatment (MEF2A/D).

TF Module	Module description	Z-Score	Known Factor(s)	Binding Domain	Function
Differentiation					
V$HAND V$MEF2	Twist subfamily of class B bHLH transcription factors	4.33	Hand1, Hand2, Lyl1, Mesp1, Mesp2 Nhlh1, Nhlh2, Scx, Tal1, Tal2, Tcf3, Tcf4, Tcf12, Tcf15, Twist1, Twist2	bHLH	Positive regulator of striated muscle differentiation, secondary heart field specification
V$EBOX V$MEF2	E-box binding factors	4.22	Atf6, Atf6b, Max, Mga, Mlx, Mlxip, Mlxipl, Mnt, Mxd3, Mxd4, Mxi1, Myc, Mycl, Mycn, Tcfl5, Usf1, Usf2	bHLH-ZIP, bZIP	Wnt signaling pathway, positive regulator of apoptosis
V$MEF2 V$RXRF	RXR heterodimer binding sites	3.53	Nr1h2, Nr1h3, Nr1i2, Nr1i3, Rara, Rarb, Rarg, Rxra, Rxrb, Rxrg, Thra, Thrb, Vdr	C4 zinc finger domain	Cardiac muscle proliferation, canonical Wnt signaling, ventricular cardiac muscle differentiation
V$EGRF V$MEF2	EGR/nerve growth factor induced protein C & related factors	3.41	Egr1-4, Wt1	C2H2 zinc finger domain	Heart development, BMP signaling, positive regulation of cell proliferation
V$MEF2 V$RBPF	RBPJ - kappa	2.85	Rbpj, Rbpjl	RHR	Notch-binding transcriptional regulator, cardiac differentiation
V$MEF2 V$SRFF	Serum response element binding factor	2.84	Srf	MADS box	Positive regulator of cell differentiation
V$HESF V$MEF2	Vertebrate homologues of enhancer of split complex	2.73	Bhlhe40, Bhlhe41, Helt, Hes1, Hes2, Hes3, Hes5, Hes6, Hes7, Hey1, Hey2, Heyl, Itgb3bp, Sohlh1, Sohlh2	bHLH	Notch signaling in cardiac development, cardiac hypertrophy in response to stress,
V$HOXH V$MEF2	HOX - MEIS1 heterodimers	2.72	Hoxa10, Hoxa11, Hoxa13, Hoxa9, Hoxa9l, Hoxb13, Hoxb9, Hoxc10, Hoxc12, Hoxd10, Hoxd12, Hoxd13, Hoxd9, Meis1-3,	TALE class homeodomain, homeodomain	Embryonic patterning, skeletal muscle tissue development
V$MEF2 V$PBXC	PBX - MEIS complexes	2.14	Meis1-3, Pbx1-4, Pknox1, Pknox2	TALE class homeodomain	Heart development
Cell Cycle					
V$HAND V$MEF2	Twist subfamily of class B bHLH transcription factors	4.33	Hand1, Hand2, Lyl1, Mesp1, Mesp2 Nhlh1, Nhlh2, Scx, Tal1, Tal2, Tcf3, Tcf4, Tcf12, Tcf15, Twist1, Twist2	bHLH	Positive regulator of striated muscle differentiation, secondary heart field specification
V$FKHD V$MEF2	Fork head domain factors	4.1	Foxa1-3, Foxb2, Foxc1-2, Foxd1-4, Foxe1, Foxe3, Foxf1, Foxg1, Foxj1-3, Foxk1-2, Foxl1-2, Foxm1, Foxn2-3, Foxo1, Fox3-4, Foxo6, Foxp1-5, Foxq1, Foxs1	fork head domain (winged helix)	G2/M transition, anatomical structure morphogenesis, cardiac muscle proliferation, ventricular cardiac muscle morphogenesis
V$MEF2 V$RXRF	RXR heterodimer binding sites	3.53	Nr1h2, Nr1h3, Nr1i2, Nr1i3, Rara, Rarb, Rarg, Rxra, Rxrb, Rxrg, Thra, Thrb, Vdr	C4 zinc finger domain	Cardiac muscle proliferation, canonical Wnt signaling, ventricular cardiac muscle
V$AP1R V$MEF2	MAF and AP1 related factors	3.06	Bach1-2, Maf, Mafa, Mafb, Maff, Mafg, Mafk, Nfe2, Nfe2l1-3, Nrl, RGD1562865	BTB-POZ bZIP, bZIP	Regulator of anatomical structure morphogenesis, embryonic development
V$MEF2 V$SRFF	Serum response element binding factor	2.84	Srf	MADS box	Positive regulator of cell differentiation
V$IRXF V$MEF2	Iroquois homeobox factors	2.63	Irx1-6, Mkx	Homeodomain	Heart development, negative regulator of myoblast differentiation
V$MEF2 V$P53F	p53 tumor supressor	2.47	Tp53, Tp63, Tp73	p53 Domain	Cell cycle arrest, DNA damage response, regulator of mitotic cell cycle
V$GLIF V$MEF2	GLI zinc finger family	2.05	Gli1-3, Glis1-3, Zic1-5	C2H2 zinc finger domain	Heart development/looping, cell proliferation, Hedgehog signaling

Table 4.4 Genomatix enriched transcription factor binding site analysis. Binding site enrichment analysis was performed using the Genomatix software suite to determine enriched motifs adjacent (within 50 bp) of MEF2 consensus binding sites in the regulatory region 5kb upstream of the putative transcriptional start site of antagonistically regulated genes (differentiation genes top, cell cycle/proliferation genes bottom). The table provides a description of each candidate co-regulator for each enriched motif with a Z-score (Z-scores > 2.0 were considered significantly enriched). The known binding factor and their relevant binding domains are included when known. Finally, a brief summary of relevant regulatory function is provided.

CHAPTER FIVE: EGR1 functions as a potent repressor of MEF2 transcriptional activity

This research was originally presented in PLOS ONE. Feng Y*, **Desjardins CA***, Cooper O, Kontor A, Nocco SE, Naya FJ. (2015) EGR1 Functions as a Potent Repressor of MEF2 Transcriptional Activity. PLOS ONE 10(6): e0131619. doi.org/10.1371/journal.pone.0127641

* Equal contribution

5.1 Introduction

Members of the myocyte enhancer factor 2 (MEF2) family of transcription factors play essential and diverse roles in tissue development and function as exemplified by mutant phenotypes in mice and other animal model systems (Potthoff *et al.* 2007). The transcriptional function of MEF2 is primarily modulated through signaling pathways and interactions with co-regulators that can either enhance or abrogate its activity in specific biological settings (McKinsey *et al.* 2002). While this notion is firmly established, considerably less is known about the mechanism (Pak *et al.*) by which MEF2 coordinately regulates defined gene programs in muscle.

We previously reported that cardiomyocyte cytoarchitecture and survival is dependent on MEF2A (Naya *et al.* 2002, Ewen *et al.* 2011). MEF2A was shown to modulate the integrity of the cardiomyocyte cytoskeleton through its direct regulation of a collection of genes encoding proteins localized to the costamere, a muscle-specific focal adhesion which connects the myofibrils to the plasma membrane (sarcolemma) and functions to transmit contractile forces throughout the myocyte (Danowski *et al.* 1992,

Ervasti 2003, Ewen *et al.* 2011). To gain further insight into the mechanism by which MEF2A regulates a costamere gene program, a bioinformatics analysis of transcription factor binding sites was performed using the proximal promoter regions of costamere genes (Ewen *et al.* 2011). This computational approach identified a number of candidate *cis*-elements that may function as binding sites for transcriptional co-regulators of MEF2A-dependent costamere genes. One of these predicted sites belonged to the early growth response (EGR) family of zinc finger transcription factors (Delbridge *et al.* 1997).

The involvement of the EGR1 transcription factor in cardiovascular and neuronal pathways, systems in which MEF2 functions as a central regulator, makes it a particularly attractive candidate coregulatory factor. For example, EGR1 is a downstream effector in atherosclerosis, angiogenesis, and cardiac hypertrophy (Khachigian 2006), and has been shown to regulate gene expression in vascular smooth muscle downstream of mechanical stretch (Grote *et al.* 2004), a stimulus that modulates costamere/focal adhesion activity. Additionally, like MEF2, EGR1 responds to neuronal activity and regulates expression of genes involved in synapse remodeling (O'Donovan *et al.* 1999, Li *et al.* 2005, Shalizi *et al.* 2005, Greer *et al.* 2008).

In this study, we examined the ability of EGR1 to modulate MEF2A transcriptional activity. We found that EGR1 is a potent repressor of MEF2A transcriptional activity on MEF2-dependent promoters in both non-cardiac and cardiac cells. Consistent with its function as a repressor of MEF2 activity, overexpression and inhibition of EGR1 resulted in down- and up-regulated expression of costamere genes,

respectively. Taken together, these results suggest a potential role for EGR1 to modulate MEF2 activity in the regulation of costamere gene expression in cardiomyocytes.

5.2 EGR1 potently represses MEF2 transcriptional activity

To investigate the possibility that EGR1 functions as a coregulator of MEF2A, we initially examined the effect of EGR1 on MEF2A transcriptional activity using the proximal promoter region of the mouse *Tcap* gene. The *Tcap* gene encodes a myofibrillar Z-disc protein associated with the costameric protein network whose expression in cardiomyocytes is directly regulated by MEF2A (Ewen *et al.* 2011). In addition to the MEF2 site, the 2.0 kilobase (kb) proximal promoter region of the mouse *Tcap* gene is predicted to harbor 5 EGR binding sites located at positions -127, -646, -1407, -1533, and -1851, relative to the transcription start site. HEK293T cells were co-transfected with the *Tcap*-luciferase reporter and MEF2A in the presence or absence of EGR1. As shown in Figure 5.1A, EGR1 alone had no significant effect on the basal activity of the *Tcap* reporter, whereas MEF2A robustly activated this reporter. In contrast, co-transfection of EGR1 significantly repressed MEF2A activation of the *Tcap* reporter. It is worth noting that this repressive effect was not due to EGR1 inhibiting the expression of the MEF2A expression plasmid as there was no decrease in overexpressed MEF2A in cells transfected with EGR1 (Figure 5.1B).

In a parallel series of experiments, we asked whether EGR1-mediated repression of MEF2A required DNA binding as previous studies have shown that EGR1 is able to repress NF-κB activity in a non-DNA binding manner (Chapman *et al.* 2000). Therefore, we examined the ability of EGR1 to repress a MEF2-dependent promoter not known to

have EGR binding sites. For these experiments we used the 3xMEF2 reporter, which harbors three tandem copies of the MEF2 site from the *desmin* gene and flanking sequences that do not contain the consensus EGR DNA binding site (Naya *et al.* 1999). The 3xMEF2 reporter was transfected in HEK293T cells along with MEF2A, EGR1, or both. EGR1 alone had no effect on the multimerized 3xMEF2 reporter but, similar to the Tcap promoter, significantly repressed this reporter in the presence of MEF2A (Figure 5.2). These results suggest that EGR1 is capable of repressing MEF2A activity in a non-DNA binding fashion.

We next asked whether EGR1-mediated repression of MEF2A was restricted to this protein isoform or whether other MEF2 protein isoforms could also be inhibited by this factor. Although EGR1 was identified by analyzing the promoter regions of costamere associated genes regulated by MEF2A, we found that EGR1 also significantly repressed MEF2D transcriptional activity on the 3xMEF2 reporter (Figure 5.3). EGR1 overexpression did not significantly repress transcriptional activity of MEF2B and MEF2C, but we noted a trend towards repression with these MEF2 isoforms. These results indicate that, in addition to MEF2A, EGR1 is capable of significantly repressing the transcriptional activity of an additional MEF2 isoform.

To determine whether EGR1 specifically represses the MEF2 family or whether it is able to repress other members of the MADS-box transcription factor superfamily, we examined the effect of EGR1 on serum response factor (SRF) transcriptional activity. Like the MEF2 proteins, SRF possesses a MADS box DNA binding and dimerization domain but is unable to dimerize with these factors and it binds to a different A/T-rich

consensus DNA binding sequence known as a CArG box (Miano *et al.* 2007). HEK293T cells were co-transfected with SRF and the SRF-dependent *SM22*-luc reporter, with or without EGR1. As shown in Figure 5.4A, EGR1 failed to repress SRF activity on the *SM22-luc* reporter, demonstrating that EGR1 functions as a specific co-repressor of the MEF2 subclass of MADS-box transcription factors.

To investigate if this was a reciprocal repression of transcriptional activity, we transfected HEK293T cells with an EGR1-specific promoter, *p300*, reporter construct (Yu *et al.* 2004). This promoter region lacks consensus MEF2 binding sites, and this promoter was selected to determine if MEF2A:EGR1 protein-protein interactions have similar effects on EGR1-activated genes. Unlike the MEF2-specific reporters, *p300-luc* was not repressed by the co-transduction of MEF2A and EGR1 (Figure 5.4B). These results demonstrate that the EGR1-mediated repressive effect on MEF2A transcriptional activity is not reciprocal and suggest that repression is specific for genes directly regulated by MEF2.

5.3 EGR1 represses endogenous MEF2 transcriptional activity

To determine whether EGR1 represses endogenous MEF2 activity in cardiac muscle cells we examined the activity of MEF2-dependent reporters in neonatal rat ventricular myocytes (NRVMs) transduced with EGR1 adenovirus. Initially, we used the *Tcap* and 3xMEF2 reporters for these assays but their variable and low activities, respectively, in NRVMs precluded us from further analyzing the effect of EGR1 on these MEF2-dependent constructs. As an alternative, we used the 1.5 kb proximal promoter region of *myomaxin/Xirp2*, which has been shown to display consistently high MEF2-

dependent activity in primary cardiomyocytes (McCalmon *et al.* 2010). Additionally, similar to the 3xMEF2 reporter, the 1.5 kb *myomaxin* promoter region is predicted to lack EGR binding sites, thus any effect on reporter activity is likely to be mediated via DNA binding-independent effects of EGR1. As shown in Figure 5.5, overexpression of EGR1 significantly repressed the activity of the wild type 1.5 kb *myomaxin* promoter. In contrast, the mutant 1.5 kb *myomaxin* ΔMEF2 reporter, harboring a mutation in the -75 MEF2 site which results in reduced basal activity in NRVMs, was not significantly repressed by EGR1. These results reveal that EGR1-mediated repression of a MEF2 target gene in cardiomyocytes is primarily occurring through the inhibition of MEF2 activity.

5.4 EGR1 interacts with MEF2A

The DNA-binding independent mechanism by which EGR1 represses MEF2-dependent transcription suggests that EGR1 represses MEF2 activity through protein-protein interaction. Therefore, a co-immunoprecipitation assay was performed to determine whether or not EGR1 and MEF2A interact in transfected cells.

Co-immunoprecipitation was performed using epitope-tagged fusion proteins MEF2A-FLAG (C-terminal tag) and MYC-EGR1 (N-terminal tag). To confirm the expression of these two epitope-tagged fusion proteins, MEF2A-Flag and EGR1were transfected into HEK293T cells and protein was harvested 36–48 hr post-transfection. Western blot analysis confirmed the expression of both MEF2A-FLAG (Figure 5.6A) as well as MYC-EGR1 (Figure 5.6B). Lysates from cells cotransfected with empty MYC vector or MYC-EGR1, and MEF2A-FLAG were then subjected to a co-

immunoprecipitation assay to test for a protein-protein interaction. As shown in Fig 3A left panel, MEF2A was immunoprecipated effectively indicating an interaction between EGR1 and MEF2A. When empty MYC vector was immunoprecipitated, no MEF2A--FLAG was detectable (Figure 5.6A, right panel), suggesting that the immunoprecipitation of MEF2A-FLAG was mediated by interaction with EGR1 rather than nonspecific immunoprecipitation.

5.5 Costamere gene expression and cardiomyocyte survival are sensitive to EGR1 expression

EGR1 repression of MEF2 activity suggests that overexpression of this factor might impair cardiomyocyte survival in a manner similar to that observed in MEF2A-deficient NRVMs (Ewen *et al.* 2011). We investigated this hypothesis by transducing NRVMs with adenoviruses expressing either EGR1 (AdEGR1) or a beta-galactosidase (Adβgal) control. Quantitative RT-PCR analysis showed increased Egr1 expression in AdEGR1 treated NRVMs compared to Adβgal controls (Figure 5.7). At 72 hr post transduction, we noted widespread cardiomyocyte detachment in EGR1-transduced NRVMs, similar to MEF2A-depleted NRVMs (Figure 5.8A, right panels). The cellular detachment phenotype suggested reduced viability of cardiomyocytes overexpressing EGR1. Analysis of cellular viability revealed significantly reduced survival in EGR1 expressing cells (Figure 5.8B). Measurement of Caspase 3 activity, a marker of apoptosis, showed a significant increase in Caspase 3 activity in EGR1 overexpressing cells, suggesting induction of apoptosis as a mechanism for the decreased viability of EGR1 overexpressing cell (Figure 5.8C). We next examined the expression of thirteen

costamere genes previously characterized by our lab to be downregulated in MEF2A-depleted NRVMs (Ewen *et al.* 2011). Consistent with the ability of EGR1 to repress MEF2 activity, EGR1 overexpression in NRVMs led to significantly decreased expression of eleven of the thirteen MEF2-dependent costamere genes analyzed (Figure 5.9).

In a complementary set of experiments EGR1 was depleted in NRVMs using an *Egr1*-specific siRNA (Ambion). Unlike EGR1 overexpression, siRNA-mediated knockdown of EGR1 had no obvious morphological effect on NRVMs 72 hr post-transfection (Figure 5.10A). To determine the efficiency of EGR1 knockdown, HEK293T cells were transfected with pcDNA3-EGR1-Flag with either negative control siRNA or *Egr1* siRNA. Cell lysates were probed for Flag expression and EGR1-Flag expression is observed at the expected size (80kD) when cotransfected with negative control siRNA, but expression is lost when co-transfected with *Egr1* siRNA (Figure 5.10B). There is a confounding non-specific band just above the relevant EGR1-Flag band that is observed in all samples, including the untransfected control, and does not vary with siRNA treatment. Subsequently, expression of costamere genes was analyzed by qRT-PCR. As predicted by our model of EGR1-mediated MEF2 repression, MEF2-dependent costamere gene expression was elevated in *Egr1* siRNA knockdown NRVMs (Figure 5.11). Eight of the thirteen genes were significantly upregulated upon EGR1 knockdown. Taken together, the EGR1 overexpression and knockdown experiments clearly support its role in MEF2-dependent costamere gene expression in cardiomyocytes.

5.6 Discussion

The present report reveals that the EGR1 transcription factor interacts with MEF2A and functions as a potent repressor of MEF2 activity in cardiomyocytes. EGR1 was shown to repress MEF2A transcriptional activity on MEF2-dependent promoters that either harbored multiple, predicted EGR binding sites or lacked a consensus EGR DNA binding sequence. Moreover, although we previously identified EGR1 through computational analysis of predicted transcription factor binding sites on costamere genes primarily dependent on MEF2A, our investigation revealed that EGR1 represses additional MEF2 protein isoforms in transient reporter assays. Finally, this repressive effect was found to be specific for the MEF2 subclass of MADS box transcription factors as EGR1 failed to repress SRF transcriptional activity.

While EGR1 was selected as a candidate co-regulator of MEF2A through analysis of consensus DNA binding sequences on a collection of costamere promoters, it is interesting that the repressive effect of EGR1 could also occur in a DNA-binding independent manner. This suggests that the role of DNA-binding, as it relates to the repressive action of EGR1, may be to more effectively target the EGR1 protein to promoters that are directly bound by MEF2. It is unclear whether EGR1 DNA-binding plays an additional non-MEF2 related role in the regulation of cardiomyocyte costamere and survival, and further study is required to better understand how the repressive interaction of EGR1 and MEF2 is reprised in a physiological context.

Consistent with the notion that EGR1 repressed MEF2, overexpression of EGR1 in NRVMs resulted in significantly decreased expression of MEF2-dependent costamere

genes. Interestingly, overexpression of EGR1 also caused cardiomyocyte detachment and significantly reduced survival, which is reminiscent of the MEF2A depletion phenotype in NRVMs [4]. These observations support our model that EGR1 and MEF2 function in the same pathway to transcriptionally co-regulate MEF2-dependent costamere genes in cardiomyocytes.

The ability of EGR1 to function as a repressor of gene expression in cardiomyocytes has been documented (McKinsey *et al.* 2001, McCalmon *et al.* 2010). However, EGR1 has not been previously demonstrated to regulate a distinct gene program or specifically interact with and repress the activity of a core cardiac transcription factor such as MEF2. Of particular interest is the connection of these transcription factors in cardiac hypertrophy pathways. MEF2 is a known downstream mediator of hypertrophic signaling (Chabane *et al.* 2009), particularly in calcineurin-induced hypertrophy by Ca^{2+}-activated NFAT signaling that promotes chamber dilation and loss of contractility (Wang *et al.* 2005). In this regard, EGR1 has been shown to induce Cav3.2 T-type calcium channels, which plays a role in inducing calcineurin/NFAT signaling during cardiac hypertrophy (Kasneci *et al.* 2009), to play an important role in adaptive response to hypertrophic stimuli (Czubryt *et al.* 2004), and to be targeted and suppressed by Atf3during endothelin-1 induced cardiomyocyte hypertrophy (van Oort *et al.* 2006). Additionally, Nab1, a repressor of EGR, has been shown to be a potent inhibitor of pathological cardiac hypertrophy (Hsu *et al.* 2013) and EGR1 deficient mice have a blunted catecholamine-induced hypertrophy response and are more sensitive to stress (Pacini *et al.* 2013). Given the wide variety of

cardiopathologies in which both EGR1 and MEF2 have been implicated, further investigation of EGR1's function as a potent MEF2 repressor will provide additional insight into mechanisms of various cardiopathologies and into potential targets for treatment of cardiac disease.

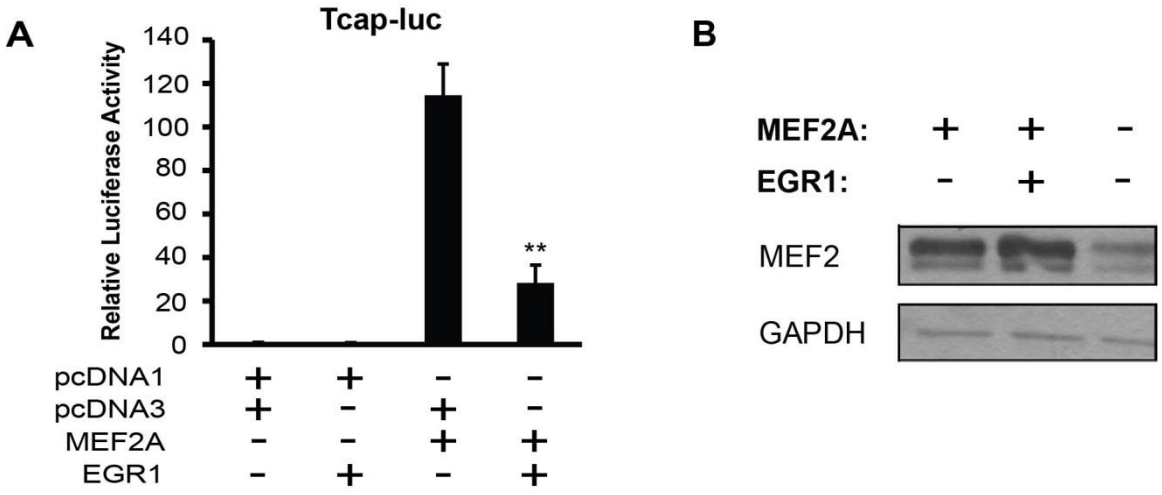

Figure 5.1 EGR1 is a potent repressor of MEF2A transcriptional activity. A, HEK293T cells were transfected with the *Tcap*-Luc, pcDNA3-EGR1 and pcDNA1-MEF2A. pcDNA1 and pcDNA3 were used as empty plasmid controls for the MEF2A and EGR1 expression vectors, resepectively. Firefly luciferase readings were normalized by Bradford assay. ($n = 6$, $p<0.003$). **B**, Western blot analysis shows that EGR1 overexpression does not decrease the expression of MEF2A. Data are mean ± SEM. *$p<0.05$, **$p<0.01$, ***$p<0.001$, n.s. not significant.

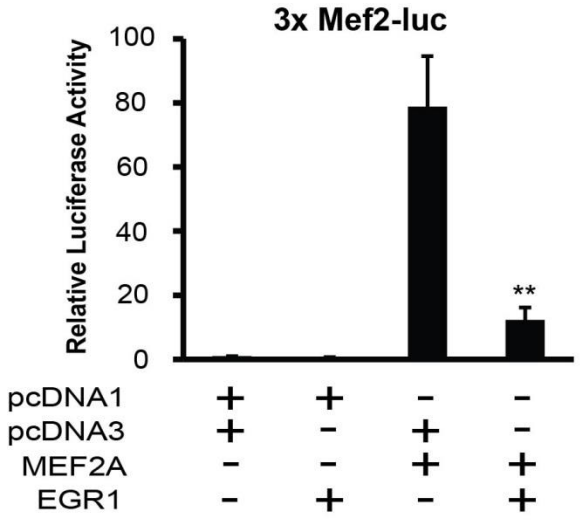

Figure 5.2 EGR1 repression does not require EGR1 DNA-binding activity. HEK293T cells were co-transfected with a3xMEF2-luc lacking any putative EGR1 binding sites. MEF2A alone robustly induced reporter activity, and introduction of EGR1 was sufficient to repress MEF2A-mediated activation. Firefly luciferase readings were normalized by Bradford assay (n=4, $p<0.007$). Data are mean ± SEM. *$p<0.05$, **$p<0.01$, ***$p<0.001$, n.s. not significant.

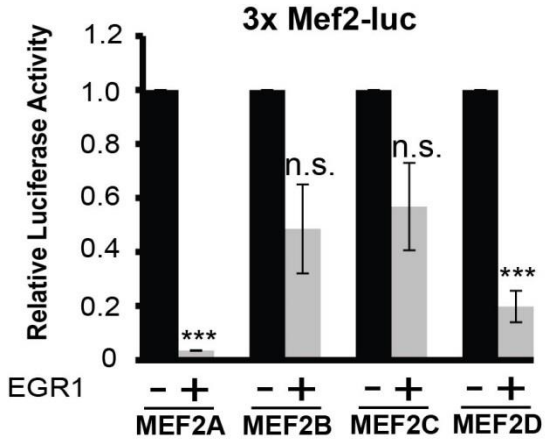

Figure 5.3 EGR1 significantly represses MEF2A and –D mediated transcriptional activation, but not MEF2B or –C. HEK293T cells were co-transfected with 3xMEF2-luc and MEF2A, B, C, or D in the presence or absence of EGR1. EGR1 was sufficient to robustly repress MEF2A and –D transcriptional activity, but not MEF2B, or –D. Data are mean ± SEM. *p<0.05, **p<0.01, ***p<0.001, n.s. not significant.

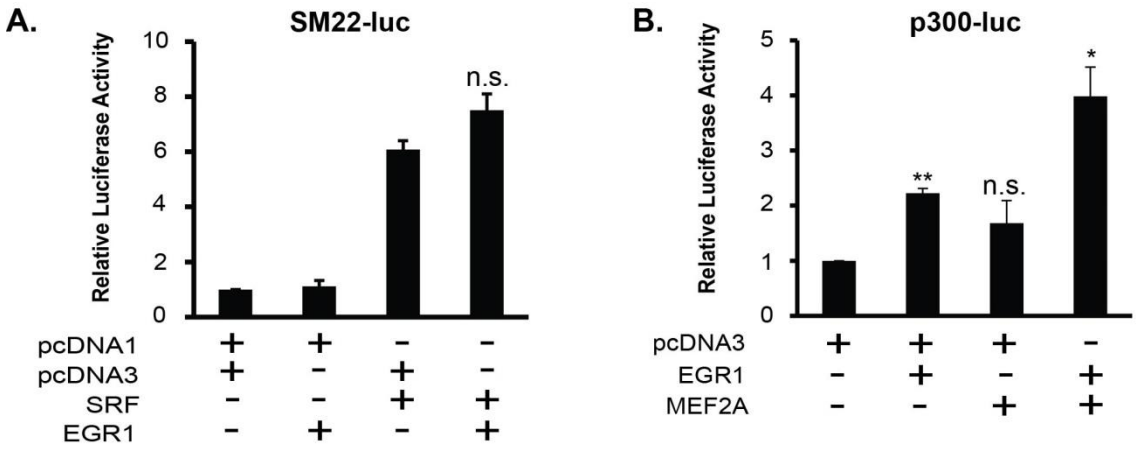

Figure 5.4 EGR1 repression is unidirectional and specific to MEF2. A, EGR1 does not repress SRF activity on an SRF-specific reporter construct. No significant difference was measured in the luciferase activation in the absence or presence of EGR1 (n=4, n.s.). **B**, MEF2A does not repress EGR1 transcriptional activity on a EGR1-specific promoter construct, p300-luc, lacking MEF2 binding sites (n = 3). Luciferase data are normalized to Bradford assay. Data are mean ± SEM. *p<0.05, **p<0.01, ***p<0.001, n.s. not significant.

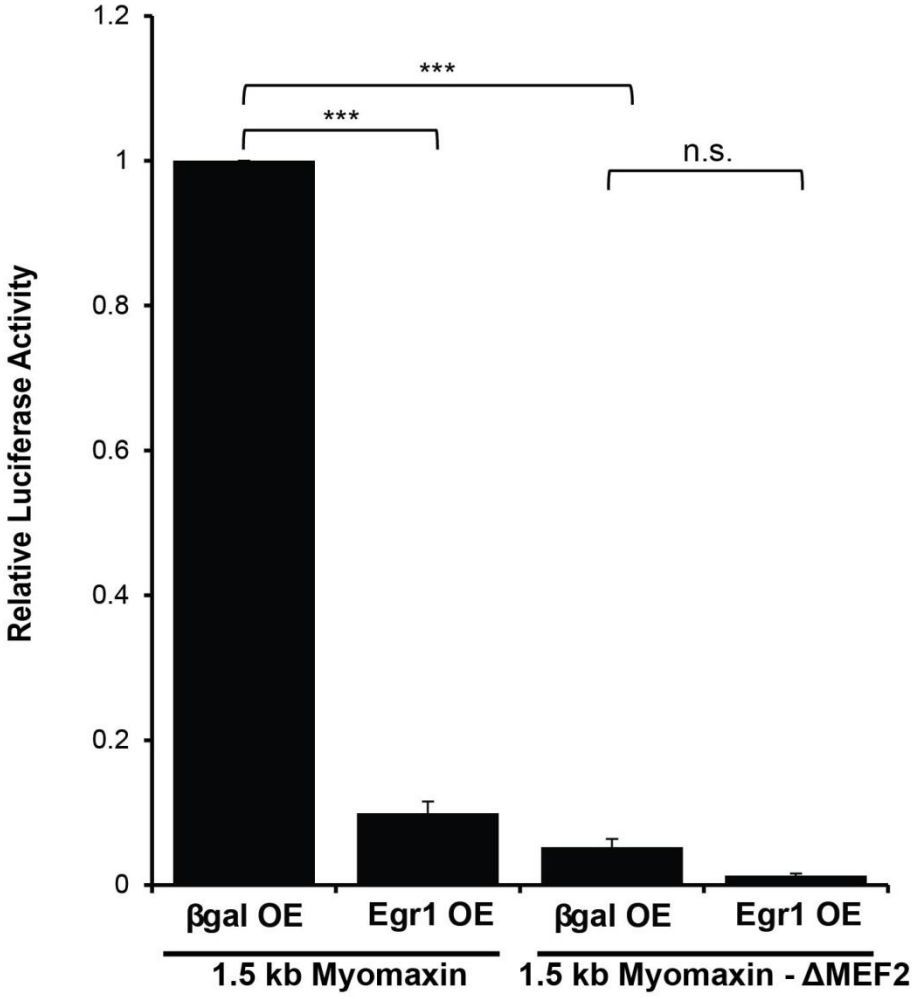
1.2
1
0.8
0.6
0.4
0.2
0
Relative Luciferase Activity
***
***
n.s.
βgal OE
Egr1 OE
βgal OE
Egr1 OE
1.5 kb Myomaxin
1.5 kb Myomaxin - ΔMEF2

Figure 5.5 EGR1-mediated repression of MEF2A activity requires MEF2 DNA-binding. NRVMs were transduced with AdEGR1 and Adβgal at an MOI of 25. Twenty four hr post-transduction, 1.5 kb myomaxin-Luc and 1.5 kb myomaxinΔMEF2-Luc were transfected. Luciferase activity was measured 48 hr after transfection. Firefly luciferase readings were normalized to Renilla luciferase readings. Data are mean ± SEM. ***p<0.001, n.s. not significant.

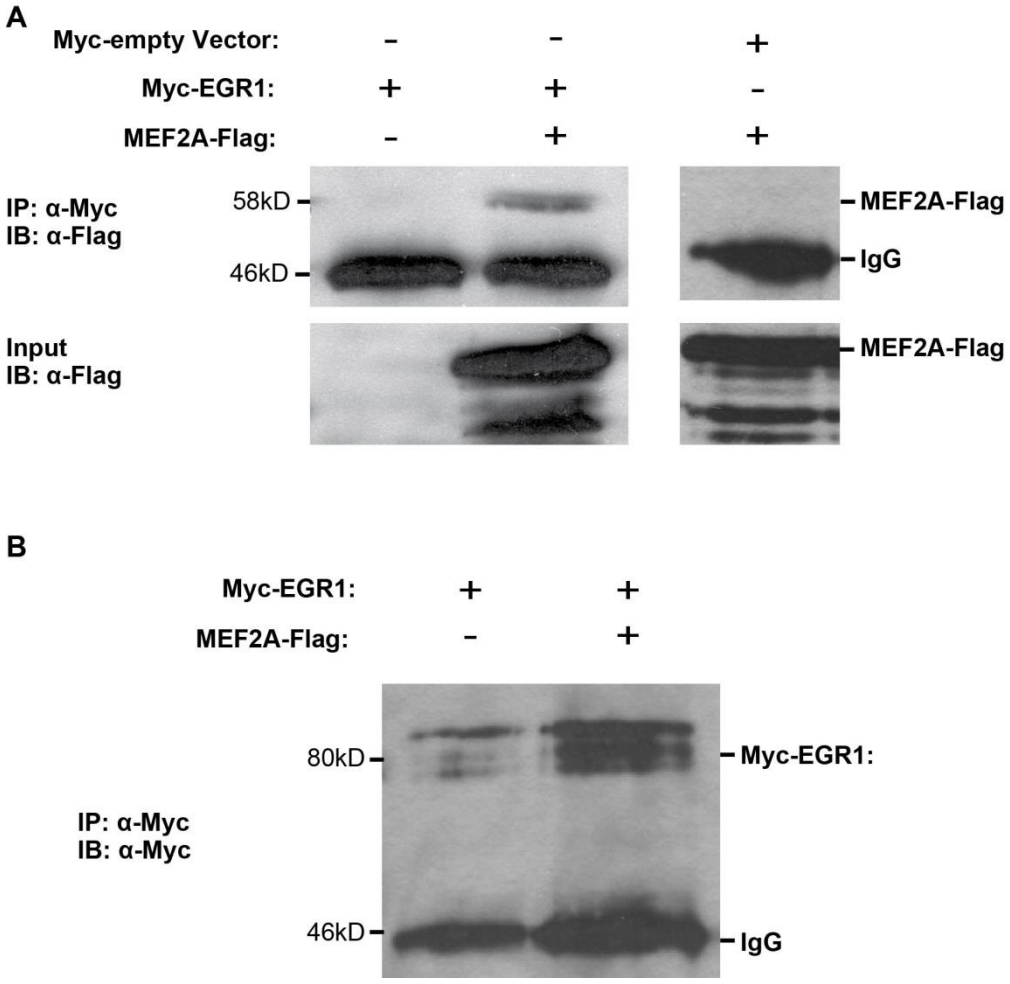

Figure 5.6 MEF2A and EGR1 physically interact *in vitro*. A, HEK293T cells were transfected with pcDNA3-myc (empty vector) or pcDNA3-Myc-EGR1 (N-terminal epitope tag) and pCMV-MEF2A-FLAG (C-terminal epitope tag). Whole cell lysates in AT buffer were incubated with Protein G Sepharose Beads (GE Healthcare) and 1 μg of anti-Flag and incubated at 4°C, rotating overnight on a nutator. Precipitated samples were fractionated on an 8% SDS-PAGE gel followed by a western blot incubated with anti-Flag (1:2,000). **B**, Self-immunoprecipitation of the myc-EGR1 protein shows efficient expression and purification.

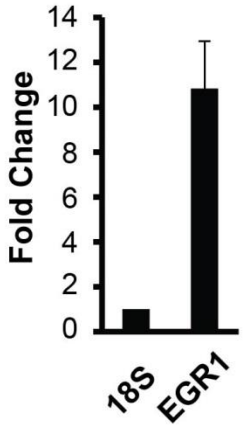

Figure 5.7 AdEGR1 transduction induces an increase in *Egr1* transcripts. Quantitative RT-PCR analysis confirms expression of *Egr1* transcripts 48 hr post-transduction with AdEGR1; fold change is in comparison to expression levels in the Adβgal control, results were normalized to 18s.

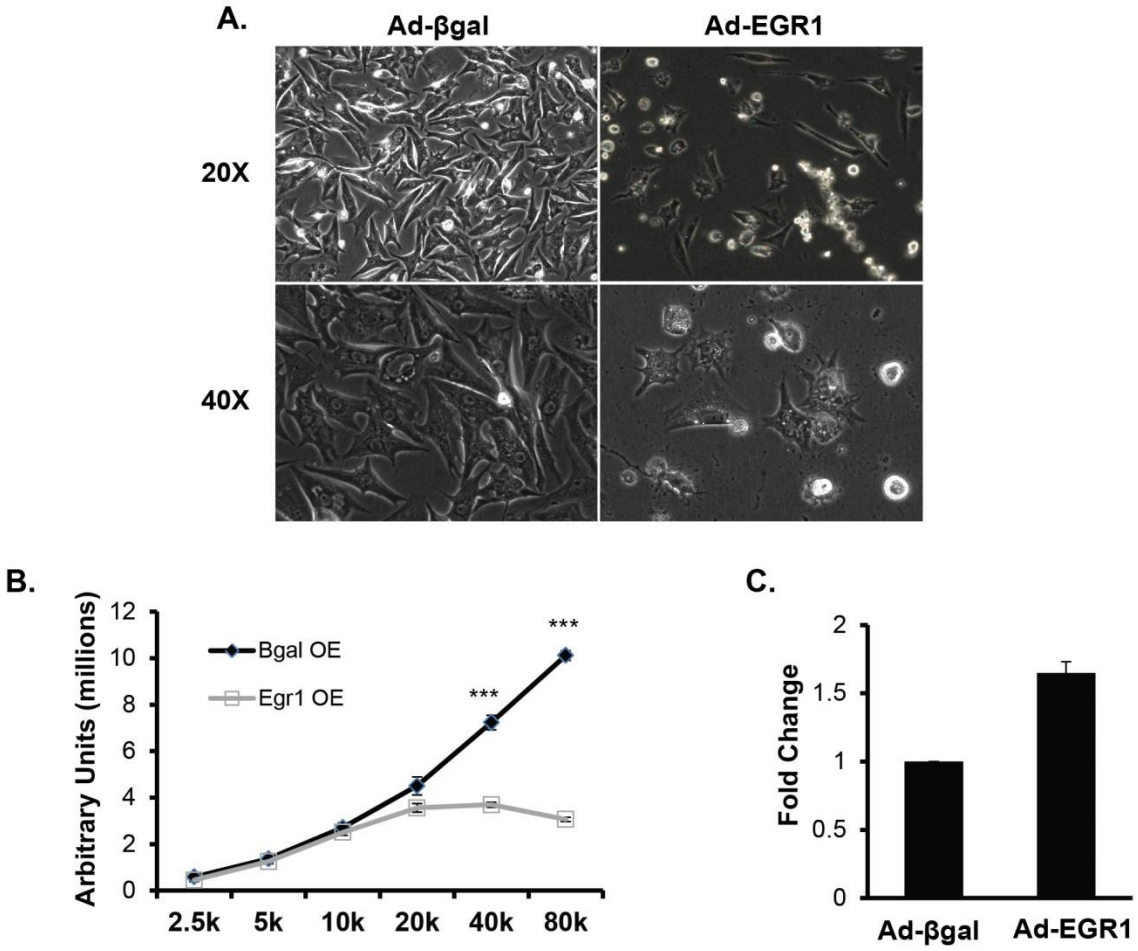
A.
Ad-βgal
Ad-EGR1
20X
40X
B.
Arbitrary Units (millions)
Bgal OE
Egr1 OE
***
***
2.5k
5k
10k
20k
40k
80k
C.
Fold Change
Ad-βgal
Ad-EGR1

Figure 5.8 Overexpression of EGR1 impairs NRVM viability. A, NRVMs were transduced with AdEGR1 and Adβgal at an MOI of 25 and observed 48 hr post transduction. Extensive cell detachment is seen in the AdEGR1 transduced NRVMs in comparison to the Adβgal transduced NRVMs. **B**, NRVMs were seeded in increasing cell densities and transduced with AdEGR1 or Adβgal at an MOI of 25 and assayed for cell viability 48 hr post-transduction. Cell titer blue assay shows a significant decrease in viability in AdEGR1 transduced NRVMs but not the control. **C**, NRVMs were transduced with AdEGR1 or Adβgal at an MOI of 25 and assayed for Caspase 3 activity 72 hr post-transduction. The assay shows significant upregulation of Caspase 3 activity at 72 hr post-transduction in the AdEGR1-transduced, but not Adβgal-transduced NRVMs. Data are mean ± SEM, n = 3, *p<0.05, **p<0.01, ***p<0.001.

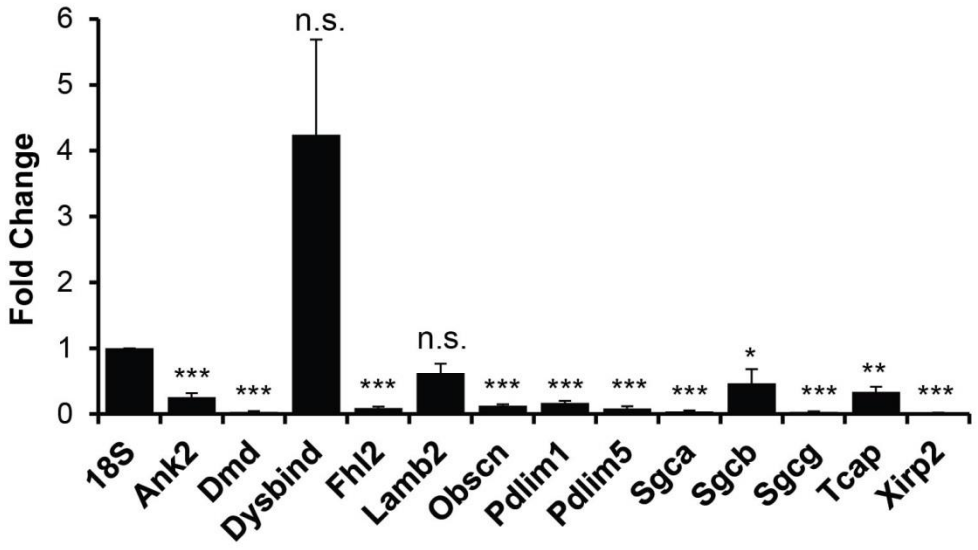

Figure 5.9 Costamere gene expression is sensitive to EGR1 levels in NRVMs. Quantitative RT-PCR analysis of 13 MEF2-dependent costamere genes shows 11 of these genes are down-regulated when EGR1 is overexpressed in NRVMs; fold change is in comparison to expression levels in the Adβgal control. Results were normalized to 18s. Data are mean ± SEM, n = 3, *p<0.05, **p<0.01, ***p<0.001.

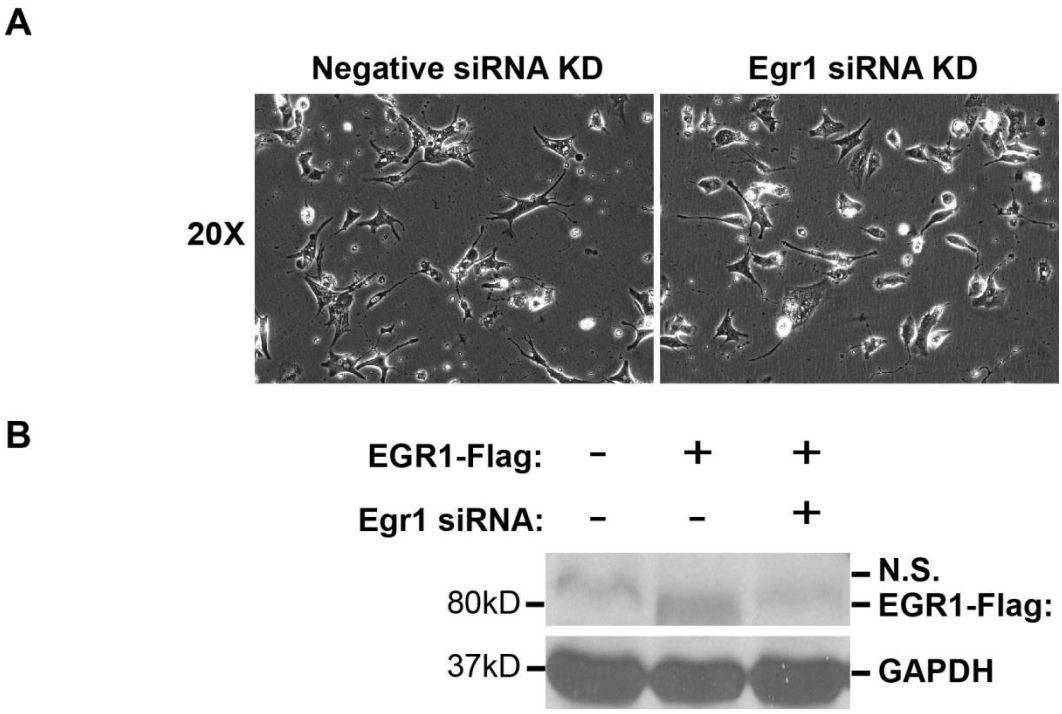

Figure 5.10 EGR1 depleted NRVMs display no obvious morphological defects. A, NRVMs were transfected with 100 nM EGR1 siRNA and analyzed 72 hr post transfection. **B**, HEK 293T cells were transfected with pcCMV-EGR1-Flag, and either a negative control or Egr1 siRNA. Western blot analysis probing for the Flag epitope shows loss of EGR1-Flag expression upon co-transfection with the Egr1 siRNA, though a confounding non-specific band is present slightly above the EGR1-Flag band.

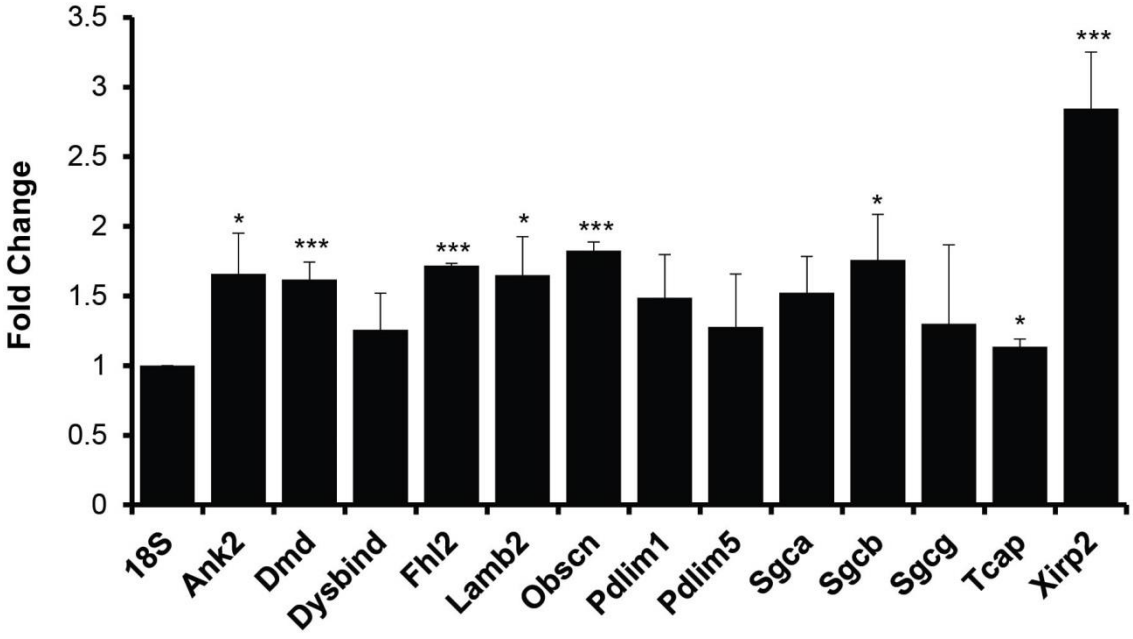

Figure 5.11 Costamere gene expression is upregulated in EGR1-depleted NRVMs. EGR1-depletion results in upregulated costamere gene expression in NRVMs. qRT-PCR analysis of 13 MEF2-dependent costamere genes in EGR1 siRNA knockdown NRVMs shows that eight of the genes are significantly upregulated, and the majority of the remaining genes show a nonsignificant trend towards upregulation when EGR1 is knocked down; fold change is in comparison to expression levels in the negative siRNA knockdown controls, results were normalized to 18s. Sample size for Ank2, Dmd, Dysbind, Lamb2, Pdlim1, Sgcb, and 18s is n = 6. Sample size for Pdlim5, Sgca, Sgcg, and Tcap is n = 5. Sample size for Fhl2 and Obscn is n = 4, and the sample size for Xirp2 is n = 3., *$p<0.05$, ** $p<0.01$, ***$p<0.001$.

CHAPTER SIX: Discussion

6.1 Discussion

The position of the MEF2 as a core regulatory element in both skeletal and cardiac muscle has been well established. Extensive research has shown its importance in muscle development, homeostasis, and disease. However, genome-wide gene regulatory analysis of the individual roles of the four MEF2 isoforms in muscle has not been performed. Previous research has typically focused on a single member of the MEF2 family and much of the research has been based on the assumption that the function of the family members are either largely redundant, and/or their regulatory roles are defined by their spatiotemporal expression patterns. Through acute isoform-specific ablation of MEF2 expression we have been able to reveal the requirement of individual MEF2 isoforms in the regulation of distinct and shared gene programs in striated muscle.

Interestingly, acute ablation of MEF2 expression in neonatal cardiomyocytes does not perfectly recapitulate the observed global *in vivo* MEF2-deficient phenotypes in mouse models. The global MEF2A-deficient mouse does display cardiac abnormalities, but these are not characterized by the loss of cardiomyocyte viability we observe in our *in vitro* MEF2A-deficient cardiomyocytes. Additionally, while MEF2C activity was thought to be dispensable after early development, we show a distinct role for MEF2C in neonatal cardiomyocytes that isn't shared by other MEF2 isoforms, suggesting that MEF2C continues to play a role in the homeostasis of differentiated cardiomyocytes. Finally, MEF2D-deficient mice display no overt cardiac phenotype until stressed, in response to which, they exhibit a blunted remodeling response. This appears to be at odds with the

drastic loss of cardiomyocyte viability we observe in acute *Mef2d* depletion in cardiomyocytes. It remains unclear why acute depletion of MEF2 activity leads to a different phenotype than chronic depletion, and we believe that reconciling these apparent discrepancies will allow us a greater understanding of the regulatory network that is at play in cardiomyocyte differentiation and homeostasis.

In Chapter Three we present a requirement for MEF2A expression in differentiating C2C12 cells that is distinct from the other MEF2 isoforms. Additionally, overexpression of MEF2B, -C, or -D was not sufficient to rescue the myotube differentiation defect observed in MEF2A-deficient C2C12 cells. This result suggests the presence of regulatory mechanisms that are specific to individual MEF2 isoforms in skeletal muscle. We hypothesized that a global analysis of genes dysregulated in C2C12 cells acutely depleted of individual MEF2 isoforms would reveal a series of distinct transcriptional programs that are preferentially associated with each MEF2 isoform.

Comparative microarray analysis supports our hypothesis that transcriptional regulation by the MEF2 family is far more nuanced than previously appreciated. We observed gene cohorts that are preferentially regulated by a single MEF2 isoform. Additionally, analysis of the cellular programs dysregulated in individual MEF2 isoform depletion revealed very little overlap, suggesting that a large part of the function of each MEF2 isoform in skeletal muscle is distinct from the function of the other MEF2 isoforms. We found this result surprising considering the substantial *in vitro* data supporting the binding and activation of a single consensus sequence by all members of the MEF2 family. We attempted to verify the consensus binding site by determining

putative MEF2 binding sites in genes preferentially dysregulated by individual MEF2 isoforms, and a compilation of all these sites yielded the same consensus site for all four MEF2 isoforms. Since this analysis was based on the JASPAR position-weight matrix, we suspect that the site prediction analysis was already biased towards the consensus sequence. We believe that an unbiased approach is possible, and have begun a collaboration to determine the consensus MEF2 binding site for each MEF2 isoform using protein binding microarray (PBM) technology and an unbiased array of oligonucleotide sequences.

In light of an apparent lack of variation in the binding sequence associated with genes preferentially sensitive to each MEF2 isoform, we considered the alternate hypothesis that the complex regulatory patterns we observe are due to association with distinct pools of co-regulatory proteins. To assess this hypothesis we evaluated the enrichment of non-MEF2 consensus binding sites in the proximal 5kb region upstream of the putative transcriptional start site. We observed several candidate co-regulatory factors that could explain the differential effects of MEF2A, -B, and -D, but failed to identify any preferentially enriched transcriptional co-regulator associated with the MEF2C-sensitive gene cohorts. We suspect that additional refinement of this analysis through use of ChIP-seq would allow us to create a dataset of genes being directly bound by the MEF2 factors, and potentially further refine the set of co-regulatory factors that may be mediating these differential regulatory effects.

In Chapter Four, we evaluate the requirement for MEF2A, -C, and -D in neonatal cardiomyocytes. Interestingly, quantitative RT-PCR analysis has allowed us to evaluate

the relative transcript expression levels the three other MEF2 isoforms in cardiomyocytes relative to *Mef2a* transcripts. Contrary to previously published *in* situ hybridization data, expression of *Mef2c* transcripts is not absent postnatally, though it is downregulated in late development. Additionally, we find that *Mef2c* and *Mef2d* transcripts are expressed at similar levels, suggesting that MEF2C maintains regulatory relevance even after its downregulation in development. Unlike skeletal muscle, MEF2B appears to be absent from neonatal cardiomyocytes and was not investigated. Abrogation of MEF2A and -D activity was associated with loss of neonatal cardiomyocyte viability in low-serum culture conditions, and overexpression of MEF2A, -D, or the constitutively-active MEF2-VP16 was sufficient to partially rescue viability. In conjunction with our skeletal muscle findings, these data support the hypothesis that the individual members of the MEF2 family regulate distinct cellular pathways in striated muscle. These observations are supported by comparative transcriptomic analysis which reveals genes sets that are preferentially dysregulated in the loss of individual MEF2 isoforms.

Interestingly, this analysis has allowed us to observe a previously uncharacterized antagonistic relationship between the MEF2 factors in the regulation of cell cycle and sarcomeric differentiation genes. We hypothesize that this represents a developmentally relevant regulatory switch which may mediate the transition from proliferative early cardiomyocytes into terminally differentiated mature cardiomyocytes during embryonic development. The temporal expression of the MEF2 family during cardiac development suggests that MEF2C plays a role in the maintenance of this immature cardiomyocyte state that shares both proliferative capacity and contractile function, and that the

emergence of MEF2A as the primary MEF2 isoform later in development may represent a switch away from proliferation and towards terminal differentiation and quiescence. Additionally, the ability to measure this antagonistic relationship in neonatal cardiomyocytes suggests that cardiomyocytes maintain an active equilibrium between proliferation and quiescence as they mature. While mature cardiomyocytes maintain their terminally differentiated state indefinitely, understanding the regulatory equilibrium observed in the relationship between MEF2 factors might provide insight into therapeutic interventions that can coerce mature cardiomyocytes to regain proliferative capacity to compensate for the loss of cardiomyocytes in cardiac dysfunction.

We hypothesize that the ability to regulate gene expression in opposite directions by the MEF2 isoforms is likely mediated by association with co-regulatory proteins. We evaluated the presence of enriched binding sites for co-regulatory proteins adjacent (within 50 bp) of putative MEF2 binding sites on antagonistically regulated genes and observed binding sites associated with two signaling pathways, Hedgehog and Notch. To assess the role of these pathways on MEF2-mediated regulation of the antagonistically regulated gene cohort we overexpressed constitutively active elements of each pathway in MEF2A and -D depleted NRVMs. We observed little interaction between the Hedgehog signaling pathway and depletion of MEF2A or -D in NRVMs, and Hedgehog signaling downregulated cell cycle genes universally. Additionally, we observed that Notch regulation of cell cycle genes was inhibited by the activity of MEF2A or -D, and that Notch activation of sarcomeric genes required the presence of MEF2A or -D.

In Chapter Five we assessed the ability of a repressive co-regulatory protein, EGR1, to mediate MEF2 function on a subset of known MEF2 target genes. We observed a repressive effect of EGR1 on the transcriptional activity of MEF2A that did not require EGR1 DNA-binding activity. Additionally, we identified a direct protein-protein interaction between EGR1 and MEF2A *in vitro*. Interestingly, while the repressive potential of EGR1 has been documented, we believe this is the first time it has been characterized to repress an entire gene program through association with a core cardiac transcription factor.

Additionally, the lack of observed repressive effect of EGR1 co-expression with other MEF2 isoforms provides substantial evidence for the existence of MEF2 isoform specific co-regulatory interactions which may help explain the observed regulatory patterns in Chapters Three and Four.

6.2 Future Perspectives

6.2.1 Further refinement of the MEF2 gene cohorts

Comparative transcriptomics has provided us with a wealth of data about the transcriptional regulatory roles of the MEF2 factors in both skeletal and cardiac muscle. To date we have only focused on small subsets of each of these data sets, but there are many interactions that remain to be explored. Most notably, while we have hypothesized potential co-regulatory proteins that may mediate the preferential regulation of gene cohorts by individual MEF2 isoforms, we have yet to evaluate these candidates. Additionally, assessing the direct binding of MEF2 factors to their sensitive genes will be

an essential contribution to further refinement of these gene sets, allowing us to create cohorts of direct and indirect targets.

Additionally, pathway analysis has revealed largely distinct roles for each of the MEF2 isoforms, but we have not had the opportunity to truly delve into the cellular pathways preferentially-sensitive to the individual MEF2 isoforms. Of particular interest is the emergence of metabolic pathways preferentially-regulated by MEF2C in neonatal cardiomyocytes. These pathways are interesting because canonical literature suggests that MEF2C activity is dispensable in mature cardiomyocytes, yet our transcriptomic analysis reveals the potential for a well-defined function for MEF2C in these cells. Additionally, while depletion of *Mef2c* did not yield an overt morphological phenotype under normal culture conditions, we suspect that its putative role in cardiomyocyte metabolism may manifest as sensitivity to altered nutrient availability. We believe that characterization of a novel role for MEF2C in mature cardiomyocytes is an interesting avenue to continue investigating, especially considering the lack of studies focused on this factor in cardiac homeostasis.

6.2.2 Characterization of the transcriptional landscape of antagonistically regulated genes

While the role of MEF2 in the regulation of many of the sarcomere genes has been characterized, very little is known about the mechanism through which MEF2 regulated cell cycle genes. Additionally, nothing is known about the ability of the MEF2 family to antagonistically regulate either gene cohort. While we have identified putative MEF2 binding sites on some of the proximal promoter regions of these genes, it is not

known whether MEF2 is capable of directly binding these sites, if the regulatory effects are indirect, or potentially some combination of both. We do know that the MEF2D is capable of mediating the regulation of cell cycle genes through direct regulation of PTEN expression, but interestingly, *Pten* transcripts are not affected by depletion of MEF2A or MEF2C activity, suggesting that there exist multiple and potentially unique regulatory mechanisms.

Further characterization of these antagonistically regulated genes will require assessment of direct binding using ChIP-seq technology to further define subsets that are direct targets. We wish to focus analysis on these direct targets because they may be able to shed light onto the co-regulatory proteins that are necessary to mediate this complex regulatory relationship. Additionally, we will proceed with analysis of the relationship between the MEF2 factors and candidate co-regulatory proteins. Of particular interest is the ability to form protein-protein complexes with individual MEF2 factors. We know from our analysis of EGR1-mediated repression that this co-repressor associates with MEF2A to mediate its repressive effect.

Additionally, identification of functional MEF2 sites will allow us to produce reporter constructs through which we can evaluate the activating or repressing activity of the individual MEF2 isoforms in a more controlled context. This is particularly relevant because standard transfection techniques are particularly ineffective in neonatal cardiomyocytes, leaving us only transduction as an efficient means of manipulation. The ability to recapitulate this system into a more permissive cell line would be technically beneficial and allow us more leeway for the complex manipulations of MEF2 isoforms

and other co-regulatory proteins that may be necessary to fully grasp the antagonistic relationship observed in cardiomyocytes.

6.2.3 Is the transition from a MEF2C-dominant to a MEF2A-dominant transcriptional landscape developmentally relevant?

In addition to the biochemical analysis proposed above, consideration of the developmental relevance of the observed antagonistic gene regulation is also critical. Of particular importance is whether these genes act as we might hypothesize at the relevant developmental time points. Specifically, do we observe high expression of cell cycle gene and repressed expression of sarcomere genes in early development, and do we see a shift in later development. Additionally, are potential shifts in these gene programs associated with the ratio of MEF2 isoforms in cardiomyocytes?

Previous *in vivo* studies in mice have established a role for MEF2C early in development, and a role for MEF2A much later in development, but in both cases we are observing the effects of chronic depletion. Through the use of established MEF2-flox mice lines, we may be able to better asses the roles of each MEF2 factor at developmentally relevant time points through acute ablation of MEF2 factor activity. The power this affords us is the ability to pinpoint the specific developmental relevance of each of the MEF2 isoforms. We believe this is a necessary set of information because it allows us to return to the developing embryo and assess what transcriptional profiles are associated with that time point, specifically the relationship between proliferative and cardiac differentiation gene programs at these time points. These experiments will allow us to evaluate the hypothesis that the composition of the MEF2 factor ratio may act as a

phenotypic switch between pro-proliferation and pro-quiescence gene programs. Understanding this will also allow us to probe the induction of this process by the myriad developmentally relevant signaling pathways at play in the developing cardiac heart. Our hope is that through this precise developmental analysis, in conjunction with the above mentioned biochemical analysis, we can build a transcriptionally network involving MEF2 that describes key transcriptional events in the development of the mature cardiomyocyte.

While we feel that this is a critical facet of cardiac embryonic development that is lacking, we also believe that these types of analysis will provide us with knowledge essential to the understanding of postnatal cardiac disease. It is believed that cardiac disease causes adult cardiomyocytes to re-acquire fetal gene expression, and this shift may be due to shifts in the relative expression levels of the MEF2 family in adult cardiac disease. We believe that understanding the relationship between MEF2 and terminal differentiation may inform new therapies focused on the induction of proliferative capacity in the remaining cardiomyocytes after induction of cardiac disease.

6.3 Conclusion

In combination, the above mentioned experiments will allow us to build a much more detailed cardiac transcriptional network that accounts for the differential regulatory roles of individual MEF2 factors in cardiomyocytes. We believe that considering transcription factors as discrete regulatory players rather than as members of broad families is essential to dissecting the underlying mechanisms of development and disease.

LIST OF JOURNAL ABBREVIATIONS

Am J Physiol Cell Physiol	American Journal of Physiology - Cell Physiology
Annu Rev Cell Dev Biol	Annual Review of Cell and Developmental Biology
Biochim Biophys Acta	Biochimica et Biophysica Acta
Bioinformatics	Bioinformatics
Can J Physiol Pharmacol	Canadian Journal of Physiology and Pharmacology
Cancer Cell	Cancer Cell
Cardiovasc Res	Cardiovascular Research
Cell	Cell
Cell Mol Life Sci	Cell and Molecular Life Sciences
Circ Res	Circulation Research
Circulation	Circulation
Cold Spring Harb Perspect Med	Cold Spring Harbor Perspectives in Medicine
Curr Opin Cell Biol	Current Opinion in Cell Biology
Curr Opin Genet Dev	Current Opinion in Genetics & Development
Curr Opin Pharmacol	Current Opinion in Pharmacology
Curr Top Dev Biol	Current Topics in Developmental Biology
Current Biology	Current Biology
Dev Biol	Developmental Biology
Dev Cell	Developmental Cell
Dev Dyn	Developmental Dynamics

Dev Genes Evol	Development Genes and Evolution
Development	Development
Differentiation	Differentiation
EMBO J	EMBO Journal
Eur J Hum Genet	European Journal of Human Genetics
FEBS Lett	FEBS Letters
Gene	Gene
Genes and Development	Genes and Development
Genes Dev	Genes & Development
Genesis	Genesis
Genome Res	Genome Research
Heredity (Edinb)	Heredity (Edinb)
J Biol Chem	Journal of Biological Chemistry
J Cardiovas Dev Dis	Journal of Cardiovascular Development and Disease
J Cell Biochem	Journal of Cellular Biochemistry
J Cell Biol	Journal of Cell Biology
J Cell Physiol	Journal of Cellular Physiology
J Cell Sci	Journal of Cell Science
J Clin Invest	Journal of Clinical Investigation
J Mol Biol	Journal of Molecular Biology
Mech Dev	Mechanisms of Development
Mol Cell Biol	Molecular and Cellular Biology

Mol Cell	Molecular Cell
Nat Cell Biol	Nature Cell Biology
Nat Genet	Nature Genetics
Nat Med	Nature Medicine
Neuron	Neuron
Nucleic Acids Res	Nucleic Acids Research
Pediatr Cardiol	Pediatric Cardiology
Physiol Genomics	Physiological Genomics
Physiol Rev	Physiological Reviews
PLoS Genet	PLoS Genetics
PLoS One	PLoS One
Proc Natl Acad Sci U S A	Proceedings of the National Academy of Science of the United States of America
Recent Prog Horm Res	Recent Progress in Hormone Research
Science	Science
Trends Biochem Sci	Trends in Biochemical Sciences
Trends Cardiovasc Res	Trends in Cardiovascular Research
Trends Neurosci	Trends in Neuroscience

REFERENCES

Ahuja, P., P. Sdek and W. R. MacLellan (2007). Cardiac myocyte cell cycle control in development, disease, and regeneration. Physiol Rev **87**(2): 521-544.

Ashburner, M., C. A. Ball, J. A. Blake, D. Botstein, H. Butler, J. M. Cherry, A. P. Davis, K. Dolinski, S. S. Dwight, J. T. Eppig, M. A. Harris, D. P. Hill, L. Issel-Tarver, A. Kasarskis, S. Lewis, J. C. Matese, J. E. Richardson, M. Ringwald, G. M. Rubin and G. Sherlock (2000). Gene ontology: tool for the unification of biology. The Gene Ontology Consortium. Nat Genet **25**(1): 25-29.

Backs, J. and E. N. Olson (2006). Control of cardiac growth by histone acetylation/deacetylation. Circ Res **98**(1): 15-24.

Barnes, R. M., I. S. Harris, E. J. Jaehnig, K. Sauls, T. Sinha, A. Rojas, W. Schachterle, D. J. McCulley, R. A. Norris and B. L. Black (2016). MEF2C regulates outflow tract alignment and transcriptional control of Tdgf1. Development **143**(5): 774-779.

Bendall, A. J. and C. Abate-Shen (2000). Roles for Msx and Dlx homeoproteins in vertebrate development. Gene **247**(1-2): 17-31.

Berry, F. B., Y. Miura, K. Mihara, P. Kaspar, N. Sakata, T. Hashimoto-Tamaoki and T. Tamaoki (2001). Positive and negative regulation of myogenic differentiation of C2C12 cells by isoforms of the multiple homeodomain zinc finger transcription factor ATBF1. J Biol Chem **276**(27): 25057-25065.

Bi, W., C. J. Drake and J. J. Schwarz (1999). The transcription factor MEF2C-null mouse exhibits complex vascular malformations and reduced cardiac expression of angiopoietin 1 and VEGF. Dev Biol **211**(2): 255-267.

Black, B. L., J. D. Molkentin and E. N. Olson (1998). Multiple roles for the MyoD basic region in transmission of transcriptional activation signals and interaction with MEF2. Mol Cell Biol **18**(1): 69-77.

Black, B. L. and E. N. Olson (1998). Transcriptional control of muscle development by myocyte enhancer factor-2 (MEF2) proteins. Annu Rev Cell Dev Biol **14**: 167-196.

Blais, A., M. Tsikitis, D. Acosta-Alvear, R. Sharan, Y. Kluger and B. D. Dynlacht (2005). An initial blueprint for myogenic differentiation. Genes Dev **19**(5): 553-569.

Bondue, A. and C. Blanpain (2010). Mesp1: a key regulator of cardiovascular lineage commitment. Circ Res **107**(12): 1414-1427.

Bour, B. A., M. A. O'Brien, W. L. Lockwood, E. S. Goldstein, R. Bodmer, P. H. Taghert, S. M. Abmayr and H. T. Nguyen (1995). Drosophila MEF2, a transcription factor that is essential for myogenesis. Genes & Development **9**: 730-741.

Braun, T. and H. H. Arnold (1996). Myf-5 and myoD genes are activated in distinct mesenchymal stem cells and determine different skeletal muscle cell lineages. EMBO J **15**(2): 310-318.

Bryantsev, A. L. and R. M. Cripps (2009). Cardiac gene regulatory networks in Drosophila. Biochim Biophys Acta **1789**(4): 343-353.

Buettner, F. F., A. Ashikov, B. Tiemann, L. Lehle and H. Bakker (2013). C. elegans DPY-19 is a C-mannosyltransferase glycosylating thrombospondin repeats. Mol Cell **50**(2): 295-302.

Campa, V. M., R. Gutierrez-Lanza, F. Cerignoli, R. Diaz-Trelles, B. Nelson, T. Tsuji, M. Barcova, W. Jiang and M. Mercola (2008). Notch activates cell cycle reentry and progression in quiescent cardiomyocytes. J Cell Biol **183**(1): 129-141.

Carnegie, G. K., J. Soughayer, F. D. Smith, B. S. Pedroja, F. Zhang, D. Diviani, M. R. Bristow, M. T. Kunkel, A. C. Newton, L. K. Langeberg and J. D. Scott (2008). AKAP-Lbc mobilizes a cardiac hypertrophy signaling pathway. Mol Cell **32**(2): 169-179.

Chabane, N., X. Li and H. Fahmi (2009). HDAC4 contributes to IL-1-induced mPGES-1 expression in human synovial fibroblasts through up-regulation of Egr-1 transcriptional activity. J Cell Biochem **106**(3): 453-463.

Chapman, N. R. and N. D. Perkins (2000). Inhibition of the RelA(p65) NF- B Subunit by Egr-1. J Biol Chem **275**(7): 4719-4725.

Conway, S. J., B. Firulli and A. B. Firulli (2010). A bHLH code for cardiac morphogenesis. Pediatr Cardiol **31**(3): 318-324.

Czubryt, M. P. and E. N. Olson (2004). Balancing contractility and energy production: the role of myocyte enhancer factor 2 (MEF2) in cardiac hypertrophy. Recent Prog Horm Res **59**: 105-124.

D'Amato, G., G. Luxan, G. del Monte-Nieto, B. Martinez-Poveda, C. Torroja, W. Walter, M. S. Bochter, R. Benedito, S. Cole, F. Martinez, A. K. Hadjantonakis, A. Uemura, L. J. Jimenez-Borreguero and J. L. de la Pompa (2016). Sequential Notch activation regulates ventricular chamber development. Nat Cell Biol **18**(1): 7-20.

Danowski, B. A., K. Imanaka-Yoshida, J. M. Sanger and J. W. Sanger (1992). Costameres Are Sites of Force Transmission to the Substratum in Adult Rat Cardiomyocytes. J Cell Biol **118**(6): 1411-1420.

de la Pompa, J. L. and J. A. Epstein (2012). Coordinating tissue interactions: Notch signaling in cardiac development and disease. Dev Cell **22**(2): 244-254.

Delbridge, G. J. and L. M. Khachigian (1997). FGF-1-induced platelet-derived growth factor-A chain gene expression in endothelial cells involves transcriptional activation by early growth response factor-1. Circ Res **18**(2): 282-288.

Desjardins, C. A. and F. J. Naya (2016). The Function of the MEF2 Family of Transcription Factors in Cardiac Development, Cardiogenomics, and Direct Reprogramming. J Cardiovasc Dev Dis **3**(3).

Dichoso, D., T. Brodigan, K. Y. Chwoe, J. S. Lee, R. Llacer, M. Park, A. K. Corsi, S. A. Kostas, A. Fire, J. Ahnn and M. Krause (2000). The MADS-Box factor CeMEF2 is not essential for Caenorhabditis elegans myogenesis and development. Dev Biol **223**(2): 431-440.

Doerks, T., R. R. Copley, J. Schultz, C. P. Ponting and P. Bork (2002). Systematic identification of novel protein domain families associated with nuclear functions. Genome Res **12**(1): 47-56.

Du, M., R. L. Perry, N. B. Nowacki, J. W. Gordon, J. Salma, J. Zhao, A. Aziz, J. Chan, K. W. Siu and J. C. McDermott (2008). Protein kinase A represses skeletal myogenesis by targeting myocyte enhancer factor 2D. Mol Cell Biol **28**(9): 2952-2970.

Durham, J. T., O. M. Brand, M. Arnold, J. G. Reynolds, L. Muthukumar, H. Weiler, J. A. Richardson and F. J. Naya (2006). Myospryn is a direct transcriptional target for MEF2A that encodes a striated muscle, alpha-actinin-interacting, costamere-localized protein. J Biol Chem **281**(10): 6841-6849.

Edmonson, D. G., G. E. Lyons, J. F. Martin and E. N. Olson (1994). *Mef2* expression marks the cardiac and skeletal muscle lineages during mouse embryogenesis. Development **120**: 1251-1263.

Ervasti, J. M. (2003). Costameres: the Achilles' heel of Herculean muscle. J Biol Chem **278**(16): 13591-13594.

Estrella, N. L., A. L. Clark, C. A. Desjardins, S. E. Nocco and F. J. Naya (2015). MEF2D deficiency in neonatal cardiomyocytes triggers cell cycle re-entry and programmed cell death in vitro. J Biol Chem **290**(40): 24367-24380.

Estrella, N. L., C. A. Desjardins, S. E. Nocco, A. L. Clark, Y. Maksimenko and F. J. Naya (2015). MEF2 transcription factors regulate distinct gene programs in mammalian skeletal muscle differentiation. J Biol Chem **290**(2): 1256-1268.

Estrella, N. L. and F. J. Naya (2014). Transcriptional networks regulating the costamere, sarcomere, and other cytoskeletal structures in striated muscle. Cell Mol Life Sci **71**(9): 1641-1656.

Evans, R. M. and D. J. Mangelsdorf (2014). Nuclear Receptors, RXR, and the Big Bang. Cell **157**(1): 255-266.

Ewen, E. P., C. M. Snyder, M. Wilson, D. Desjardins and F. J. Naya (2011). The Mef2A transcription factor coordinately regulates a costamere gene program in cardiac muscle. J Biol Chem **286**(34): 29644-29653.

Feng, Y., C. A. Desjardins, O. Cooper, A. Kontor, S. E. Nocco and F. J. Naya (2015). EGR1 Functions as a Potent Repressor of MEF2 Transcriptional Activity. PLoS One **10**(5): e0127641.

Foglia, M. J. and K. D. Poss (2016). Building and re-building the heart by cardiomyocyte proliferation. Development **143**(5): 729-740.

Gabori, N., R. Sakuma, J. N. Wylie, K. H. Kim, S. S. Zhang, C. C. Hui and B. G. Bruneau (2012). Cooperative and antagonistic roles for Irx3 and Irx5 in cardiac morphogenesis and postnatal physiology. Development **139**: 4007-4019.

Gianakopoulos, P. J. and I. S. Skerjanc (2005). Developmental roles and clinical significance of hedgehog signaling. J Biol Chem **280**(22): 21022-21028.

Gossett, L. A., D. J. Kelvin, E. A. Sternberg and E. N. Olson (1989). A new myocyte-specific enhancer-binding factor that recognizes a conserved element associated with multiple muscle-specific genes. Mol Cel. Biol **9**(11): 5022-5033.

Grade, C. V., M. S. Salerno, F. R. Schubert, S. Dietrich and L. E. Alvares (2009). An evolutionarily conserved Myostatin proximal promoter/enhancer confers basal levels of transcription and spatial specificity in vivo. Dev Genes Evol **219**(9-10): 497-508.

Grant, C. E., T. L. Bailey and W. S. Noble (2011). FIMO: scanning for occurrences of a given motif. Bioinformatics **27**(7): 1017-1018.

Greer, P. L. and M. E. Greenberg (2008). From synapse to nucleus: calcium-dependent gene transcription in the control of synapse development and function. Neuron **59**(6): 846-860.

Grote, K., U. Bavendiek, C. Grothusen, I. Flach, D. Hilfiker-Kleiner, H. Drexler and B. Schieffer (2004). Stretch-inducible expression of the angiogenic factor CCN1 in vascular smooth muscle cells is mediated by Egr-1. J Biol Chem **279**(53): 55675-55681.

Guo, Y., S. J. Kuhl, A. S. Pfister, W. Cizelsky, S. Denk, L. Beer-Molz and M. Kuhl (2014). Comparative analysis reveals distinct and overlapping functions of Mef2c and Mef2d during cardiogenesis in Xenopus laevis. PLoS One **9**(1): e87294.

Han, A., J. He, Y. Wu, J. O. Liu and L. Chen (2005). Mechanism of recruitment of class II histone deacetylases by myocyte enhancer factor-2. J Mol Biol **345**(1): 91-102.

He, A., S. W. Kong, Q. Ma and W. T. Pu (2011). Co-occupancy by multiple cardiac transcription factors identifies transcriptional enhancers active in heart. Proc Natl Acad Sci U S A **108**(14): 5632-5637.

Heidt, A. B., A. Rojas, I. S. Harris and B. L. Black (2007). Determinants of myogenic specificity within MyoD are required for noncanonical E box binding. Mol Cell Biol **27**(16): 5910-5920.

Hinits, Y. and S. M. Hughes (2007). Mef2s are required for thick filament formation in nascent muscle fibres. Development **134**(13): 2511-2519.

Hinits, Y., L. Pan, C. Walker, J. Dowd, C. B. Moens and S. M. Hughes (2012). Zebrafish Mef2ca and Mef2cb are essential for both first and second heart field cardiomyocyte differentiation. Dev Biol **369**(2): 199-210.

Ho Sui, S. J., J. R. Mortimer, D. J. Arenillas, J. Brumm, C. J. Walsh, B. P. Kennedy and W. W. Wasserman (2005). oPOSSUM: identification of over-represented transcription factor binding sites in co-expressed genes. Nucleic Acids Res **33**(10): 3154-3164.

Hsu, S. C., Y. T. Chang and C. C. Chen (2013). Early growth response 1 is an early signal inducing Cav3.2 T-type calcium channels during cardiac hypertrophy. Cardiovasc Res **100**(2): 222-230.

Huang, H. T., O. M. Brand, M. Mathew, C. Ignatiou, E. P. Ewen, S. A. McCalmon and F. J. Naya (2006). Myomaxin is a novel transcriptional target of MEF2A that encodes a Xin-related alpha-actinin-interacting protein. J Biol Chem **281**(51): 39370-39379.

Junion, G., T. Jagla, S. Duplant, R. Tapin, J. P. Da Ponte and K. Jagla (2005). Mapping Dmef2-binding regulatory modules by using a ChIP-enriched in silico targets approach. Proc Natl Acad Sci U S A **102**(51): 18479-18484.

Kanehisa, M., M. Furumichi, M. Tanabe, Y. Sato and K. Morishima (2017). KEGG: new perspectives on genomes, pathways, diseases and drugs. Nucleic Acids Res **45**(D1): D353-D361.

Karamboulas, C., G. D. Dakubo, J. Liu, Y. De Repentigny, K. Yutzey, V. A. Wallace, R. Kothary and I. S. Skerjanc (2006). Disruption of MEF2 activity in cardiomyoblasts inhibits cardiomyogenesis. J Cell Sci **119**(Pt 20): 4315-4321.

Kasneci, A., N. M. Kemeny-Suss, S. V. Komarova and L. E. Chalifour (2009). Egr-1 negatively regulates calsequestrin expression and calcium dynamics in ventricular cells. Cardiovasc Res **81**(4): 695-702.

Khachigian, L. M. (2006). Early growth response-1 in cardiovascular pathobiology. Circ Res **98**(2): 186-191.

Kim, Y., D. Phan, E. van Rooij, D. Z. Wang, J. McAnally, X. Qi, J. A. Richardson, J. A. Hill, R. Bassel-Duby and E. N. Olson (2008). The MEF2D transcription factor mediates stress-dependent cardiac remodeling in mice. J Clin Invest **118**(1): 124-132.

Knoepfler, P. S., D. A. Bergstrom, T. Uetsuki, I. Dac-Korytko, Y. H. Sun, W. E. Wright, S. J. Tapscott and M. P. Kamps (1999). A conserved motif N-terminal to the DNA-binding domains of myogenic bHLH transcription factors mediates cooperative DNA binding with pbx-Meis1/Prep1. Nucleic Acids Res **27**(18): 3752-3761.

Kolodziejczyk, S. M., L. Wang, K. Balazsi, Y. DeRepentigny, R. Kothary and L. A. Megeney (1999). MEF2 is upregulated during cardiac hypertrophy and is required for normal post-natal growth of the myocardium. Current Biology **9**(20): 1203-1206.

Lazic, S. and I. C. Scott (2011). Mef2cb regulates late myocardial cell addition from a second heart field-like population of progenitors in zebrafish. Dev Biol **354**(1): 123-133.

Lee, R. T., Z. Zhao and P. W. Ingham (2016). Hedgehog signalling. Development **143**(3): 367-372.

Lehmann, L. H., B. C. Worst, D. A. Stanmore and J. Backs (2014). Histone deacetylase signaling in cardioprotection. Cell Mol Life Sci **71**(9): 1673-1690.

Li, L., J. Carter, X. Gao, J. Whitehead and W. G. Tourtellotte (2005). The neuroplasticity-associated arc gene is a direct transcriptional target of early growth response (Egr) transcription factors. Mol Cell Biol **25**(23): 10286-10300.

Lilly, B., S. Galewsky, A. B. Firulli, R. A. Schulz and E. N. Olson (1994). D-MEF2: a MADS box transcription factor expressed in differentiating mesoderm and muscle cell lineages during Drosophila embryogenesis. Proc Natl Acad Sci U S A **91**(12): 5662-5666.

Lilly, B., B. Zhao, G. Ranganayakulu, B. M. Paterson, R. A. Schulz and E. N. Olson (1995). Requirement of MADS domain transcription factor D-MEF2 for muscle formation in Drosophila. Science **267**(5198): 688-693.

Lin, Q., J. Lu, H. Yanagisawa, R. Webb, G. E. Lyons, J. A. Richardson and E. N. Olson (1998). Requirement of the MADS-box transcription factor MEF2C for vascular development. Development **125**(22): 4565-4574.

Lin, Q., J. J. Schwarz, C. Bucana and E. N. Olson (1997). Control of Mouse Cardiac Morphogenesis and Myogenesis by Transcription Factor MEF2C. Science **276**: 1404-1407.

Liu, J. and G. D. Stormo (2008). Context-dependent DNA recognition code for C2H2 zinc-finger transcription factors. Bioinformatics **24**(17): 1850-1857.

Lovato, T. L., C. A. Sensibaugh, K. L. Swingle, M. M. Martinez and R. M. Cripps (2015). The Drosophila Transcription Factors Tinman and Pannier Activate and Collaborate with Myocyte Enhancer Factor-2 to Promote Heart Cell Fate. PLoS One **10**(7): e0132965.

Lu, J., T. A. McKinsey, R. L. Nicol and E. N. Olson (2000). Signal-dependent activation of the MEF2 transcription factor by dissociation from histone deacetylases. Proc Natl Acad Sci U S A **97**(8): 4070-4075.

Lu, J., T. A. McKinsey, C. L. Zhang and E. N. Olson (2000). Regulation of skeletal myogenesis by association of the MEF2 transcription factor with class II histone deacetylases. Mol Cell **6**(2): 233-244.

Mayer, U. (2003). Integrins: redundant or important players in skeletal muscle? J Biol Chem **278**(17): 14587-14590.

McCalmon, S. A., D. M. Desjardins, S. Ahmad, K. S. Davidoff, C. M. Snyder, K. Sato, K. Ohashi, O. M. Kielbasa, M. Mathew, E. P. Ewen, K. Walsh, H. Gavras and F. J. Naya (2010). Modulation of angiotensin II-mediated cardiac remodeling by the MEF2A target gene Xirp2. Circ Res **106**(5): 952-960.

McKinsey, T. A. and E. N. Olson (2005). Toward transcriptional therapies for the failing heart: chemical screens to modulate genes. J Clin Invest **115**(3): 538-546.

McKinsey, T. A., C. L. Zhang and E. N. Olson (2001). Control of muscle development by dueling HATs and HDACs. Curr Opin Genet Dev **11**(5): 497-504.

McKinsey, T. A., C. L. Zhang and E. N. Olson (2002). MEF2: a calcium-dependent regulator of cell division, differentiation and death. Trends Biochem Sci **27**(1): 40-47.

Miano, J. M., X. Long and K. Fujiwara (2007). Serum response factor: master regulator of the actin cytoskeleton and contractile apparatus. Am J Physiol Cell Physiol **292**(1): C70-81.

Miska, E. A., C. Karlsson, E. Langley, S. J. Nielsen, J. Pines and T. Kouzarides (1999). HDAC4 deacetylase associates with and represses the MEF2 transcription factor. EMBO J **18**(18): 5099-5107.

Molkentin, J. D., A. B. Firulli, B. L. Black, J. F. Martin, C. M. Hustad, N. Copeland, N. Jenkins, G. E. Lyons and E. N. Olson (1996). MEF2B is a potent transactivator expressed in early myogenic lineages. Mol Cell Biol **16**(7): 3814-3824.

Molkentin, J. D. and E. N. Olson (1996). Combinatorial control of muscle development by basic helix-loop-helix and MADS-box transcription factors. Proc Natl Acad Sci U S A **93**(18): 9366-9373.

Moorman, A. F. and V. M. Christoffels (2003). Cardiac Chamber Formation: Development, Genes, and Evolution. Physiol Rev **83**: 1223-1267.

Motoyama, J., J. Liu, R. Mo, Q. Ding, M. Post and C. C. Hui (1998). Essential function of Gli2 and Gli3 in the formation of lung, trachea and oesophagus. Nat Genet **20**(1): 54-57.

Murphy, A. M. (1996). Contractile protein phenotypic variation during development. Cardiovasc Res **31**: 25-33.

Murray, T. V., A. Ahmad and A. C. Brewer (2014). Reactive oxygen at the heart of metabolism. Trends Cardiovasc Med **24**(3): 113-120.

Narlikar, L., N. J. Sakabe, A. A. Blanski, F. E. Arimura, J. M. Westlund, M. A. Nobrega and I. Ovcharenko (2010). Genome-wide discovery of human heart enhancers. Genome Res **20**(3): 381-392.

Naya, F. J., B. L. Black, H. Wu, R. Bassel-Duby, J. A. Richardson, J. A. Hill and E. N. Olson (2002). Mitochondrial deficiency and cardiac sudden death in mice lacking the MEF2A transcription factor. Nat Med **8**(11): 1303-1309.

Naya, F. J., C. Wu, J. A. Richardson, P. Overbeek and E. N. Olson (1999). Transcriptional activity of MEF2 during mouse embryogenesis monitored with a MEF2-dependent transgene. Development **126**(10): 2045-2052.

Niu, Z., A. Li, S. X. Zhang and R. J. Schwartz (2007). Serum response factor micromanaging cardiogenesis. Curr Opin Cell Biol **19**(6): 618-627.

Ntziachristos, P., J. S. Lim, J. Sage and I. Aifantis (2014). From fly wings to targeted cancer therapies: a centennial for notch signaling. Cancer Cell **25**(3): 318-334.

O'Donovan, K. J., W. G. Tourtellotte, J. Millbrandt and J. M. Baraban (1999). The EGR family of transcription-regulatory factors: progress at the interface of molecular and systems neuroscience. Trends Neurosci **22**(4): 167-173.

O'Mahoney, J. V., K. L. Guven, J. Lin, J. E. Joya, C. S. Robinson, R. P. Wade and E. C. Hardeman (1998). Identification of a novel slow-muscle-fiber enhancer binding protein, MusTRD1. Mol Cell Biol **18**(11): 6641-6652.

Olson, E. N. (2006). Gene regulatory networks in the evolution and development of the heart. Science **313**(5795): 1922-1927.

Pacini, L., S. Suffredini, D. Ponti, R. Coppini, G. Frati, G. Ragona, E. Cerbai and A. Calogero (2013). Altered calcium regulation in isolated cardiomyocytes from Egr-1 knock-out mice. Can J Physiol Pharmacol **91**(12): 1135-1142.

Paige, S. L., K. Plonowska, A. Xu and S. M. Wu (2015). Molecular regulation of cardiomyocyte differentiation. Circ Res **116**(2): 341-353.

Pak, E. and R. A. Segal (2016). Hedgehog Signal Transduction: Key Players, Oncogenic Drivers, and Cancer Therapy. Dev Cell **38**(4): 333-344.

Pallavi, S. K., D. M. Ho, C. Hicks, L. Miele and S. Artavanis-Tsakonas (2012). Notch and Mef2 synergize to promote proliferation and metastasis through JNK signal activation in Drosophila. EMBO J **31**(13): 2895-2907.

Paris, J., C. Virtanen, Z. Lu and M. Takahashi (2004). Identification of MEF2-regulated genes during muscle differentiation. Physiol Genomics **20**(1): 143-151.

Parra, M. and E. Verdin (2010). Regulatory signal transduction pathways for class IIa histone deacetylases. Curr Opin Pharmacol **10**(4): 454-460.

Pasumarthi, K. B. S. (2002). Cardiomyocyte Cell Cycle Regulation. Circulation Research **90**(10): 1044-1054.

Pereira, A. H., C. F. Clemente, A. C. Cardoso, T. H. Theizen, S. A. Rocco, C. C. Judice, M. C. Guido, V. D. Pascoal, I. Lopes-Cendes, J. R. Souza and K. G. Franchini (2009). MEF2C silencing attenuates load-induced left ventricular hypertrophy by modulating mTOR/S6K pathway in mice. PLoS One **4**(12): e8472.

Pollock, R. and R. Treisman (1991). Human SRF-related proteins: DNA-binding properties and potential regulatory targets. Genes Dev **5**(12A): 2327-2341.

Porrello, E. R., A. I. Mahmoud, E. Simpson, J. A. Hill, J. A. Richardson, E. N. Olson and H. A. Sadek (2011). Transient regenerative potential of the neonatal mouse heart. Science **331**(6020): 1078-1080.

Potthoff, M. J., M. A. Arnold, J. McAnally, J. A. Richardson, R. Bassel-Duby and E. N. Olson (2007). Regulation of skeletal muscle sarcomere integrity and postnatal muscle function by Mef2c. Mol Cell Biol **27**(23): 8143-8151.

Potthoff, M. J. and E. N. Olson (2007). MEF2: a central regulator of diverse developmental programs. Development **134**(23): 4131-4140.

Puri, P. L. and V. Sartorelli (2000). Regulation of Muscle Regulatory Factors by DNA-Binding, Interacting Proteins, and Post-Transcriptional Modification. J Cell Physiol **185**: 155-173.

Quandt, K., K. Frech, H. Karas, E. Wingender and T. Werner (1995). MatInd and MatInspector: new fast and versatile tools for detection of consensus matches in nucleotide sequence data. Nucleic Acids Res **23**(23): 4878-4884.

Ramachandran, B., G. Yu, S. Li, B. Zhu and T. Gulick (2008). Myocyte enhancer factor 2A is transcriptionally autoregulated. J Biol Chem **283**(16): 10318-10329.

Rochais, F., K. Mesbah and R. G. Kelly (2009). Signaling pathways controlling second heart field development. Circ Res **104**(8): 933-942.

Sandmann, T., L. J. Jensen, J. S. Jakobsen, M. M. Karzynski, M. P. Eichenlaub, P. Bork and E. E. Furlong (2006). A temporal map of transcription factor activity: mef2 directly regulates target genes at all stages of muscle development. Dev Cell **10**(6): 797-807.

Santelli, E. and T. J. Richmond (2000). Crystal structure of MEF2A core bound to DNA at 1.5 A resolution. J Mol Biol **297**(2): 437-449.

Sartorelli, V., J. Huang, Y. Hamamori and L. Kedes (1997). Molecular mechanisms of myogenic coactivation by p300: direct interaction with the activation domain of MyoD and with the MADS box of MEF2C. Mol Cell Biol **17**(2): 1010-1026.

Schlesinger, J., M. Schueler, M. Grunert, J. J. Fischer, Q. Zhang, T. Krueger, M. Lange, M. Tonjes, I. Dunkel and S. R. Sperling (2011). The cardiac transcription network modulated by Gata4, Mef2a, Nkx2.5, Srf, histone modifications, and microRNAs. PLoS Genet **7**(2): e1001313.

Sebastian, S., H. Faralli, Z. Yao, P. Rakopoulos, C. Palii, Y. Cao, K. Singh, Q. C. Liu, A. Chu, A. Aziz, M. Brand, S. J. Tapscott and F. J. Dilworth (2013). Tissue-specific splicing of a ubiquitously expressed transcription factor is essential for muscle differentiation. Genes Dev **27**(11): 1247-1259.

Sengupta, A., V. V. Kalinichenko and K. E. Yutzey (2013). FoxO1 and FoxM1 transcription factors have antagonistic functions in neonatal cardiomyocyte cell-cycle withdrawal and IGF1 gene regulation. Circ Res **112**(2): 267-277.

Shalizi, A. K. and A. Bonni (2005). Brawn for Brains: The Role of MEF2 Proteins in the Developing Nervous System. Curr Top Dev Biol **69**: 239-266.

Shen, H., A. S. McElhinny, Y. Cao, P. Gao, J. Liu, R. Bronson, J. D. Griffin and L. Wu (2006). The Notch coactivator, MAML1, functions as a novel coactivator for MEF2C-mediated transcription and is required for normal myogenesis. Genes Dev **20**(6): 675-688.

Shen, T., I. Aneas, N. Sakabe, R. J. Dirschinger, G. Wang, S. Smemo, J. M. Westlund, H. Cheng, N. Dalton, Y. Gu, C. J. Boogerd, C. L. Cai, K. Peterson, J. Chen, M. A. Nobrega and S. M. Evans (2011). Tbx20 regulates a genetic program essential to adult mouse cardiomyocyte function. J Clin Invest **121**(12): 4640-4654.

Skerjanc, I. S., H. Petropoulos, A. G. Ridgeway and S. Wiilton (1998). Myocyte Enhancer Factor 2C and Nkx2–5 Up-regulate Each Other's Expression and Initiate Cardiomyogenesis in P19 Cells. J. Biol. Chem **273**(52): 34904-34920.

Snyder, C. M., A. L. Rice, N. L. Estrella, A. Held, S. C. Kandarian and F. J. Naya (2013). MEF2A regulates the Gtl2-Dio3 microRNA mega-cluster to modulate WNT signaling in skeletal muscle regeneration. Development **140**(1): 31-42.

Sorimachi, H. and Y. Ono (2012). Regulation and physiological roles of the calpain system in muscular disorders. Cardiovasc Res **96**(1): 11-22.

Sparrow, D. B., E. A. Miska, E. Langley, S. Reynaud-Deonauth, S. Kotecha, N. Towers, G. Spohr, T. Kouzarides and T. J. Mohun (1999). MEF-2 function is modified by a novel co-repressor, MITR. EMBO J **18**(18): 5085-5098.

Srivastava, D. (2006). Making or breaking the heart: from lineage determination to morphogenesis. Cell **126**(6): 1037-1048.

Svingen, T. and K. F. Tonissen (2006). Hox transcription factors and their elusive mammalian gene targets. Heredity (Edinb) **97**(2): 88-96.

Tassabehji, M., M. Carette, C. Wilmot, D. Donnai, A. P. Read and K. Metcalfe (1999). A transcription factor involved in skeletal muscle gene expression is deleted in patients with Williams syndrome. Eur J Hum Genet **7**: 737-747.

Thomas, N. A., M. Koudijs, F. J. van Eeden, A. L. Joyner and D. Yelon (2008). Hedgehog signaling plays a cell-autonomous role in maximizing cardiac developmental potential. Development **135**(22): 3789-3799.

Ticho, B. S., D. Y. Stainier, M. C. Fishman and R. E. Breitbart (1996). Three zebrafish MEF2 genes delineate somitic and cardiac muscle development in wild-type and mutant embryos. Mech Dev **59**(2): 205-218.

Tsukui, T., J. Capdevila, K. Tamura, P. Ruiz-Lozano, C. Rodriguez-Esteban, S. Yonei-Tamura, J. Magallon, R. A. S. Chandraratna, K. Chien, B. Blumberg, R. M. Evans and J.

C. I. Belmonte (1999). Multiple left-right asymmetry defects in Shh・/・ mutant mice unveil a convergence of the Shh and retinoic acid pathways in the control of Lefty-1. Proc Natl Acad Sci U S A **96**: 11376-11381.

Untergasser, A., I. Cutcutache, T. Koressaar, J. Ye, B. C. Faircloth, M. Remm and S. G. Rozen (2012). Primer3--new capabilities and interfaces. Nucleic Acids Res **40**(15): e115.

van Oort, R. J., E. van Rooij, M. Bourajjaj, J. Schimmel, M. A. Jansen, R. van der Nagel, P. A. Doevendans, M. D. Schneider, C. J. van Echteld and L. J. De Windt (2006). MEF2 activates a genetic program promoting chamber dilation and contractile dysfunction in calcineurin-induced heart failure. Circulation **114**(4): 298-308.

VanDusen, N. J. and A. B. Firulli (2012). Twist factor regulation of non-cardiomyocyte cell lineages in the developing heart. Differentiation **84**(1): 79-88.

Vincent, S. D. and M. E. Buckingham (2010). How to make a heart: the origin and regulation of cardiac progenitor cells. Curr Top Dev Biol **90**: 1-41.

Vincentz, J. W., R. M. Barnes, B. A. Firulli, S. J. Conway and A. B. Firulli (2008). Cooperative interaction of Nkx2.5 and Mef2c transcription factors during heart development. Dev Dyn **237**(12): 3809-3819.

Vogler, G. and R. Bodmer (2015). Cellular Mechanisms of Drosophila Heart Morphogenesis. J Cardiovasc Dev Dis **2**(1): 2-16.

Vong, L. H., M. J. Ragusa and J. J. Schwarz (2005). Generation of conditional Mef2cloxP/loxP mice for temporal- and tissue-specific analyses. Genesis **43**(1): 43-48.

Voronova, A., A. Al Madhoun, A. Fischer, M. Shelton, C. Karamboulas and I. S. Skerjanc (2012). Gli2 and MEF2C activate each other's expression and function synergistically during cardiomyogenesis in vitro. Nucleic Acids Res **40**(8): 3329-3347.

Waardenberg, A. J., M. Ramialison, R. Bouveret and R. P. Harvey (2014). Genetic networks governing heart development. Cold Spring Harb Perspect Med **4**(11): a013839.

Wales, S., S. Hashemi, A. Blais and J. C. McDermott (2014). Global MEF2 target gene analysis in cardiac and skeletal muscle reveals novel regulation of DUSP6 by p38MAPK-MEF2 signaling. Nucleic Acids Res **42**(18): 11349-11362.

Wang, C., S. Dostanic, N. Servant and L. E. Chalifour (2005). Egr-1 negatively regulates expression of the sodium-calcium exchanger-1 in cardiomyocytes in vitro and in vivo. Cardiovasc Res **65**(1): 187-194.

Wang, Y. X., L. X. Qian, Z. Yu, Q. Jiang, Y. X. Dong, X. F. Liu, X. Y. Yang, T. P. Zhong and H. Y. Song (2005). Requirements of myocyte-specific enhancer factor 2A in zebrafish cardiac contractility. FEBS Lett **579**(21): 4843-4850.

Watanabe, K., H. Takebayashi, A. K. Bepari, S. Esumi, Y. Yanagawa and N. Tamamaki (2011). Dpy19l1, a multi-transmembrane protein, regulates the radial migration of glutamatergic neurons in the developing cerebral cortex. Development **138**(22): 4979-4990.

Wilson-Rawlins, J., J. D. Molkentin, B. L. Black and E. N. Olson (1999). Activated Notch Inhibits Myogenic Activity of the MADS-Box Transcription Factor Myocyte Enhancer Factor 2C. Mol Cel. Biol **19**(4): 2853-2862.

Wright, W. E., M. Binder and W. Funk (1991). Cyclic amplification and selection of targets (CASTing) for the myogenin consensus binding site. Mol Cell Biol **11**(8): 4104-4110.

Xu, J., N. L. Gong, I. Bodi, B. J. Aronow, P. H. Backx and J. D. Molkentin (2006). Myocyte enhancer factors 2A and 2C induce dilated cardiomyopathy in transgenic mice. J Biol Chem **281**(14): 9152-9162.

Yu, J., I. de Belle, H. Liang and E. D. Adamson (2004). Coactivating factors p300 and CBP are transcriptionally crossregulated by Egr1 in prostate cells, leading to divergent responses. Mol Cell **15**(1): 83-94.

Yu, Y. T., R. E. Breitbart, L. B. Smoot, Y. Lee, V. Mahdavi and B. Nadal-Ginard (1992). Human myocyte-specific enhancer factor 2 comprises a group of tissue-restricted MADS box transcription factors. Genes Dev **6**(9): 1783-1798.

Yu, Z., T. G. Pestell, M. P. Lisanti and R. G. Pestell (2012). Cancer stem cells. Int J Biochem Cell Biol **44**(12): 2144-2151.

Zacchigna, S. and M. Giacca (2014). Extra- and intracellular factors regulating cardiomyocyte proliferation in postnatal life. Cardiovasc Res **102**(2): 312-320.

Zhang, C. L., T. A. McKinsey, S. Chang, C. L. Antos, J. A. Hill and E. N. Olson (2002). Class II Histone Deacetylases Act as Signal-Responsive Repressors of Cardiac Hypertrophy. Cell **110**: 479-488.

Zhang, X. M., M. Ramalho-Santos and A. P. McMahon (2001). Smoothened mutants reveal redundant roles for Shh and Ihh signaling including regulation of L/R asymmetry by the mouse node. Cell **105**(6): 781-792.

Zhu, B., B. Ramachandran and T. Gulick (2005). Alternative pre-mRNA splicing governs expression of a conserved acidic transactivation domain in myocyte enhancer factor 2 factors of striated muscle and brain. J Biol Chem **280**(31): 28749-28760.

CURRICULUM VITAE